Addis Ababa University
አዲስ፡አበባ፡ዩኒቨርሲቲ
SEEK WISDOM, ELEVATE YOUR INTELLECT AND SERVE HUMANITY !


ADDIS ABABA UNIVERSITY

COLLEGE OF NATURAL AND COMPUTATIONAL SCIENCES

CENTER FOR ENVIRONMENTAL SCIENCE


# DESIGN OF ECO - FRIENDLY HYBRID ELECTRICITY OPTIONS FOR CENTERAL RIFT VALLEY CLIMATIE CONDTIONS, ETHIOPIA

PhD DISSERTATION


MINTESNOT GIZAW TEREFE


A DISSERTATION SUBMITTED TO THE CENTER FOR ENVIRONMENTAL SCIENCE PRESENTED IN PARTIAL FULFILLMENTS OF THE REQUIREMENTS FOR THE DEGREE OF DOCTOR OF PHILOSOPHY IN ENVIRONMENTAL SCIENCE


ADDIS ABABA UNIVERSITY

ADDIS ABABA, ETHIOPIA

OCTOBER, 2024

**Addis Ababa University**

**College of Natural and Computational Sciences**

**Center for Environmental Science**

This is to certify that the dissertation prepared by Mintesnot Gizaw Terefe, entitled: *Design of Eco-friendly Hybrid electricity options for Central Rift Valley Climate condition, Ethiopia* and submitted to the center for environmental science, college of natural and computational sciences, Addis Ababa university, in partial fulfillment of the requirements for the Degree of Doctor of Philosophy (Environmental Science), complies with the regulations of the University and meets the accepted standards with respect to originality and quality.

Signed by the Examining Committee:

| | | |
|---|---|---|
| Dr.-Ing. Belachew Bantyirga | ____________ | 11-11-2024 |
| External Examiner | Signature | Date |
| Dr.-Ing. Wondwosen Bogale | ____________ | 11-11-2024 |
| Internal Examiner | Signature | Date |
| Dr.-Ing. Getachew Bekele Beyene | ____________ | 11-11-2024 |
| Advisor | Signature | Date |
| Prof. Ahmed Hussen | ____________ | 11-11-2024 |
| Chair of the Center for Environmental Science | Signature | Date |

## ABSTRACT

Energy poverty in Sub-Saharan Africa necessitates innovative and sustainable solutions. This dissertation addresses this challenge by investigating low-carbon hybrid microgrid systems (MiGs) for electrifying a typical 250-household remote community in the Ethiopian Central Rift Valley (E.C.R.V.). The study focuses on integrating renewable energy sources (wind, solar, floating photovoltaics - FPV) with diverse storage technologies (lithium-ion batteries, pumped hydro storage - PHS). To assess the region's renewable energy potential, wind speeds were measured at various heights throughout a year and analyzed alongside solar radiation data from existing databases (PVGIS 5.2, NASA Power). This comprehensive evaluation revealed significant potential for both wind and solar energy generation, informing the design of sustainable MiGs. Additionally, the potential for pumped hydro storage (PHS) was assessed using LiDAR-based digital elevation models (DEM) with a resolution of 12.5 meters, identifying Tedecha Island, with its unique volcanic crater pond, as a prime location for a small-scale PHS system. Leveraging this natural feature, a novel MiG design incorporating the Energy-Water-Food Nexus (E-W-F-N) was proposed, aiming to optimize excess energy for water management and agricultural productivity. Extensive simulations and optimization using HOMER Pro, PVsyst, and MATLAB identified optimal hybrid systems tailored to the specific needs of mainland and island communities. For the mainland, a 35.8 KW solar PV system, 20.4 KW wind turbines, and 72 KWh lithium-ion batteries proved the most cost-effective, with a levelized cost of electricity (LCOE) of $0.190/KWh. For the island community, the lowest-cost option was a 41 KW solar PV coupled with a 254 KWh PHS system (LCOE: $0.061/KWh), highlighting the potential for locally available resources to reduce costs. An alternative 32.2 KWp (FPV-PHS) configuration was also identified, showcasing a 7% higher energy yield and significant water savings (2.19 $m^3/m^2$/year) compared to land-mounted PV, at a reasonable LCOE of $0.140/KWh. Sensitivity analysis of the land-based PV-PHS system revealed its robustness under varying conditions, achieving an LCOE of $0.0882/KWh while maintaining 75% of PHS capacity, thereby yielding a surplus of 750 $m^3$ of water annually for E-W-F-N applications. This demonstrates the system's potential to simultaneously address energy and water scarcity challenges. Furthermore, this dissertation addresses critical gaps in the literature by proposing a novel microgrid design paradigm that incorporates the Energy-Water-Food Nexus (E-W-F-N) and developing a comprehensive methodological framework for designing and evaluating FPV-based systems, particularly small-scale (20-50 KWp) configurations. This research confirms the technical and economic feasibility of hybrid MiGs within the Ethiopian context, offering a pathway to expand electricity access and foster sustainable development in the E.C.R.V. and similar regions. The study's focus on small-scale FPV-PHS systems and E-W-F-N integration provides valuable insights for the widespread adoption of sustainable energy solutions in underserved communities. Future research directions include exploring the integration of bioenergy, assessing the long-term performance of mainland systems, conducting a detailed geological assessment for the PHS reservoir, and investigating the use of locally-sourced materials for FPV platforms to further enhance sustainability and cost-effectiveness.

**Keywords:** Ethiopia, Central Rift Valley, hybrid microgrid, renewable energy, energy storage, pumped hydro storage, floating PV, Energy-Water-Food Nexus, off-grid electrification

## ACKNOWLEDGEMENTS

I gratefully acknowledge the invaluable guidance and mentorship of Dr. Getachew Bekele, Associate Professor of Energy Technology at Addis Ababa University. I also extend my sincere thanks to the Coimbra Group for their generous scholarship, the Department of Industrial Engineering at the University of Padova, Italy for providing a stimulating academic environment, and the staff of the Center for Environmental Science for their dedicated partnership in this research.

Dedicated to my grandmother and father ASHEBERU and TEREFE

## TABLE OF CONTENTS

# LIST OF FIGURES

# LIST OF TABLES

# ACRONYMS

| | |
|---|---|
| CCM | Capital Cost Multiplier |
| CRGE | Climate Resilient Green Economy |
| DGe | Diesel Electricity Generator |
| DERs | Distributed Energy Resources |
| E.C.R.V | Ethiopian Central Rift Valley |
| EgoLMPV | Energy Gain Over Land mounted PV |
| E-W-F-N | Energy-Water-Food Nexus |
| FPV | Floating Photovoltaic |
| HDGEs | Hybrid and Decentralized Green Energy Systems |
| HESS | Hybrid Energy supply system |
| Lab | Lead Acid Battery |
| Lib | Lithium Ion Battery |
| LMPV | Land Mounted PV |
| KW/MW | Kilo/Mega Watt |
| MiGs | Microgrid System |
| NPC | Net Present Cost |
| PHS | Pumped Hydro Storage |
| PHSP | Pumped Hydro Storage Potential |
| PV/s | Solar Photovoltaics |
| PVFBO | PV Field Behavior Optimization |
| SOCmin | Minimum State of Charge |
| RF | Renewable Fraction |
| WSP | Water Saving Potential |
| WTa | Wind Turbine |

## LIST OF PUBLICATIONS

**Paper I:**

**Mintesnot Gizaw** and Getachew Bekele, Investigation of Sustainable Technology options: Wind, Pumped-hydro-storage and Solar potential to electrify Isolated Ziway Islanders in Ethiopia.

*EAI Endorsed Transactions on Energy Web* 10 (2023).; https://doi.org/10.4108/ew.88

**Paper II:**

**Mintesnot Gizaw** and Getachew Bekele, Design of a solar island with a water-battery storage system for Lake Ziway islanders in Ethiopia. *Cogent Engineering, 2024.* ***11****(1): p. 2363001*.; https://doi.org/10.1080/23311916.2024.2363001

**Paper III:**

**Mintesnot Gizaw** and Getachew Bekele, Design and evaluation of a sustainable electricity supply system using different storage technologies for Ethiopian central rift valley climate conditions *Under review*

**Additional papers not included in this dissertation:**

**Paper IV:**

**Mintesnot Gizaw** and Getachew Bekele, Design and testing of a small scale Wind turbine for island energy system in Ethiopia.

*In preparation*

**International conference proceedings**

**Mintesnot Gizaw** and Getachew Bekele, Study of the Potential of Sea-Water Pumped Storage for Power Generation: Zway Islands in Ethiopia. Easy Chair; 2021 Jun 12.

# CHAPTER 1: INTRODUCTION

## 1.1. Background

The global transition towards renewable energy is undeniable, particularly in Sub-Saharan Africa where over half a billion people lack electricity access [1-4]. This reliance on polluting fuels hinders socioeconomic development and progress towards international sustainable development goals. Hybrid renewable energy systems (HRES), defined as integrated systems utilizing multiple renewable energy sources, offer a promising solution for electrifying remote areas, providing greater reliability, lower costs, and reduced environmental impact compared to traditional energy sources [2] .

Ethiopia, despite abundant renewable energy potential, faces a significant electricity access deficit as illustrated in Figure 1. As of 2022, only 55 % of the population had access to electricity, while a mere 7.6% utilized clean cooking fuels, with the majority still relying on biomass [5, 6]. This energy poverty, coupled with a rapidly growing economy and a large population lacking modern energy access, underscores the urgency of expanding electrification efforts across the country.

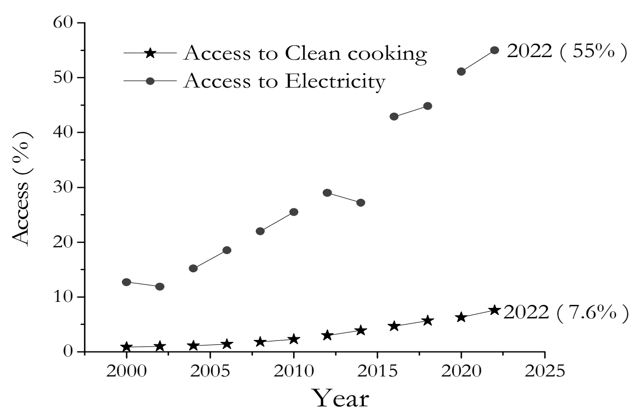


Figure 1. Progress in access to clean cooking and electricity in Ethiopia from 2000 to 2022 [5, 6].

While grid extension remains a priority, microgrids (MiGs) powered by wind, solar, and hydro, often combined with energy storage, are recognized as cost-effective alternatives for remote areas [7]. These decentralized systems not only provide electricity but also contribute to local economic development and climate change mitigation. Ethiopia's commitment to a Climate Resilient Green Economy (CRGE) highlights the importance of increasing renewable electricity generation from different power sources (Figures 2- 4) for domestic and regional markets.

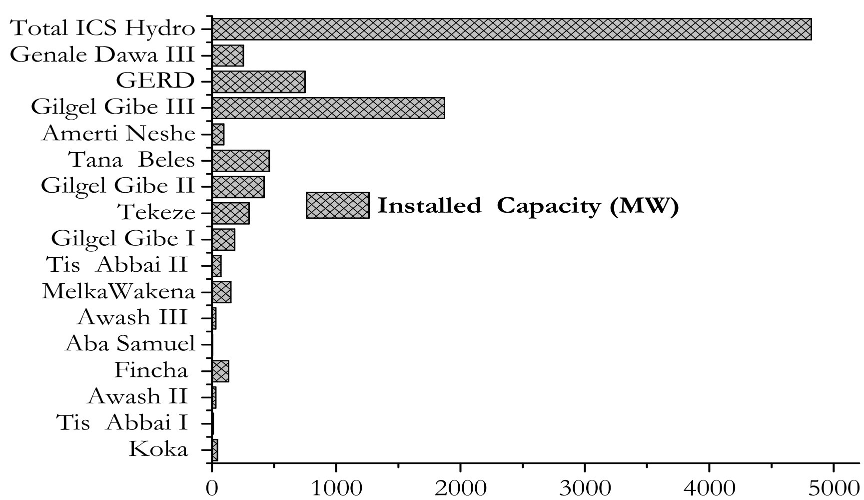


Figure 2. Hydro Power, Installed Capacity (MW) of inter connected system (ICS) as of 2023 [8].

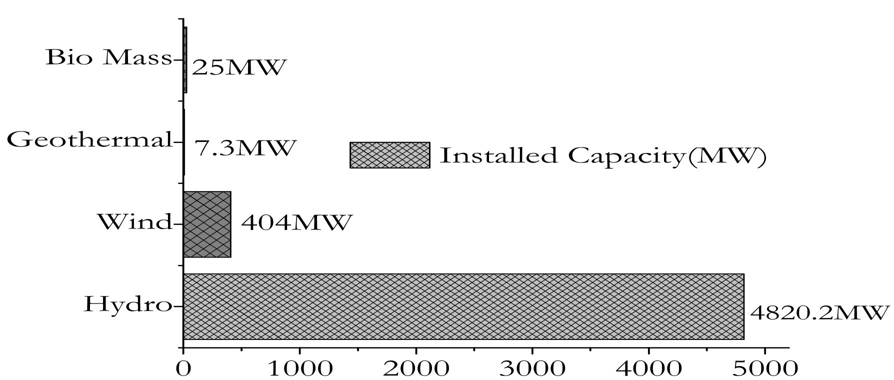


Figure 3. Share of Installed Capacity(MW) by source as of 2023 [8] .

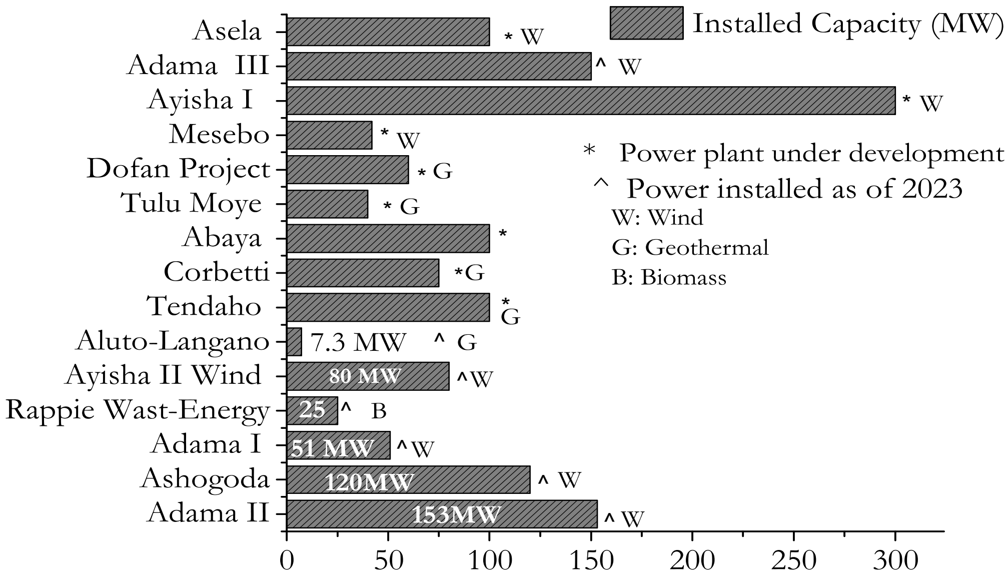


Figure 4. Installed and underdevelopment Power plants(Wind, Geothermal and Biomass) [8].

These figures (2 - 4) illustrate the installed capacity and power plants under development in Ethiopia, emphasizing the country's commitment to increasing clean energy generation. This dissertation focuses on the Ethiopian Central Rift Valley (E.C.R.V.), a region targeted for electrification by national electrification program (NEP) [9, 10]. This area, encompassing mainland and island communities, faces unique energy challenges due to its geography and reliance on non-grid energy sources (Figure 5). The predominantly semi-arid climate supports livelihoods like livestock rearing and small-scale farming, often vulnerable to rainfall variability [11-13]. Island communities, dependent on micro-agriculture and fishing, face additional challenges in accessing electricity, relying on costly and polluting fuels for basic needs [14] .

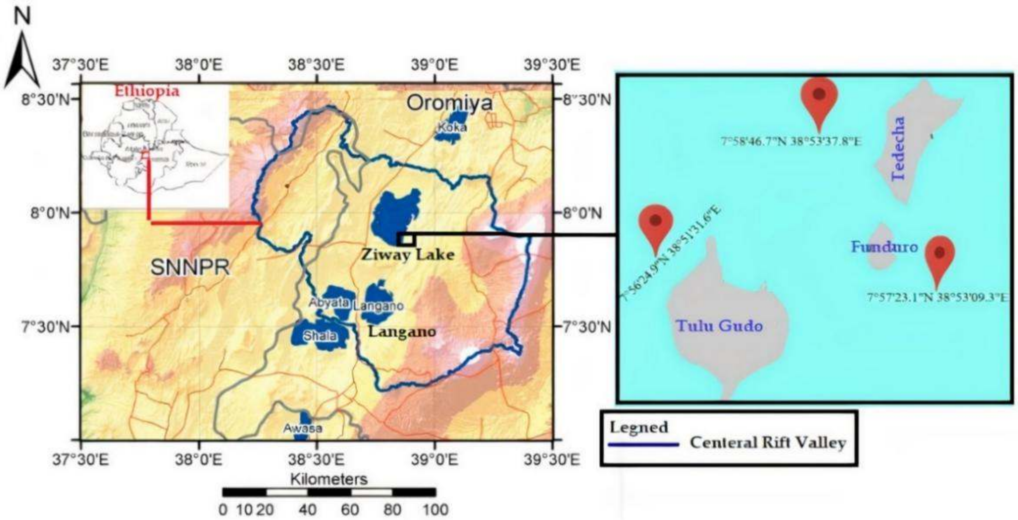


Figure 5. Location of Central Rift valley, districts and Lakes

The unique geographical and climatic condition of the E.C.R.V. make it particularly well-suited for harnessing solar and wind energy, as well as potentially developing pumped hydro storage systems. However, the lack of basic infrastructure and business centers forces islanders to travel to nearby Ziway town for essential supplies like kerosene, diesel, and milling services. This reliance on fossil fuels and biomass for cooking (see Appendix 6) not only strains resources but also puts pressure on the island's natural vegetation.

Hybrid and Decentralized Green Energy Systems (HDGEs), primarily powered by green energy with backup from batteries or diesel generators (DGe), offer a promising pathway to energy stability and economic feasibility in off-grid communities like those in the E.C.R.V. This dissertation will explore the design and implementation of such systems to address the energy challenges and promote sustainable development in this region.

### 1.2. Problem Description and Motivation

The Ethiopian Central Rift Valley (E.C.R.V.) faces a complex energy crisis, with limited electricity access, environmental degradation, and potential water scarcity deeply intertwined [15-17]. Over half of the region's population, particularly those in remote rural and island communities, lacks access to reliable electricity, hindering socioeconomic progress and perpetuating dependence on polluting energy sources like biomass, kerosene, and diesel fuel (Appendix 6) [11-13]. This reliance not only exacerbates local environmental issues, such as deforestation and air pollution, but also contributes to the global climate crisis.

The magnitude of the energy deficit in the E.C.R.V. is evident in Appendix 5 (Power Africa Geospatial Analysis map), revealing a high concentration of households relying on non-grid lighting sources, predominantly in areas where grid extension is not economically feasible [15]. Recent research by [17] corroborates this, reporting that 96% of households in the E.C.R.V. depend on forest energy, dung cakes, kerosene, or diesel for their energy needs. This heavy reliance on unsustainable energy sources not only poses health risks due to indoor air pollution but also contributes to greenhouse gas emissions and deforestation.

Further compounding the region's challenges is the continuous abstraction of water from the E.C.R.V. lakes for irrigation, which, coupled with climate change impacts, has intensified water scarcity and threatened the ecological balance and livelihoods of communities reliant on these water bodies[17]. This situation underscores the urgent need for sustainable solutions that can address both energy and water scarcity in an integrated manner.

While the E.C.R.V. boasts abundant solar and wind resources, their widespread utilization has been hampered by technical, financial, and institutional barriers [3]. Traditional grid extension, often financially unviable in remote areas, leaves many communities underserved [5]. To address these interconnected challenges, this dissertation investigates innovative and sustainable hybrid microgrid systems (MiGs) that integrate wind, solar, and floating photovoltaic (FPV) technologies with energy storage options such as pumped hydro storage (PHS) and batteries. These decentralized systems offer the potential to provide reliable and affordable electricity, reduce environmental impact, and address water scarcity concerns through an integrated Energy-Water-Food Nexus (E-W-F-N) approach [18, 19].

### 1.3. Objectives of this Research

**General objective:**

- ❖ To design and evaluate innovative, low-carbon hybrid electricity systems with diesel generator (DGe) backup for sustainable electrification of communities in the Ethiopian Central Rift Valley (E.C.R.V.), considering both technical, economic and environmental aspects.

**Specific objectives**:

- To investigate the technical potential of Wind, Pumped-hydro-storage (PHS), and solar resources in the E.C.R.V and evaluating their capacity to meet the electricity demands of both mainland and island communities.
- To design and evaluate a stand-alone offshore hybrid floating solar PV (FPV) – PHS – DGe based micro grid system (MiGs) for island community, considering techno-economic and environmental viability.
- To design and conduct techno-economic evaluation of eco-friendly hybrid Wind (WTa)-Solar (PVs)-batteries (Lithium-ion (Lib) and lead acid (Lab)) – PHS - DGe electricity options for the Island and mainland communities.
- To investigate the extra benefit packages linked with the FPV and the E-W-F-N integration potential of the optimized hybrid MiGs.

### 1.4. Important Terms and Concepts

1. **Distributed Energy Resources (DERs)**: DERs are small-scale power generation units located close to the point of use. They can include renewable sources like solar panels and wind turbines, as well as energy storage technologies and controllable loads.

2. **Microgrid System (MiGs)**: A microgrid is a localized group of interconnected electricity sources and loads that can operate independently of the main grid or in parallel with it. MiGs typically incorporate DERs and energy storage, providing enhanced reliability and flexibility for communities or facilities with specific energy needs.

3. **Onshore (on land)/Offshore (on Water) Micro grids:** In this dissertation, we categorize microgrid systems based on their deployment location (land and water): onshore or offshore. Specifically, we classify floating photovoltaic (FPV) (Solar Island) systems as offshore energy supply systems, while traditional land-mounted photovoltaic (PV) systems fall under the onshore category [13].

5. **Pumped Hydro Storage (PHS)**: is a renewable energy storage method that uses two water reservoirs at different elevations to store and generate electricity by pumping water to the upper reservoir during low demand and releasing it to produce power during high demand [20].

6. **PH 245 KWh**: is a Homer Pro pumped hydro storage(PHS) component with various range of minimum state of charge (PHS: SOCmin) (0-100%).This storage is categorized under mechanical energy storage [13].

7. **Floating PV (FPV) extra benefit packages**: FPV systems offer extra benefits beyond electricity generation, including water conservation due to reduced evaporation from shaded water surfaces, and improved energy yield due to the cooling effect of water on the panels [13].

### 1.5. Rationale and Significance

This dissertation is of critical significance due to several factors. First, it directly addresses the pressing need for sustainable energy solutions in the Ethiopian Central Rift Valley (E.C.R.V.), a region grappling with limited electricity access and environmental challenges. By investigating and designing eco-friendly hybrid electricity options, this research has the potential to improve the quality of life for thousands of residents, enhance local economic development, and contribute to national sustainable development goals.

Second, the focus on floating photovoltaic (FLPV) systems is particularly relevant given Ethiopia's unique context. As a country heavily reliant on hydropower (Table 1) and known as a water tower of Africa , exploring alternative renewable energy sources like FLPV can diversify the energy mix, reduce pressure on land resources, and potentially mitigate water scarcity concerns. The vast network of existing hydropower reservoirs and lakes in Ethiopia provides ample opportunity for deploying FLPV systems, making it a promising avenue for increasing clean energy generation without exacerbating water-related issues [21, 22].

Third, this research contributes to the growing body of knowledge on hybrid renewable energy systems and microgrids, especially in the context of developing countries. By evaluating the technical, economic, and environmental feasibility of different system configurations, this study will provide valuable insights for policymakers, energy planners, and communities seeking sustainable electrification solutions in similar contexts.

Finally, the focus on floating solar PV is timely and innovative. While this technology has gained traction globally, research on its application in Ethiopia remains limited [13] . This dissertation aims to fill this gap by providing a comprehensive assessment of FLPV's potential in the E.C.R.V., including its technical performance, economic viability, and environmental benefits.

By addressing these critical issues, this dissertation seeks to contribute to the advancement of sustainable energy solutions, both in Ethiopia and beyond. The findings of this research will not only inform policy and practice but also serve as a catalyst for further innovation in the field of renewable energy.

Table 1.Available areas suitable for off-shore solar PV from HPR and Lakes [21].

| HPR | Area ( $km^2$ ) | Lake | Area ( $km^2$ ) |
|---|---|---|---|
| GERD | 1763.3 | Tana | 3050 |
| Gilgel Gibe I | 62 | Ziway | 435 |
| Koysha | 113 | Abaya & Chamo | 1160 |
| Tekeze | 147 | Langano | 233 |
| Karadobi | 445 | Hawassa | 129 |
| Gilgel Gibe III | 210 | Abiyata | 148 |
| Fincha | 345 | Shala | 310 |
| Koka | 263 | Turkana | 7560 |

(GERD): Grand Ethiopien Renaissance Dam, (HPR): Hydro power réservoirs

The remainder of the next section is organized as follows: Chapter 2 reviews related literature in sequence, namely:(Modeling and sizing of hybrid micro-grid systems) and Floating photovoltaics energy supply system. These three chapters (3, 4, 5) form the core of this study. Each of these chapters can be read independently, even though they are related. Chapter 3 discusses the study's methodological aspects, and the next section, chapter (4) highlights key findings. In Chapter 5, the dissertation concludes by presenting a summary of its main findings along with directions for further research.

# CHAPTER 2: REVIEW OF RELATED LITERATURE

## 2.1. Introduction

The literature review aims to provide a comprehensive understanding of prior research relevant to the offshore and onshore Hybrid Energy supply systems (HESS)(MiGs), particularly in the context of rural electrification. This dissertation offers valuable insights into the planning and implementation of green energy solutions for off-grid communities. Micro-grids(MiGs) (Figure 6), characterized by small-scale-energy- generation ranging from 10 KW to 10 MW, have emerged as cost-effective solutions for providing electricity to rural areas lacking access to traditional power grids [23].

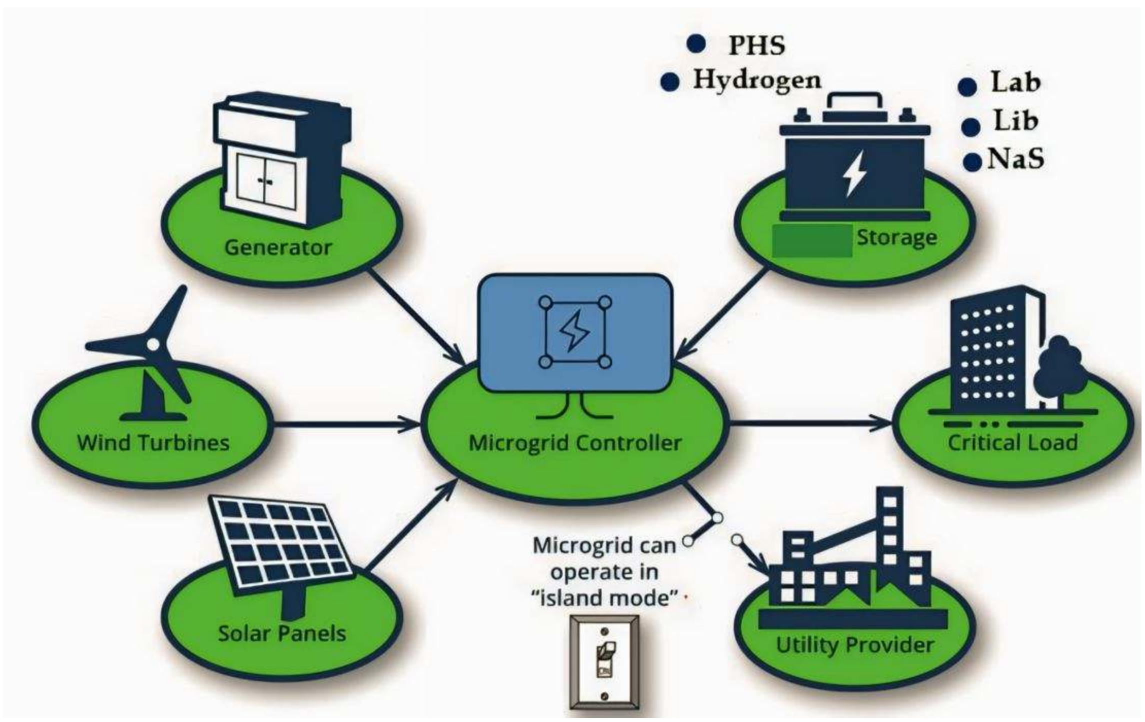


Figure 6.MiGs with various energy storing mechanisms [23].

While **pumped hydro storage (PHS)** offers a valuable energy storage solution for MiGs, recent advancements in other technologies present promising alternatives and complements. **Lithium-**

**ion batteries (Lib)** are becoming increasingly cost-effective with high energy density, making them suitable for various applications, especially where fast response times and frequent charge-discharge cycles are needed. **Lead-acid batteries (Lab)**, while having lower lifespan and energy density, remain a viable option for budget-constrained MiGs, with ongoing advancements improving their performance. **Sodium-sulfur batteries (NaS)** offer high energy density and long cycle life, making them suitable for large-scale, long-duration storage. **Hydrogen storage** is emerging as a promising long-duration solution, using excess renewable energy to produce hydrogen that can be stored and used to generate electricity via fuel cells when needed. These diverse energy storage technologies offer increased flexibility, improved reliability, and cost optimization for MiGs design[24-26].

Furthermore, the integration of **smart grid technologies** can further enhance MiGs performance. Advanced MiGs controllers optimize energy flows, maximizing renewable usage and grid stability. Demand-side management techniques, such as load shifting and demand response, help balance energy supply and demand, reducing peak loads and improving efficiency. Grid-forming inverters provide grid-supporting functions, enhancing stability, especially in islanded mode. Predictive analytics, using weather forecasting and machine learning, enable proactive energy management strategies. These smart grid technologies optimize energy dispatch, improve grid stability, enable demand response, and increase resilience, leading to more efficient and sustainable MiGs operation[26].

Numerous studies have explored the development of onshore [25-35] and offshore [40-45] micro-hybrid electricity systems in Ethiopia and abroad, contributing to the body of knowledge in this field. While an exhaustive review of all relevant studies is beyond the scope of this research, a selection of key studies is highlighted in the following section (2.2 and 2.3) to identify research gaps and emphasize the significance of this dissertation to the scientific community.

## 2.2.Onshore Hybrid Micro grids system (MiGs)

Microgrids (MiGs) are poised to become crucial in the shift toward decentralized and sustainable energy systems, particularly in providing electricity to remote areas without main grid access. Operational microgrid examples worldwide (China, Canada, Italy, Greece, Portugal, and Japan), as documented by [27], showcase their diverse energy sources, including distributed generators, solar PV, micro-hydro, wind turbines, batteries, and flywheels.

The effort to bring sustainable electricity systems to off-grid communities in Ethiopia has been steadily increasing. Recent studies conducted by [28, 29] focused on assessing the electrification possibilities in two remote Ethiopian locations: Wolega and a remote school in the southern region. These studies shared a primary objective, which was to evaluate the economic viability of hybrid electricity systems specifically, WTa-PVs-DGe and PVs-DGe with battery storage. These evaluations were carried out through simulations using Homer Pro. The simulation objectives of both studies were aligned to achieve specific goals, including the minimization of the net present cost (NPC) and cost of electricity (COE), the reduction in $CO_2$ emissions, and the maximization of renewable energy fraction (RF) within proposed micro-grid systems. Results from these investigations identified optimal system configurations involving PVs with battery storage and PVs combined with DGe and batteries. The NPC and COE values derived from these configurations were $9,150 and $0.173/kWh for one study and $32,019 and $0.173/kWh for the other study, respectively.

In another study conducted in a remote Ethiopian town Gebrehiwot et al. [30] assessed the viability of diesel power with backup batteries, wind power, and solar electricity. The results showed an energy cost (COE) of $0.207/kWh and a net cost (NPC) of $82,734, clearly demonstrating the economic viability the proposed MiGs. To evaluate the feasibility of a wind-turbine (WTa) and photovoltaic (PVs) hybrid system for electrifying 200 households in rural Ethiopia, [31] employed Homer Pro optimization and sensitivity analysis. The study concluded that a diesel-only electrical system is more viable than one that incorporates solar, wind, and diesel power. Furthermore, a report published in [32] outlined the use of Homer Pro to develop a hybrid wind and micro-hydroelectric power supply system for rural areas in Ethiopia, serving approximately 600 families. The system achieved a COE of $0.112/kWh, with overall cost and carbon savings of 32% and 83%, respectively. [33] Examined a Hydro-PVs-WTa-DGe hybrid electricity systems to provide power to a hamlet of 100 households, including essential facilities like health and education centers. The study recommended an optimal system layout comprising PVs, WTa, DGe, and batteries, taking into account the potential for wind and solar electricity. This system generated 84% green electricity with an NPC of $103,914 and a COE of $0.302/kWh.

Solar-Wind-Methane hybrid System in Iran [34] investigated a hybrid energy system consisting of solar, wind, and a methane generator with a battery for remote settlements in Fars-Province, Iran. They optimized the system configuration using Homer Pro, achieving a competitive levelized cost of electricity (COE) ranging from 0.128 to 0.223 USD/kWh. Notably, variations in biomass prices significantly impacted the performance of the biogas generator. The most efficient system configuration included a methane generator, battery, and solar panels. DGe-WTa-PVs Hybrid

Table 2. Analysis of previous research on MiGs design in Ethiopia, highlighting the contributions of this dissertation.

| Previous | Aspect | Limitations | Strength | This dissertation |
|---|---|---|---|---|
| [24-35] | Data source | Reliance on readily available wind and solar data from databases or satellite readings, potentially leading to inaccuracies [35]. | Encouraged the use of locally available renewable resources to address energy poverty in off-grid communities and advanced research on hybrid microgrid systems. | Utilized meticulously measured ground-based wind speed data to enhance accuracy and avoid potential over/underestimation of system performance. This approach provides a more reliable assessment of microgrid feasibility in the E.C.R.V. and can serve as a regional reference for future studies. |
| | Energy storage | Primarily focused on electrochemical energy storage (lithium-ion or lead-acid batteries), overlooking other promising technologies. | | Explored the integration of small-scale pumped hydro storage (PHS) in HOMER Pro, addressing a gap in the literature and demonstrating its potential for enhancing energy storage, grid stability, and overall system economics. |
| | Objective function | Primarily focused on minimizing the cost of electricity and maximizing renewable energy fraction (default HOMER Pro objective function), neglecting broader sustainability considerations. | | Extended beyond cost and renewable fraction optimization by incorporating the Energy-Water-Food Nexus (E-W-F-Nexus) into MiGs design. This novel approach considers the interdependencies between energy,water, and food systems, promoting a more holistic and sustainable solution for remote communities. |

System in Sri Lanka [36] : In remote areas of Sri Lanka, a study focused on a DGe-WTa-PVs hybrid electricity system for Siyambalanduwa village families. Through rigorous analysis and Homer Pro optimization, the ideal system configuration of 30 kW, 40 kW, 222 kWh, and 25 kW for PVs, WTa, battery, and DGe respectively was determined. The system exhibited a competitive COE of $0.3/kWh, making it an excellent choice for rural electrification. PVs-WTa-DGe & Battery Systems for Nigerian Health Centers: [37] Nigeria's health centers were the subject of another study that investigated PVs-WTa-DGe & battery hybrid electricity generation systems. Using Homer Pro simulations and considering electricity generation costs, the study revealed that systems incorporating PVs, DGe, and batteries were well-suited for rural health clinics. Interestingly, DGe-only systems had the highest COE, emphasizing the importance of hybrid solutions.

Furthermore, [38] analyzes different ways of implementing a mini-grid design for displaced shelters in Rwanda. Long-term economic and ecological performance is best achieved by implementing a 100 % renewable mini-grid system comprised of PVs-batteries. El Bachtiri and colleagues [39], with Homer Pro in terms of NPC, evaluated the feasibility of a PVs-WTa-electricity generator to identify an economical system architecture capable of meeting the consumption of 4874 kWh/month of a typical city in different Moroccan climates. It was found that a hybrid PVs-WTa microgrid was the most effective option. Again, a study in Ghana [40] examined the feasibility and economics of a self-contained hybrid electricity supply system. The proposed system included PVs, WTa, DGe, and batteries. The study considered electricity generation costs and net present cost (NPC) as key metrics. While the system exhibited an LCOE of $0.382/kWh and an NPC of $8,649,054, it was noted that these costs were significantly higher than local electricity costs, posing a challenge for implementation in Ghanaian households.

### 2.2.1. Gaps in Onshore MiG Research

Previous hybrid energy supply systems-based studies above concentrated on PVs–DGe, PVs/WTa-DGe and WTa/hydro-DGe hybrid systems with electrochemical storage and discovered that green electricity-based systems are viable. In contrast, research in Ethiopia and some neighboring Sub-Saharan African countries has been less conclusive.

The existing body of research predominantly focuses on a conventional approach to microgrid (MiG) design, sharing a common objective of minimizing Life Cycle Costs (LCC). However, a noticeable gap exists in the literature. None of the existing articles [25-35] explore innovative microgrid design approaches that can both support and integrate the Energy-Water-Food (E-W-F) Nexus framework. This gap is significant, as it hinders progress toward improving the livelihoods of off-grid communities and optimizing the Microgrid-Business model. The World Economic Forum initially proposed the W-E-F Nexus as a policy framework to address the challenges of increasing resource shortage and distributional disputes in many regions worldwide [41]. Our microgrid (MiGs) design and approach go beyond already accustomed microgrids by incorporating the principles of the (E-W-F) Nexus. We utilize excess water from the PHS section (without compromising the energy service) to support micro-agricultural activities, sanitation, and household needs, utilizing gravity. This creates a holistic and sustainable E-W-F system (see Figure 21). This approach not only meets the community's energy requirements but also promotes local food production, effective water resource management, and an understanding of the social and economic dynamics of the communities it serves. In Ethiopia, where energy and food production are interdependent and partially competitive, understanding the intricate relationships between these factors is essential for optimizing MiG business models and improving the livelihoods of off-grid communities [41].

In previous versions of Homer Pro, the Water battery component was not included in its library; a newly introduced part of this software was recently introduced called PH 245KWh, dedicated to modelling and optimizing a water battery (pumped-hydro-storage system) in its library. As far as we know, all of the studies reviewed have yet to be implemented, and related studies are insufficient. None of the previous research endeavors considered the integration of small-scale Pumped Hydro Storage (PHS) systems, specifically a PHS 245 KWh, into their hybrid energy generation setups. This gap in knowledge highlights the untapped potential of PHS in enhancing energy storage and grid stability for off-grid communities. The emergence of cost-effective storage technologies, such as Pumped Hydro Storage, often referred to as a 'water battery,' presents an exciting opportunity to ensure a continuous and sustainable energy supply. This innovation plays a critical role in enhancing the competitiveness of solar PV energy in comparison to fossil fuels and other technologies. In our study, we leverage the flexibility offered by water battery technology to support Microgrid (MiGs) systems, utilizing a small-scale PHS component within Homer Pro. This research aims to enrich the literature on small-scale pumped hydro systems, providing valuable insights for application in our region and beyond.

Moreover, within the literature, it is a prevalent practice to utilize weather parameters sourced from Homer Pro databases and satellite readings, this study takes a different approach by utilizing meticulously collected, on-the-ground weather data, specifically wind speed, to enhance the accuracy of simulation results. The utilization of on-site weather data is crucial to avoid potential overestimation or underestimation of the techno-economic and environmental sustainability of the proposed MiGs [42]. Consequently, this study offers a valuable reference for validating MiGs in the region, taking into account specific load characteristics and simulation intricacies. It underscores the importance of considering the impact of satellite-based data in MiGs simulation and optimization when using tools like Homer Pro. This situation allows all renewable energy investors to identify areas where future improvement is needed. Even if the primary goal of many previous studies on hybrid off-grid energy supply systems was to improve the livelihood of the off-grid community, small-scale irrigation is the main engine for improving their lives. However, this load is ignored in most domestic and international hybrid studies. According to [43], small-scale irrigation contributes significantly to rural transformation, and fostering comprehensive rural transformation is critical to achieving long-term growth and poverty eradication in the developing world. This, too, assists poor farmers in overcoming rainfall and water scarcity by providing sustainable water sources for cultivation and animals.

### 2.3.Offshore Hybrid MiGs

Article [44] examined the technical and economic feasibility of an independent FPV battery system for an aquaculture farm. The research confirmed that a photovoltaic battery system is the best choice compared to pure diesel and diesel photovoltaic systems. A study in [45] analyzed the water-saving and FPV potential at Rajghat Dam, India. The study found that by covering 25% of the area, a capacity of 6,513 MWp could be extracted from the reservoir, with reported economic indicators for levelized cost of electricity (LCOE) and internal rate of return (IRR) at $0.036/kWh and 8.5%, respectively. Another study [46] evaluated the effect of FPV coverage in reducing water loss through evaporation from a reservoir in India. The study found that using only 30% of the water body, a capacity of 1.14 MW was achieved, with a corresponding water savings potential of 42,731.56 $m^3$ annually. As stated above the water saving potential of the FPV is one of the main advantage of the technology, but recently accurate quantification of the water saving potential of the FPV system is challenging as, [47] stated that accurately quantifying the water-saving efficiency potential of FPV projects becomes challenging due to the complex nature of the well-accepted method called Penman-Monteith. Furthermore, [48] investigated a solar PV-WTa-PHS hybrid electricity system to satisfy the electricity load of a typical region using HOMER Pro, MATLAB and MS Excel to optimize and analyze the proposed system. Notably, the PHS storage capacity was found to be 3930615 KWh with the corresponding upper reservoir volume of 43170.06$m^3$with, the electricity cost of the system is 0.27$/KWh.

In Ethiopia the domain of Floating Photovoltaic (FPV) systems, which presents an innovative approach to solar energy generation, offers a similar story of promise with gaps waiting to be filled [49]. The study conducted to supply electricity to the Deberemariam island, in Lake Tana and the analysis was carried out using MATLAB Simulink. However, the study has not developed the economic viability of the FPV system, which can be considered as crucial for decision-makers. The emerging components of FPV systems, including the floating structure, anchoring systems, and combiner boxes, differ significantly from land-mounted systems. Therefore, conducting a detailed economic analysis of these components is imperative for understanding the economic feasibility of FPV systems in Ethiopian off-grid electrification projects. Moreover, the studies have often stopped short of determining the energy sufficiency for typical islands and the potential ancillary benefits of FPV systems, such as their capacity to save water through reduced evaporation and therefore are underexplored. Additionally, accurately quantifying the water-saving efficiency potential of FPV projects has proven challenging, given the complexity of methods like Penman-Monteith. Most researchers rely on simplified methods for rough estimations [47]. This dissertation developed a user-friendly FPV-based MiGs design and analysis framework. Furthermore, acknowledges a gap in the literature regarding small-scale FPV-based microgrid systems within the 20-50 KWp range. Most published research [40-45] tends to focus on either much smaller experimental setups or larger utility-scale projects. This dissertation thus fills a crucial gap by providing empirical evidence for the effectiveness and cost-competitiveness of small-scale FPV-PHS systems, validating their potential as a sustainable and adaptable solution for electrifying remote communities in Ethiopia and beyond.

### 2.3.1. Gaps in Offshore FPV based MiG Research:

- Limited Economic Analysis: There is a lack of detailed economic analysis on the emerging components of FPV systems (floating structures, anchoring systems, combiner boxes) and their impact on the overall economic feasibility of FPV projects in Ethiopia.
- Incomplete Assessment of Benefits: Most recent studies [40-45] have focused on energy sufficiency for islands, neglecting to explore additional benefits of FPV such as water conservation and the potential for integration with other systems like PH 245 KWh.
- Lack of Practical Water-Saving Estimation Tools: Existing methods for quantifying the water-saving potential of FPV are complex and not user-friendly, hindering their widespread adoption and application.

## 2.4. Research Gap Addressed by this Dissertation

This dissertation aims to address the identified gaps in the literature by:

- Designing and evaluating hybrid microgrid systems that incorporate the E-W-F Nexus approach, considering the interconnectedness of energy, water, and food systems in the E.C.R.V.
- Investigating the integration of small-scale PHS within hybrid MiGs, assessing its impact on system reliability, stability, and overall performance.

- Conducting a comprehensive techno-economic analysis of FPV systems, including the emerging components, to determine their economic viability for off-grid electrification in Ethiopia.
- Developing a user-friendly framework for accurately quantifying the water-saving potential of FPV systems.
- Utilizing meticulously collected on-the-ground weather data to enhance the accuracy of simulation results and validate the performance of the proposed microgrid systems.

By filling these gaps, this research aims to contribute to the advancement of sustainable and resilient energy solutions for remote and island communities in Ethiopia and other regions with similar challenges.

# CHAPTER 3: METHODOLOGY

This chapter presents the comprehensive methodology employed to achieve the objectives of this dissertation. The research design encompasses a multi-faceted approach, integrating field data collection, rigorous analysis of sustainable energy technology potential, detailed modeling of both onshore and offshore hybrids decentralized green energy systems (HDGEs), and thorough assessment of system component costs and overall economic viability. The following sections outline the specific steps taken in each phase of the research, providing a clear and structured framework for understanding the methodological choices and their rationale.

## 3.1. Data Collection and Study Area

This study focuses on the Ethiopian Central Rift Valley (E.C.R.V.) and the isolated island community of Lake Ziway as pilot cases for designing and simulating sustainable energy solutions. The E.C.R.V. was chosen due to its potential for smallholder irrigation systems, supported by numerous rivers and surface waters, and its prioritization by the government for horticulture and grain seed production (Figure 7) [10]. The island community was selected due to the similarity in household economic and livelihood dependencies, facilitating the collection of a representative load profile.

Wind data were collected through field measurements using a wind mast erected at the location indicated by the red color in Figure 7. Additionally, wind speed and direction data from the NASA database at points 1, 2, and 4 were considered for comparison purposes (Figure 7). The NASA data were measured at one-hour intervals at a height of 50 meters. Field measurements, on the other hand, were taken every ten minutes for a year (2017-2018) at heights of 10, 50, and 70 meters (see Figure 8).

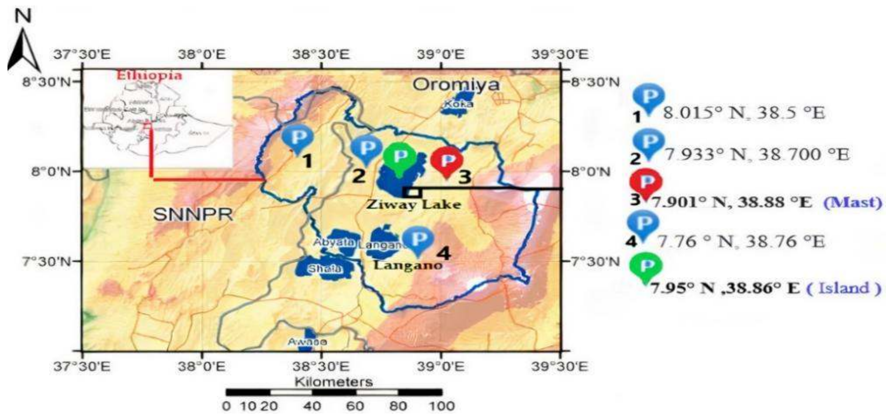


Figure 7. Data collected geographical coordinates within the E.C.R.V

Determining the solar energy potential of a location scientifically requires long-term irradiance measurements. However, in Ethiopia, such comprehensive data is not readily available. Instead, the National Meteorological Agency (NMA) provides average sunshine-hour data collected over several years NMA [33, 50]. To estimate the potential energy output of a solar electricity generator, a robust solar power yield evaluation incorporates data from multiple sources [51].

In this study, we utilized sunshine hour data from NAM and irradiance (KWh/m$^2$):

1. The nearby local weather station in Ethiopia (coordinate point 2): This provides localized data relevant to the specific climatic conditions of the E.C.R.V.
2. PVGIS 5.2 database: This database offers satellite-derived solar radiation data for various locations worldwide, including the coordinates 1, 2, 3, and 4 in Figure 7.
3. PVsyst database (metronome: 8): This database provides comprehensive solar resource data and simulation tools specifically designed for photovoltaic system analysis.

By combining data from these sources for the years 2005-2020, we aim to create a comprehensive and accurate assessment of the solar energy potential in the E.C.R.V [52].

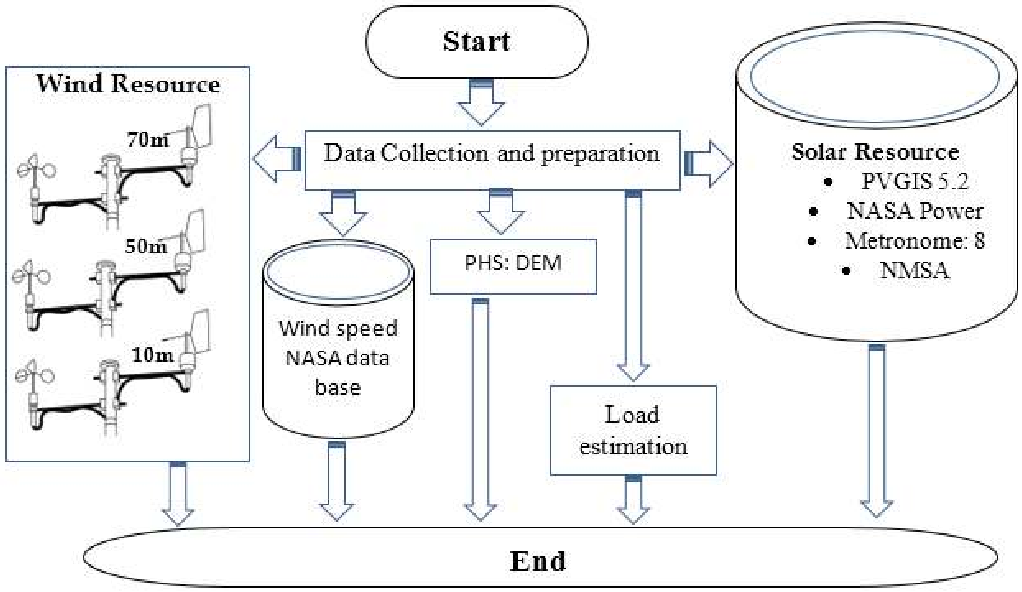


Figure 8. General framework followed to collect data for the onshore HDEs

### 3.2. Wind energy Potential and Wind Turbine(WTa) Modeling

In many studies [53-59] the wind speed frequency is closely approximated by the Weibull distribution function: Wind probability and Cumulative density function (WPDF and WPDF)

$$f(v) = \frac{k}{c}\left(\frac{v}{c}\right)^{k-1} \exp\left[-\left(\frac{v}{c}\right)^{k}\right] \tag{3.1}$$

Where: $v$ = wind speed (m/s), $k$ = the shape factor & $c$ = the scale factor (m/s)

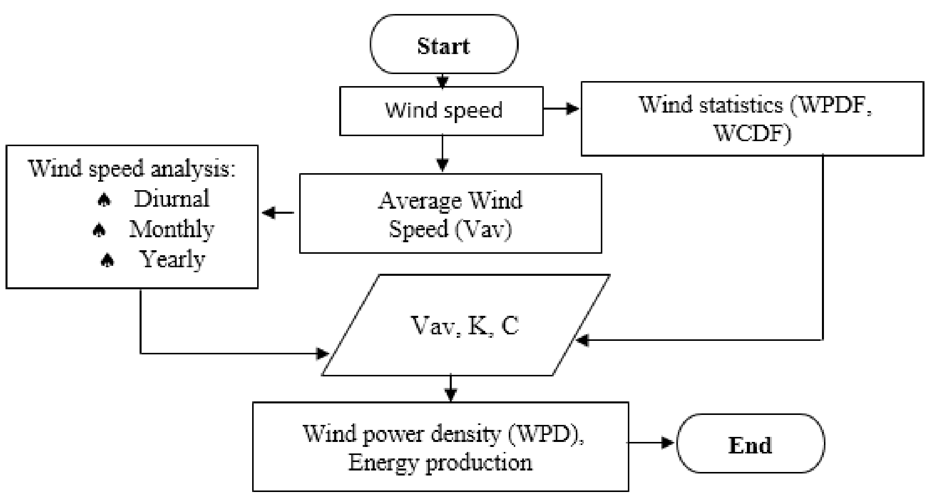


Figure 9. Conceptual frame work developed to wind power potential determination [12, 60, 61].

Equation 3.2 is essential for determining the wind turbine's operational time by calculating the probability of wind speeds falling outside or within the cut-in and cut-out limits. This information helps assess the turbine's power generation potential and overall contribution to the MiGs energy mix.

$$F(v) = 1 - exp\left[-\left(\frac{v}{c}\right)^{k}\right]; (k > 0, v > 0, c > 0) \quad (3.2)$$

The shape, scale parameters can be estimated by several methods [54, 56, 62]. This dissertation used Least-square fit method to observe distribution as it is explained after: The double logarithm of Eq. (3.2) yields:

$$\ln\{-\ln[1 - F(v)]\} = k \ln(v) - k \ln(c) \quad (3.3)$$

A plot of $\ln\{-\ln[1 - F(v)]\}$ vs $\ln(v)$ gives in a linear line. The slop of the line gives the function, and this $\ln\{-\ln[1 - F(v)]\}$ yeilds $k \ln(c)$. Hence, the shape factor $k$ and the scale factor $c$ are determined. The most occurring wind-speed, $v_{mp}(\mathrm{m}/_{\mathrm{s}})$, the maximum energy carrying speed, $v_{maxE}$ $(\mathrm{m}/_{\mathrm{s}})$, are calculated based on Eq (3.4) and (3.5) [54, 56].

$$v_{mp} = c\left(1 - \frac{1}{k}\right)^{1/k} \quad (3.4)$$

$$v_{maxE} = c\left(1 + \frac{2}{k}\right)^{1/k} \quad (3.5)$$

The wind power available per unit area A ($m^2$ ) with a speed $(v)$ is given by the (Eq 3.6 - Eq.3.8) [63-71].

$$p(v) = \frac{1}{2}\rho v^3 \quad (3.6)$$

Also, the power density of the wind, for a probability distribution $f(v)$, can be determined by:

$$WPD = \int_0^\infty p(v)f(v)dv = \frac{1}{2} * \rho * c^3 * \Gamma\left(\frac{k+3}{k}\right) \quad (3.7)$$

Where Γ is Gamma function and it is the available energy density i.e., energy per month or year $E_{an}$ $(Wh)$ can be given by:

$$WED = \frac{T}{2} * \rho * \int_{vi}^{vf} v^3 * f(v) * dv = \frac{1}{2} * \rho * c^3 * \Gamma\left(\frac{k+3}{k}\right) * T \qquad (3.8)$$

Where; $vi$ & $vf$ are the starting and the stopping(furling) wind speeds, T is the total hours per year, and $f(v)$ is the Weibull function tailored for the particular wind site. When calculating the energy on an annual basis, T was considered as 8,760 h in this dissertation.

AWS 5.1KW wind turbine is considered in this dissertation, the detailed economics and the specifications are indicated in Figure 10 and Table 5. The power output of atypical wind turbine ($WP_{out}$) with startup speed (Sst) in our case (2.7 m/s) and furling speed (Sfr) and the wind speed distribution f(vl) is modeled with: Eq (3.9).

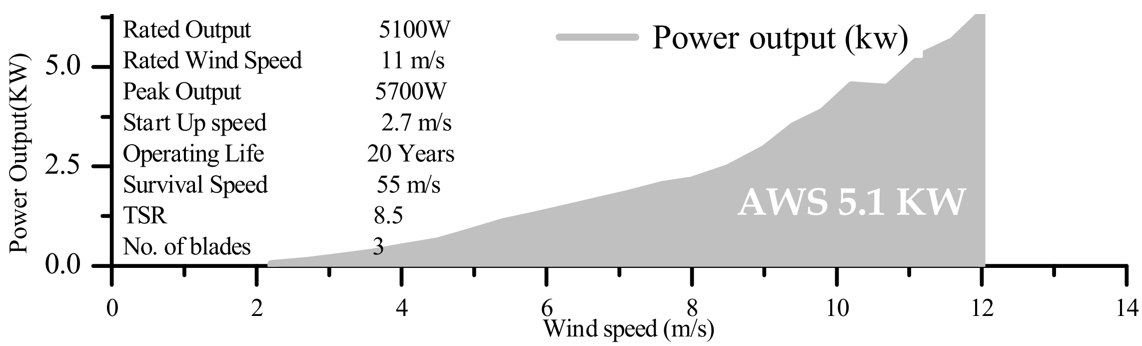


Figure 10 . Power Curve for AWS 5.1 KW Wind Turbine at 12m Height, Used in the Study.

While this dissertation utilized 10-meter height wind speed data for simulation, the AWS5.1KW wind turbines operate at a 12-meter height. To determine the wind speed variations at our study location (V interest), equation (3.10) was employed.

$$WP_{out} = \begin{cases} 0 & : \text{if, the location wind speed(vl)} < Sst \\ \int_{Sst}^{Sfr} (0.5 * \rho * \eta t * A(m^2) * vl^3) * f(vl)\, dvl & : \text{if, } Sst \le vl \le Sfr \\ 0 & : \text{if, } vl > Sfr \end{cases} \qquad (3.9)$$

$$V_{interest} = V_{initial} * (H_{interest}/H_{initial})^{Z} \qquad (3.10)$$

Here z is the coefficient of power law, 0.14 is used for this study and the reference wind speed ($V_{interest}$) is 5.86m/s at Anemo meter height ($H_{initial}$) 10m [72].

### 3.3. Solar Resource, Land Mounted (PV), and FPV Modeling

#### 3.3.1. Solar Energy Resource Potential

Electricity form the sun can be harnessed by using a solar PV. Which convert solar irradiance into electricity, using both direct and diffuse radiation see (Figure 11 and Figure 12).

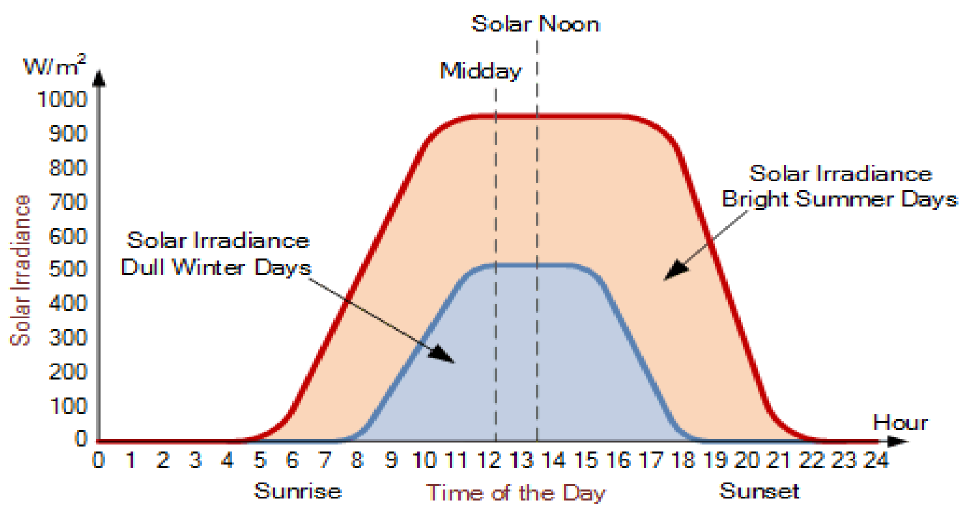


Figure 11.Solar irradiance for a typical day

Together with the mechanism mentioned in section 3.1 the solar electricity potential of the study region is obtained using the following mathematical relations see (Table 3) for the sunshine hour data. When specific location data isn't known, such as in off-grid areas, the solar radiation pattern can alternatively be described in terms of sunshine hours, and average incidence radiations is probably estimated using mathematical relationships from Table 3 Eq ( 3.11-3.16) [73].

Table 3. Mathematical equations employed for solar resource assessment [73]

| Mathematical Models | Eq. No |
|---|---|
| $\bar{N}_s = \frac{\left[\bar{H}_i / \bar{H}_O - a\right] * \bar{N}_d}{b}$ | (3.11) |
| $\bar{H}_i = \bar{H}_O \left(a + b\left(\frac{\bar{n}_s}{\bar{N}_d}\right)\right)$ | (3.12) |
| $\bar{H}_O = \frac{24*3600}{\pi} G_{sc} * \left[1 + 0.034 \cos\left(\frac{360*n_d}{365}\right)\right] * \left[\cos\varphi \cos\delta \sin\omega_s + \left(\frac{\pi\omega_s}{180}\right) \sin\varphi \sin\delta\right]$ | (3.13) |
| $\delta = 23.45 * \sin\left(360 * \frac{248+d_{nd}}{365}\right)$ | (3.14) |
| $\omega_{sh} = {}^{1}/_{\cos} (-\tan\varphi . \tan\delta)$ | (3.15) |
| $\bar{N}_d = {}^{2}/_{15} \cos^{-1}(-\tan\varphi * \tan\delta)$ | (3.16) |

Where: $\bar{H}_O$(wh/m^2/day), (a and b), $\bar{N}_d$, φ , $\omega_{sh}$ and $\delta$ represents for solar radiation at the top of the atmosphere, constants, day length, Latitude, hour of sunset and the angle of declination.

### 3.3.2. Land Mounted PV (LMPV) Modeling

Land mounted solar photovoltaics are small to large-scale solar power systems. Mounting supports located on the ground hold the module in place Figure 12 [74].

The Canadian solar (PV) module CS6K-295MS and Sunpower-E20-327 (with a nominal rating of 327 Wp and with operating temperature -40 to +85 $c^o$ ) is used in this study. The temperature coefficient, the operating temperature, efficiency (%), and the capacity rating (CR) of CS6K-295MS is -0.390, 45c°, 18.02, and 0.295 KW respectively. The financial description of the module is presented in Table 5.The energy output of CS6K-295MS or SPR-E20 in (KWh) is modeled by Homer Pro by applying Eq (3.17).

Figure 12. Land mounted solar photovoltaics (field visit 2021 Soddo woreda, Ethiopia)

$$PV_P = Y_{pva} * f_{pd} \left( {G_{sr}}/{G_{sr}, STCa} \right) [1 + \alpha_P (T_{Ca} - T_{Ca}, STCa)] \quad (3.17)$$

Where: $PV_P$ is the PV array output power, $G_{sr}$ = is the solar radiation incident on PVs array (KW/m$^2$), $G_{sr}, STCa$ is radiation at the normal situation (KW/m$^2$), $Y_{pva}$ = PV capacity (KW), $f_{pd}$ is PV derating factor (%) :88% was considered for this study, $T_{Ca}, STCa$ = module temperature at room conditions ( ºC ), and $T_C$ is PV cell temperature.

### 3.3.3. Floating Photovoltaics (FPV) and its WSP Modeling

Utilizing floating technology to install solar photovoltaic systems over water is a new idea. In this case, PV plant and floating technology combine to produce electricity. This method eliminates the need for photovoltaic power facilities to be built on valuable land. An example of a floating PV plant is shown in Figure 13 and is made up of pontoons or floats, a mooring system, anchoring, solar panels, and cables. This study proposed a novel methodological framework see (Figure 14).

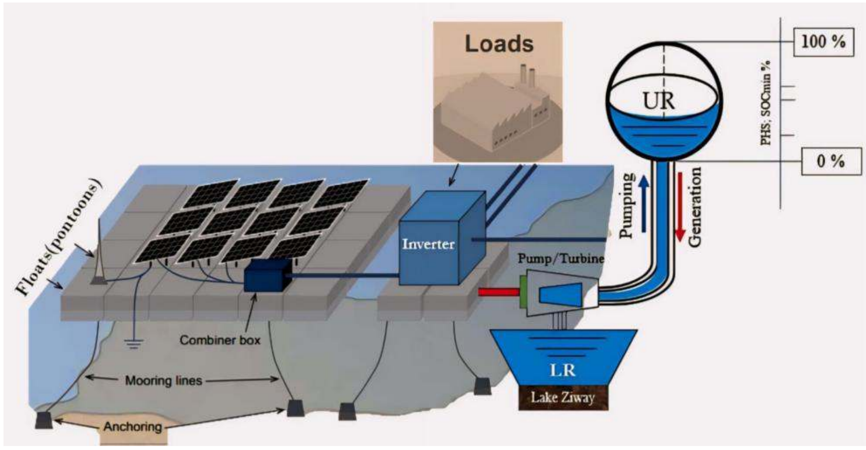


Figure 13. FPV system components adapted from [74, 75].

**Floating Photovoltaics (FPV) Thermal Modeling**

The floating photovoltaic (FPV) component of the offshore microgrid was modeled using PVsyst software, a specialized tool for simulating and analyzing the performance of photovoltaic systems. PVsyst enables accurate modeling of FPV systems by considering factors such as solar irradiance, panel tilt and orientation, shading, and temperature effects. A PVsyst unit was created and integrated into the HOMER Pro model to simulate the FPV system's energy output.

To accurately compare the aquatic and terrestrial photovoltaic systems, meticulous modeling of module cell temperature is crucial [51]. This study utilized PVsyst software to evaluate the actual field behavior of the selected SPR-E20-327 PV panel, which has an electrical efficiency of 20.1% and a temperature coefficient of -0.35% / ° C (Figure 14) [76, 77]. The Faiman relation (Equations 3.18-3.21) was employed to estimate the PV array cell temperature (Tar), incorporating the surface field temperature of the island (Tamb) obtained from PVsyst (metronome: 8), the effective irradiance on the PV array ($G_{eff}$), and other relevant parameters.

$$T_{ar} = T_{amb} + \frac{1}{Ut} * \left(\alpha * G_{eff} * (1 - \eta)\right) \tag{3.18}$$

$$\eta = \eta_{repv}\left(1 - \beta\left(T_{repv} - T_{ar}\right)\right) \tag{3.19}$$

$$Ut = \left(\frac{\alpha * G_{eff} - \eta_{repv}}{T_{ar} - T_{amb}}\right) \quad (3.20)$$

The effective irradiance ($Ge_{ff}$) accounts for various losses related to solar geometry, shading, soiling, and non-optimal tilt angles. $\eta_{repv}$ and $T_{repv}$ are the PV reference efficiency at reference temperature for 1000 $w/m^2$ of irradiance, β shows the dependence of the PV material on ambient temperature, α is solar radiation absorption coefficient, and Ut is the temperature loss factor given by ($w/m^2K$), can be expressed as:

$$Ut = Uca + Uv_w * V \quad (3.21)$$

Uca is a constant that is proportional to the velocity of the wind ($Uv_w$), and its unit is expressed as ($w/m^2.K/(m/s)$). It is important to note that a higher Ut(thermal loss factor) improves the heat exchange between PV modules and the environment, resulting in lower operating temperatures. In recent photovoltaic material science research conducted for the pilot project, experimental investigations reported ( Ut ) values of (55,57,46,71, 56) $w/m^2$ K [78]. For this study, the value was set to 50 and 15 $w/m^2$ K for the aquatic and terrestrial systems, with an optimum tilt angle of $15^o$.After consideration of all the above basic concepts behind the solar PV panel. The actual energy ($P_{fpv}$) obtained from the annual tilted irradiation (G):

$$P_{fpv} = A(m^2)*\eta_{(module,BOS)} * G(\frac{KWh}{m^2}) \quad (3.22)$$

The heat transfer procedures on a floating PV module are shown in Figure 14 (a and b). The incoming radiation from the outside world is felt by the front glass. Conduction occurs between the front and back glass as well as the EVA.

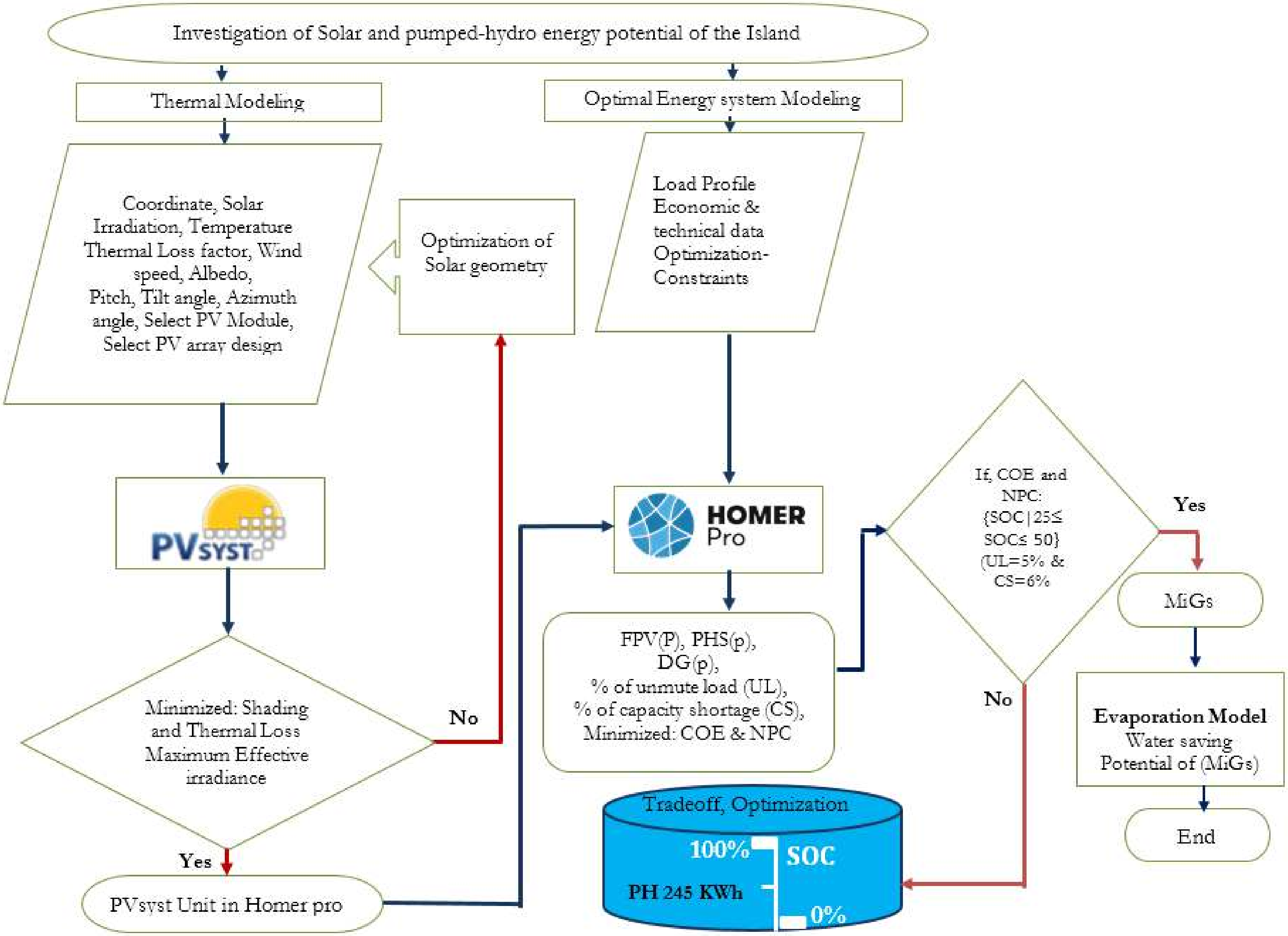


Figure 14. Integrated FPV energy, performance, and extra benefit analysis framework. (PVFBO for lost energy recovery, FPV WSP quantification)

The PV module is exposed to air convection on its front side and water surface convection on its back side, respectively. Additionally, heat is delivered from the PV module's backside to the water or canvas.

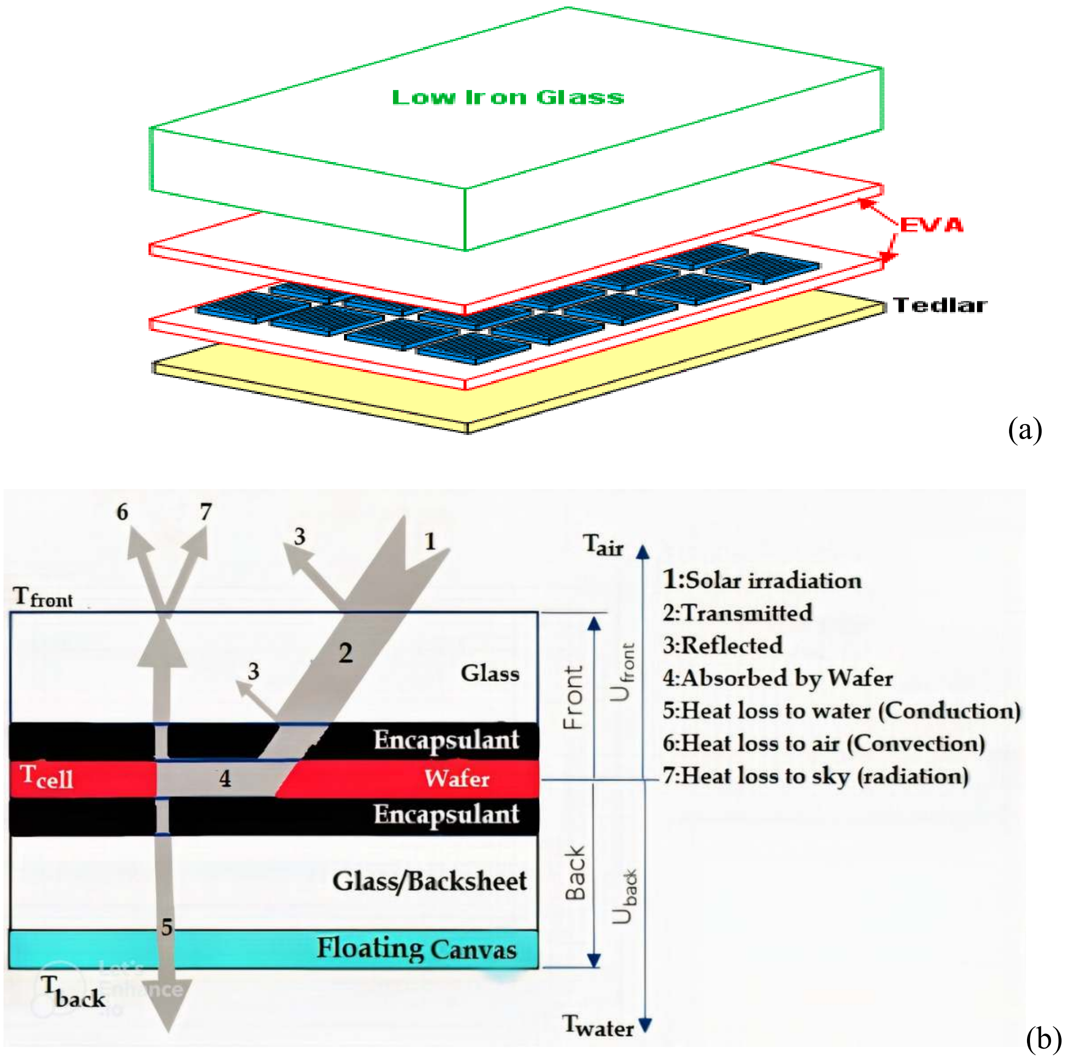


Figure 15. (a) and (b) PV panel configuration, thermal flows , and exchange in modeling [18].

### FPV MiGs Validation Methodology

To ensure the accuracy and reliability of the microgrid simulation, a rigorous validation process was conducted using System Advisor Model (SAM) and Matlab environment. This involved comparing the simulation results obtained from observed data from a real-world floating photovoltaic (PV) system. SAM is a tool developed by the National Renewable Energy Laboratory (NREL). Various PV system sizing models are available in this modular software and free to the users. The rationale behind selecting SAM as a validation software is that this software rigorously compared with data from a real-world floating photovoltaic (PV) system. And scaling factor of 110% added to SAM showed a 9% error with the observed system. This adjustment was based on previous research findings [79, 80]. To this end we conducted the simulation of the system with SAM based on the framework depicted on Figure 16.

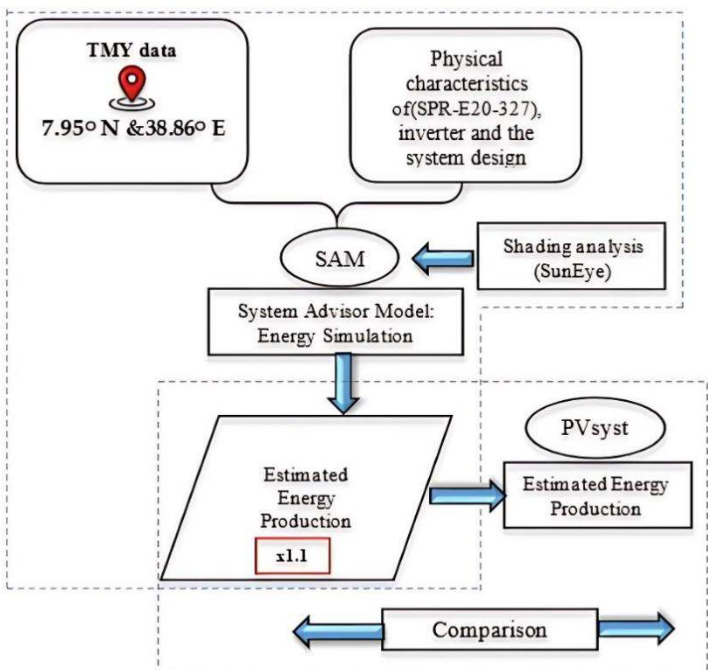


Figure 16. Validation methodology framework

Once after re-simulating the system using SAM for 32.2 KWp with the same climate data, physical characteristics of the module the study applied those formulas (3.23-3.25) .Three common statistical error metrics: Root Mean Squared Error (RMSE), Mean Bias Error (MBE), and Mean

Absolute Percentage Error (MAPE) for the observed energy (Actual)(SAM) and estimated energy (Predicted)(PVsyst) in kilowatt-hours (kWh) per month is determined based on Eq 18-20 [81].

$$\text{RMSE} = \sqrt{\frac{\sum_{i=1}^{n}(SAM_i - PVsyst_i)^2}{n}} \tag{3.23}$$

$$\text{MBE} = \frac{\sum_{i=1}^{n}(SAM_i - PVsyst_i)}{n} \tag{3.24}$$

$$\text{MAPE} = \frac{1}{n}\sum_{i=1}^{n}\left(\frac{SAM_i - PVsyst_i}{SAM_i}\right) * 100 \tag{3.25}$$

Finally, we investigated using the Mat lab Simulink environment to observe the behaviour of the system for a few time steps by employing Table 4 and Figure 17. The scope of this section is to observe the generation behaviour of the PVsyst unit for a few time steps (Appendix 4(b).

Table 4. Temperature models considered for validation in MATLAB environment.

| **No** | **PV-Type** | **Temperature model** | **Ref.** |
|---|---|---|---|
| 1 | LMPV | TPVL = 3.81+0.0282*G + 1.31*Tab – 1.65*WSL | [82] |
| 2 | FPV | TFPV = 1.8081 + 0.9282*Tab + 0.215*G – 1.221* WSw 0.0246*Tw | [83] |

Real world FPV system measured data temperature models presented in Table 3 is used in MATLAB Simulink. The water temperature (Tw) and the speed of wind on water surface (WSw) is given by; - Eq 3.26 and 3.27.

Tw = 5 +0.75*Tab (3.26)

WSw = 1.62 +1.71*WS (3.27)

Where, WS is the speed of wind on land (m/s) and Tab is ambient air temperature. For this study, we set as 20.4 °C and the solar irradiance (G) 6.10 kWh/$m^2$/day.

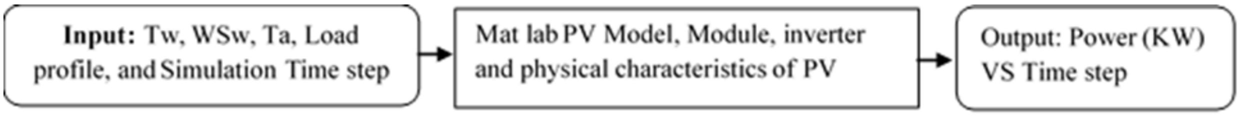


Figure 17. FPV mat lab Simulink model data input to output power [49].

**Evaporation Modeling**

FPV prevent evaporation in the region they cover and across the entire lake's surface. Two main factors cause lower evaporation. The primary issue is decreased air and water interaction within the covered area, which influences water loss through evaporation. The second explanation is the shift in the lake's thermal balance following the construction of the power plant, which makes the lake cooler and hence reduces total evaporation across the entire lake's surface [84]. To model the WSP of FPV. The study used a model developed by FAO 2020 called Crop Watt 8 with its linked New-LocClim-1.10 (see Figure 13). This model is widely used in water resource management to calculate reference evapotranspiration ($E_{Tot}$) using the Penman- Monteith method Equation (3.28). Many mathematical relations and methods have been used to perform similar actions, and the Penman-Monteith method is considered the most comprehensive and reliable [85].

$$E_{Tot} = \frac{0.408*\Delta(Rn-G)+\frac{900\gamma u_{2}(e_s-e_a)}{T+273}}{\Delta+\gamma(1+0.34U_{2w})} \qquad (3.28)$$

Where:($E_{Tot}$) is evapotranspiration(mm/day), Rn is total radiation at the surface of crop (MJ.m$^2$/day),$U_{2w}$ is the wind speed(m/s),T is the average daly temprature,$e_s$ is the average saturation vapour pressure given by (KPa),$e_a$ is the actual vapour preassure in (KPa) , Δ is the curve slop of saturation vapor preassure (KPa/°c) and γ is psychrometric constant (kPa °C$^{-1}$). The input data for the model was measured at 2m hight above the surface of the water. FAO New-LocClim-1.10 software data from 1961 to 2015 were considered for the analysis. Finally, the actual amount of water evaporated in (m$^3$) obtained using equation (3.30).

$$V\left(\frac{\mathrm{m}^3}{\mathrm{day}}\right) = \mathrm{E_{Tot}}\left(\frac{\mathrm{m}}{\mathrm{day}}\right) * \mathrm{A_{OLake}}(\mathrm{m}^2) \tag{3.29}$$

The change in evaporation from a partial or fully coverd water surface can be given by:

$$\Delta\mathrm{V}\left(\frac{\mathrm{m}^3}{\mathrm{day}}\right) = \mathrm{K} * \mathrm{E_{Tot}}\left(\frac{\mathrm{m}}{\mathrm{day}}\right) * \mathrm{A_{C.Lak}}(\mathrm{m}^2) \tag{3.30}$$

Where K represents the evaporation reduction factor coficent determined by the floating structure reflective functionality, A with subscripts stands for area of open and partially or fully coved lake.

### 3.4. Potential and Modeling of Energy Storage Technologies for Hybrid Systems

#### 3.4.1. Pumped Hydro Storage Potential (PHSP) Assessment and Modeling

Based on the location of the hybrid energy system, selecting an appropriate type of energy storage is crucial for the bankability and reliability of the proposed electricity system. PHS appears to be gaining popularity in Wind-PV hybrid systems as a superior alternative to chemical batteries for locations with high solar and wind potential, specifically islands [86]. Such a system is illustrated in Figure 18.

This dissertation employed a remote sensing technology, Arc GIS 10.5, to investigate the water battery (PHS) theoretical and technical potential of the island by using the lake as lower reservoir to support the PVs-WTa based eco-friendly electricity system for the community. Terrain attributes, for instance, slope, elevation, and available area for the upper reservoir, were extracted using digital elevation models (DEMs (LiDAR) at 12.5-m special resolution for the entire islands (Figure 5) in September 2020.

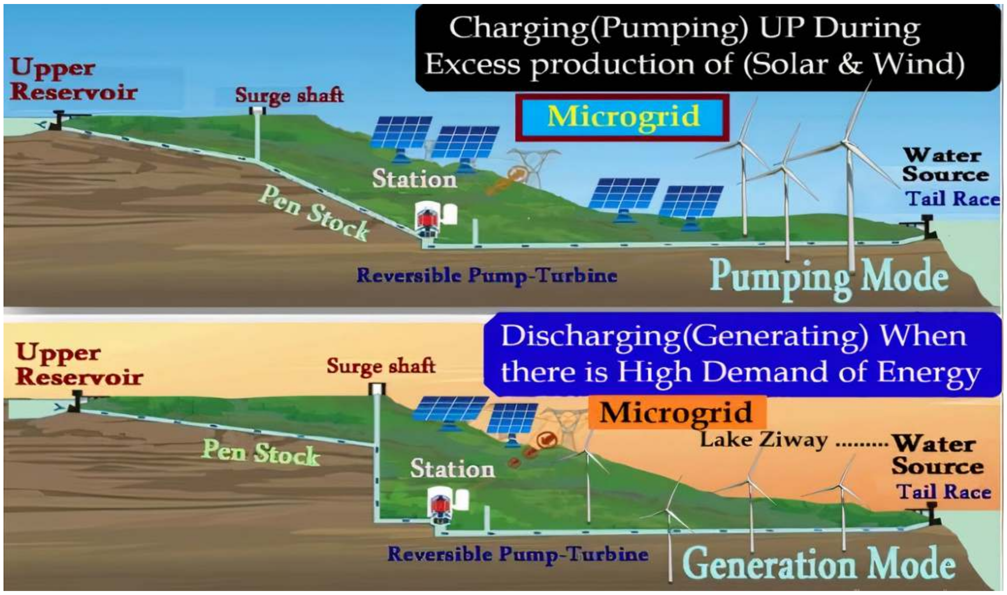


Figure 18. Hypothetical PHS system by considering E.C.RV, lake Ziway as a lower reservoir.

Arc GIS with its sub toolboxes were used to buffer and reclassification of the slop, head, area, restricted locations based on the structure in Figure 19. 0 to 20 % slope class, flat for aspect, and head 50 to 100m is considered as a highest priority during reclassification. Finally based on the criteria set during reclassification and Eq 3.31 – 3.32, the island pumped storage potential was identified.

The technical power generation and reservoir capacity is obtained using equation 3.31 and 3.32.

$$p_d = \rho * g * Q * h * \eta_T \tag{3.31}$$

$$R_{uc} = V\rho g h \eta_{Pump}/3.6 * 10^3 \tag{3.32}$$

Where: Pd = Power (W), h = head (m), Q is flow rate ($m^3$/s), $R_{uc}$ is upper reservoir capacity (energy stored in KWh): V the size of the upper reservoir in $m^3$ ; $\eta$ $(pump)$ is the Pump efficiency : factor $3.6*10^3$ is unit factor Joule to kwh.

The pumped hydro storage (PHS) system was modeled as a small-scale closed-loop system, as shown in Figure 22 (a), The system requires two reservoirs: an upper reservoir (UR),the natural volcanic crater pond at Tsedecha (Figure 41) and the lower reservoir (LR), which is Lake Ziway (Figure 5, and Figure 18). The PHS pumping station undergoes two primary operations: charging and discharging. Equation (3.31) solves the PHS discharge power, while Equation (3.33) determines the charging power (Pc) by:

$$P_c = \rho g H_C Q_C / \eta_{pump} \tag{3.33}$$

Where: the subscript c is for charging. The (PHS 245 KWh) homer component is a storage technology designed to hold 1000 $m^3$ of water in the upper reservoir, with a maximum discharge and charge current of 91.6A. The cost information for the system is in described in Table 5.

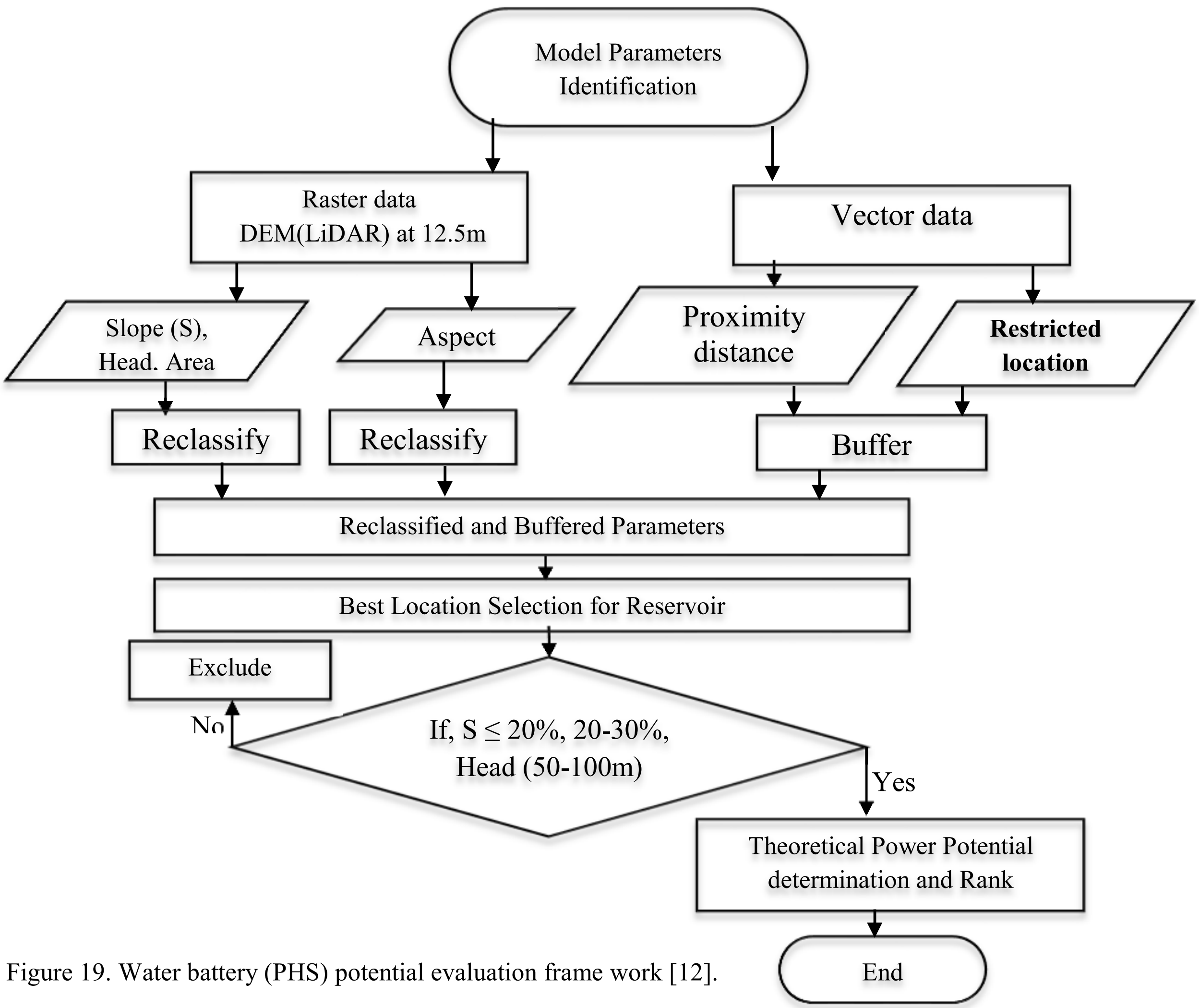


Figure 19. Water battery (PHS) potential evaluation frame work [12].

Once after identifying the PHSP of the entire island this dissertation employed the natural creator pond located on the Island Tsedcha (Figure 41) as UR and Lake Ziway as a LR for the PH 245 component.

### 3.4.2. Battery Modeling

This section will concentrate on modeling electrochemical batteries, namely lithium-ion (Lib) and lead-acid (Lab), as alternative energy storage options. Both are widely used in microgrid systems, with Li-ion batteries projected to become increasingly competitive due to anticipated cost reductions. Equation 3.34 calculates the electrical energy provided by these batteries [43].

$$\mathrm{BatEe} = \mathrm{B(io)} + \int_{\mathrm{to}}^{\mathrm{t}} \mathrm{B(vo)B(I)\,dt} \tag{3.34}$$

Where: B(io) represents the initial state of charge, B(vo) and B(I) stands for the battery voltage and current, respectively. (Lab) and (Lib) possess distinct characteristics, including lifetime and maximum charge/discharge currents [43, 72, 87, 88]. For instance, Lib batteries typically have a lifespan of 3000 cycles, while Lab batteries are often measured in total energy throughput (800 kWh). The maximum discharge/charge current for Lib is 500A/24.3A, while for Lab it is 167A/16.7A.

Electrochemical storage batteries, while useful, have limitations such as limited charge-discharge cycles, minimum state of charge requirements, and environmental concerns upon disposal. On the other hand, mechanical storage, particularly small-scale pumped hydro storage (PHS), offers greater flexibility, as excessive water withdrawal from the upper reservoir does not cause permanent damage. This PHS flexibility extends beyond the capabilities of optimization software. Consequently, this research proposes a novel approach to hybrid decentralized green energy systems (HDGEs) design and management, aiming to improve microgrid developers' business models, as illustrated in Figure 20.

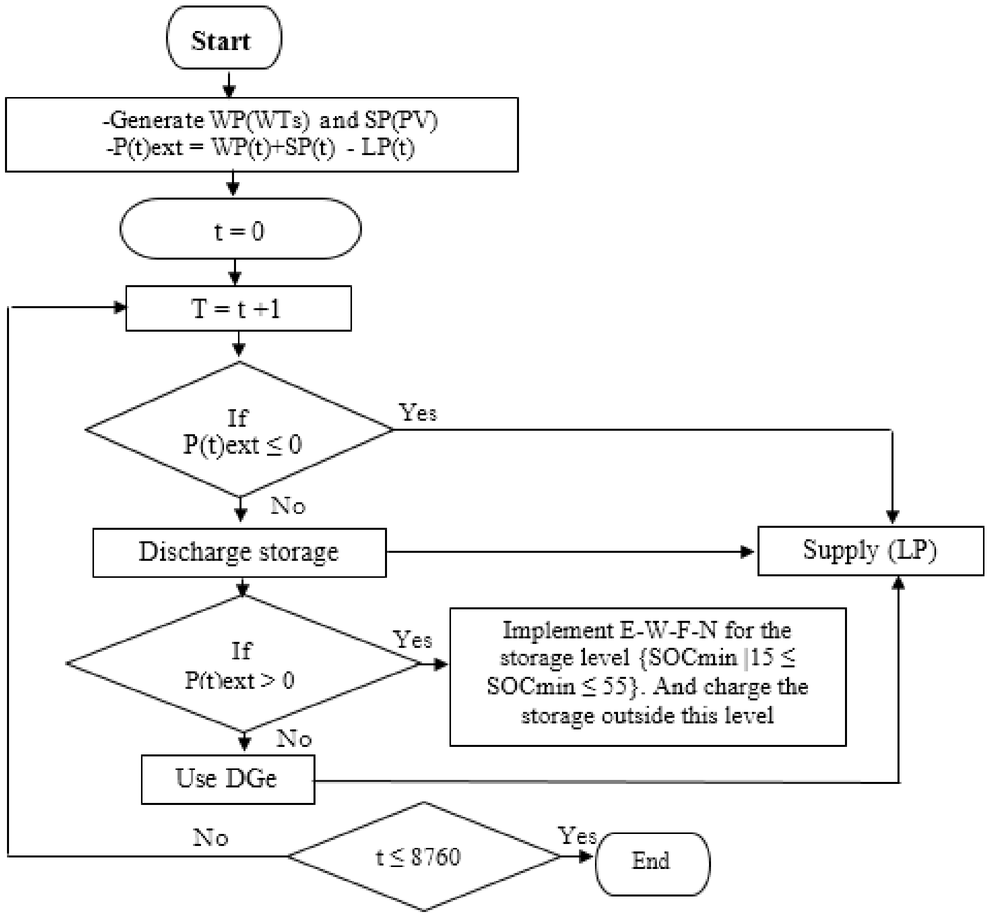


Figure 20. Proposed integrated (E-W- F-N) PHS Supported-MiGs management.

Figure 20 shows that when the wind turbine (WTa) and the solar (PV) start producing electricity, the excess power P (t)extra is the difference between the sum of (WTa), (PV) and the community load power LP (t). If P(t) extra is 0 (zero), the DHGEs are subjected to supply the LP(t) through WT & PV. In contrast, if P(t) extra is greater than zero, the DHGEs start charging the water battery (UR) to raise its SOCmin from 0 to 100% by using the excess production. Once the water battery is set to 100% and serving the LP(t). Within the interval {SOCmin |15 ≤ SOCmin ≤ 55} without affecting the energy services, implementation of the energy-water-food nexus (E-W-F-N) approaches to exploit the remaining amount of water (50%,45%…etc.) through gravity for a different activity (micro-irrigation, cattle watering, sanitation, household consumption etc.)

In essence, this management strategy prioritizes the use of renewable energy sources, utilizing excess energy for E-W-F-N initiatives when possible. PHS acts as a buffer, storing excess energy and releasing it when renewable generation is insufficient. The diesel generator serves as a last resort to ensure a continuous power supply. The SOC constraints on the PHS ensure its longevity and efficient operation.

### 3.5. Diesel Generator (DGe) Modeling

When the electricity demand surpasses the storage capacity of the HDGEs, diesel generators (DGes) are employed as a backup power source. The fuel consumption of the DGe is determined by its fuel curve, represented by Equation (3.35):

$$DG_{fc}(t) = a.\, rcDG + b.\, DG_{o}(t) \tag{3.35}$$

where a = diesel fuel curve interception coefficient, rcDG is KW rating of $DG_e$, $DG_o$ is hourly output of$DG_e$ (KW), whereas b = fuel curve slope (Litter/hour/KW) output. The fuel cost considered in this study is 0.85$/L[72].

### 3.6. Load Demand Estimation

The need for electrical energy at the research location was determined using a survey and observation that took into account the village's future demands as well as expert opinions and prior case studies in Myanmar, Indonesia and East-Africa [49, 89]. The survey participants, who systematically (purposively) selected respondents, consisted of key island and mainland community leaders, religious leaders and women. The questioner's structure encompasses the island's current power security practice (irrigation, mobile charging, playing TV and radio, etc.)

challenges they were faced with. This study adopted a well-known end-use model of United Nations Environmental program tools to estimate the energy demanded of the community. The energy needs of any business determined by two issues: the level of the activity and the intensity of energy. Besides, the breakdown of the various business that comprise the structure of energy needs affects a total community or sectoral energy demand [90].

$$\text{Energy need(Demand)} = \sum_{j=1}^{j=n} Q_j I_j \qquad (3.36)$$

Where: $Q_j$ stands for quantity of energy service j (hours/day, month or year) and $I_j$ (w, kw) is energy use intensity for energy service j (W, KW …etc.). Again $Q_j$ depends on many factors: $Q_j = N_j . p_j . M_j$ ,where $N_j$ is total number of Clients eligible for end-use(j), ($p_j$) is level of penetration of equipment's (appliances) of end user service (j) and eventually ($M_j$) stands for extent or magnitudes of use of end user service (j). From this point of view Eq5 can be rewritten as:

$$\text{Energy need(Demand)} = \sum_{j=1}^{j=n} Q_j I_j = \sum_{j=n}^{j=n} (N_j P_j . M_j). I_j \qquad (3.37)$$

### 3.7. Capital Cost Assumptions and Economic Modeling for HDGEs

Due to the technological difference between the LMPV system and the FPV, we presented the cost issue (financial description of the renewable energy technologies) in two ways as describe in Table 5 and Table 5.

#### 3.7.1. FPV Capital Cost Assumptions

These pricing estimates are based on median figures provided by FPV manufacturers and installers. Due to a lack of fencing maintenance and vegetation, some Floatvoltaic installations claim fewer O & M events per year, resulting in operating and maintenance cost exemptions.

Others, however, claim that operating and maintenance costs are equal to onshore PV system costs, operations related to FPV farms, such as standby monitoring and control of the system's basic structure (mooring lines and anchors) see Figure 13. Again, the FPV system is most sensitive to loadings related to snow and wind, float costs, the efficiency of the PV module, and variation in water depth level [91]. As a part of the operation and maintenance for floating photovoltaics, the pumped storage component of the system will supply water for cleaning the module without any additional cost consideration. This phenomenon is also a plus for saving on O & M costs. A small-scale FPV project up to 100 kW, such as the one at NUST Lake, requires no mooring lines and is inexpensive [92]. Furthermore, because the region's weather state does not present such tough tasks for the small-scale near-shore FPV system, wind, snow, and environmental disrupting components such as waves and noticeable variations in the water level are exempt in this situation. Given the preceding settings, the study presented the capital cost assumptions and considered interest and inflation rates described in Table 5 and Table 6.

Table 5. HDGEs components financial description

| Category | Main component | $(US) | O&M. cost | Repl. cost | Life time | Ref. |
|---|---|---|---|---|---|---|
| Solar | SPR-E20-327 | $620/Panel | 3$/year | $620/panel | 25 years | [93] |
| | CS6K-295MS | $900/KW | $0/year | $900/KW | 25 years | [72] |
| Storage | (Lab) | $300.0/KWh | $10/KWh | $300/KWh | 10 years | [43] |
| | (Lib) | $630.0/KWh | 0$/ year | $600/KWh | 15 years | [72, 87] |
| Converter | Fron24 | 150.0/KW | 3$/year | $150/KW | 10 years | [94] |
| Wind | AWS5.1KW WT | $2,155/KW | $20/year | $0 | 25 years | [95] |
| Backup | DGEs | 250/KW | $0.3/KW | $200/KW | 60,000hr | [30] |

Table 6. Capital cost assumption of components unique for onshore HDGEs

| Category | Main Component | $ (US) | Ref. |
|---|---|---|---|
| Balance of System (BOS) | Inverter | 150/KW | [94, 96] |
| | Floating structure | 20/Panel | |
| | Anchoring | 36/KWp | |
| Storage | PHS | 11000 | [97] [98] |
| Discount rate, inflation rate (%), and diesel fuel($/L) are 12.59,10.51& 0.43 | | | [29] |

The cost of pumped hydro is mainly sight dependent according to [98], [97] and [99] the reported price shows $470/kW, $500-2000/KW,5-100/KWh. For this study by considering the suitability of the sight the authors used values indicated in Table 5 above. The Replacement, Operation and maintenance (O & M. Cost), and duration of PHS is (100$/year, 11,054.45$ and 50 years' life) and according to the manufacturer the floating structure is granted for 25 year [29, 98] .

### 3.7.2. Economic modeling for (FPV and LMPV MiGs)

The selection of the appropriate HDGEs from the configuration is filtered out by Homer based on least neat present cost and cost of electricity and calculated by using: Eq. (3.38).

$$\mathrm{NPC} = \sum_{\mathrm{C=PHS,PV,WT.....etc.}} \mathrm{NPC_C}\ , \qquad \text{also } \mathrm{NPC_C} = \mathrm{IC_C} + \mathrm{RC_C} - \mathrm{SC_C} \tag{3.38}$$

Where: NPC = net present cost of HESS, c subscript is about the system component i.e., PHS, WTa, PVs…etc.; $IC_C$ is the net initial cost of the c component ($), $RC_C$ is the total replacement cost of the c component ($) and $SC_C$ is cost of salvage value ($). Cost of energy is given by:

$$\mathrm{COE} = \mathrm{C_{T,ann}} - \mathrm{C_B}.\mathrm{H_T} \Big/ \mathrm{TE_{served}} \tag{3.39}$$

Where: $C_{Tann}$ is the total cost of the system annually ($/year), $C_B$ is marginal cost of boiler ($/year), $H_T$ is served thermal load total (KWh/year), $TE_{served}$ stands for consumed electrical load. Here $H_T$ = zero. The project life time assumed, the real discount and inflation rate (%) is 25 years, 10.51, and 12.5 respectively. The real inflation and discount factor of the project applied in this study is based on updated information obtained from trusted source [29, 72].

### 3.8.Onshore and Offshore HDGEs Model Representation, Simulation and Optimization

This section outlines the methodology for evaluating the performance of hybrid decentralized green energy systems (HDGEs) under various storage scenarios within proposed microgrids (MiGs) in the Ethiopian Central Rift Valley (ECRV). The MiGs utilize a diverse mix of power generation sources, including photovoltaic (PV) panels, wind turbines (WTa), and diesel generators (DGes), alongside various energy storage technologies such as pumped hydro storage (PHS), lithium-ion (Lib), and lead-acid (Lab) batteries. To determine the optimal system configuration for each storage scenario, multiple batches of simulations were conducted using HOMER Pro software. These simulations were based on the MiGs configurations illustrated in Figure 21, Figure 22(a and b) and further detailed in Appendix 2 and 3. The primary goal was to identify the most suitable system for each community, considering net present cost (NPC), levelized cost of electricity (LCOE), renewable energy fraction (RF), and the capacity to support the E-W-F-N approach.

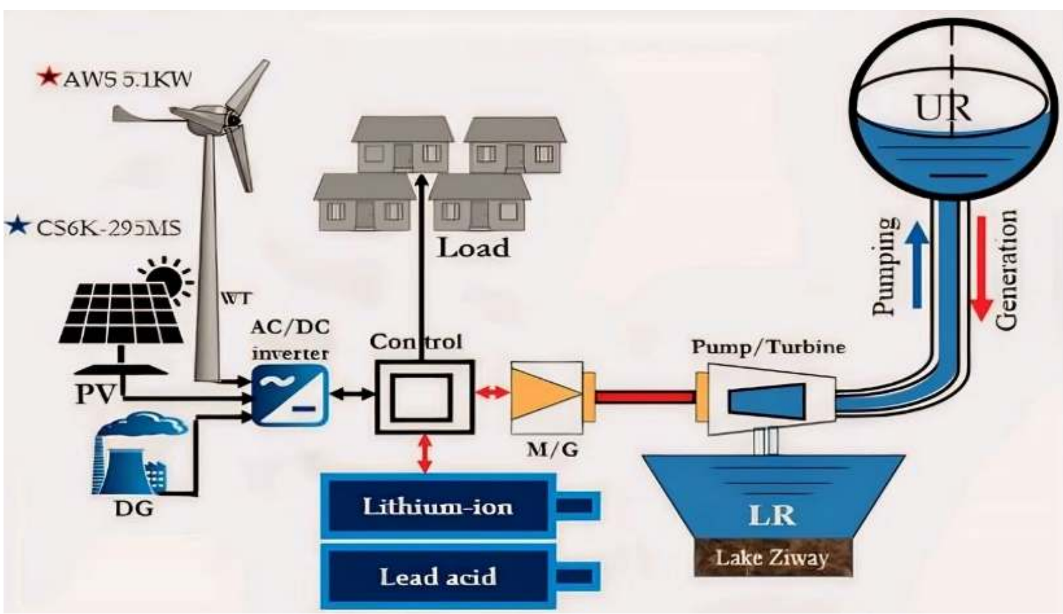


Figure 21. HDGEs schematic design of the off shore and onshore system with different storages

Figure 21 presents a comprehensive model designed to meet the electricity needs of a typical ECRV community that currently relies on a 45 kW DGe for power. This model incorporates solar PVs, wind turbines, and three distinct energy storage systems: PHS, Lib, and Lab. The system also includes a 45 kW DGe with specific fuel curve parameters.

During daylight hours, solar PVs and wind turbines generate electricity to meet the community's load. Excess energy produced during this time is used to recharge the batteries (Lib and Lab) and pump water from Lake Ziway to the upper reservoir of the PHS unit. The stored energy in the batteries and the potential energy in the PHS reservoir can be utilized when PV and WT generation is insufficient, such as during cloud cover, low irradiance, or nighttime.

These initial steps aimed to identify the most suitable microgrid types for each community and comprehensively assess the techno-economic and environmental implications of various energy storage technologies. This approach will provide valuable insights to guide informed decision-making regarding sustainable and efficient microgrid operations in the unique context of the Ethiopian Central Rift Valley.

#### 3.8.1. Solar Island Representation

The concept of a floating photovoltaic (FPV) solar island holds immense potential for transforming energy provision in island communities, particularly in regions like the Ziway Islands, where high solar irradiance coincides with limited land availability and absent grid infrastructure (Figure 22). FPV technology directly addresses two pressing challenges of land-based solar power: space constraints and solar cell overheating [100].Unlike terrestrial installations, FPV systems incorporate unique components like pontoons/floats, anchoring and mooring systems, and combiners (Figure 12) [51].

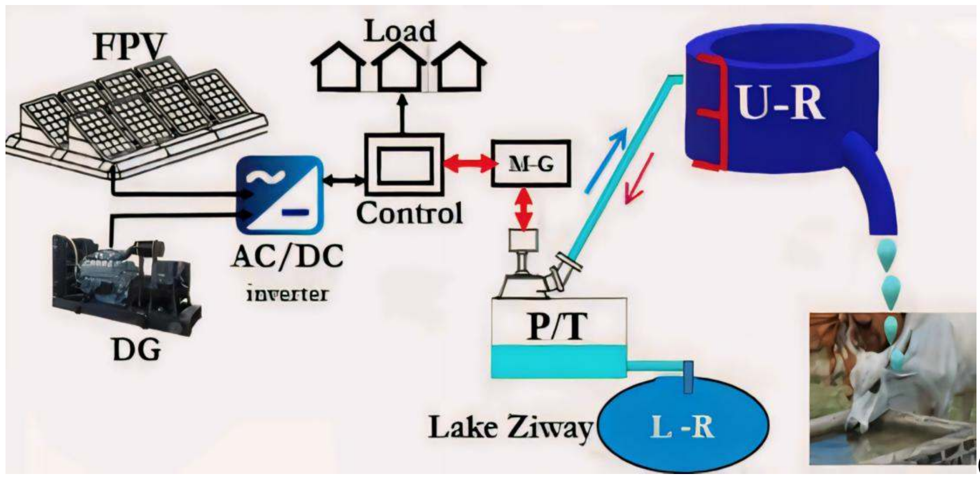

(a)

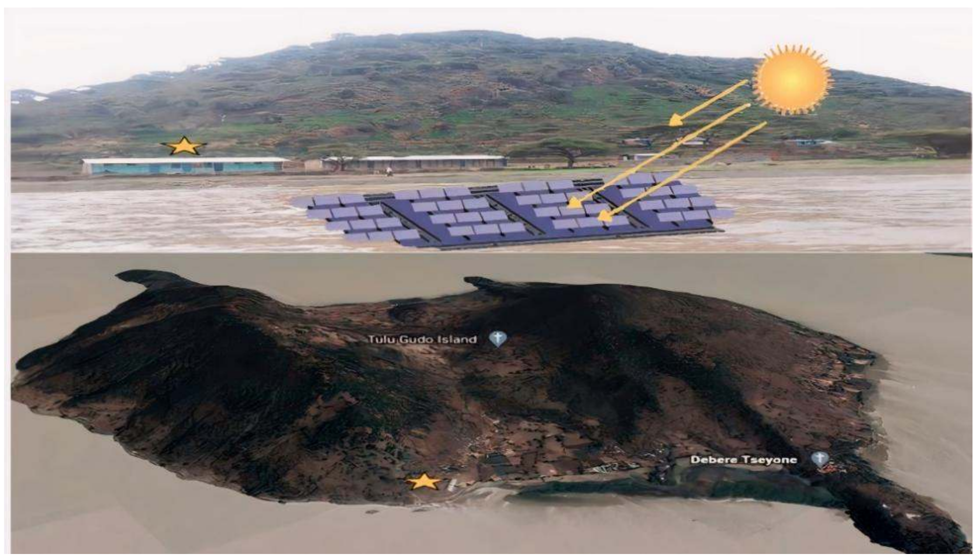

(b )

Figure 22. (a &b). Proposed hypothetical small-scale solar island electricity supply system ready for simulation and a 3D image of the case study Island with a PVsyst unit on Lake Ziway[13].

The proposed FPV-based microgrid model aims to replace the existing 45 KW diesel generator, providing a sustainable electricity source for the island community while mitigating Lake Ziway's evaporation rate. The system integrates an FPV array (modeled in PVsyst), a PHS 245 water battery component, and a 45KW CAT-45-60HZ diesel generator for backup power (Figure 21). During daylight hours, the FPV array directly supplies the load, and excess energy is used to pump water from Lake Ziway into the PHS upper reservoir. When FPV generation is insufficient due to cloud cover, low irradiance, or nighttime, the stored potential energy in the upper reservoir drives the PHS pump/turbine unit to generate electricity.

The integration of PVsyst and HOMER Pro software streamlines the design and modeling process. In PVsyst, (SPR-E20-327) 327Wp PV modules are arranged in series and parallel configurations to achieve the desired power output. The module layout, with a south-facing orientation and fixed tilt angle, is visualized in a 3D construction within HOMER Pro (Figure 14 and Figure 21(b) ) to ensure optimal solar energy capture.

### 3.9.Simulation and Optimization of the HDGEs

This section details the methodology employed to simulate and optimize the proposed hybrid microgrid systems for both the mainland and island communities in the E.C.R.V. The primary goal is to identify the optimal configuration of renewable energy sources, energy storage technologies, and diesel backup that can reliably meet the electricity demand of these communities while minimizing costs and environmental impact.

The simulations and optimizations were conducted using HOMER Pro, a widely recognized software platform designed for modeling and analyzing hybrid energy systems. HOMER Pro's comprehensive capabilities enable the evaluation of various system configurations, including different combinations of renewable energy sources, energy storage options, and diesel generators (Appendix 2 and 3). The software's built-in algorithms optimize system design based on user-defined objectives, such as minimizing the net present cost (NPC) or levelized cost of electricity (LCOE).

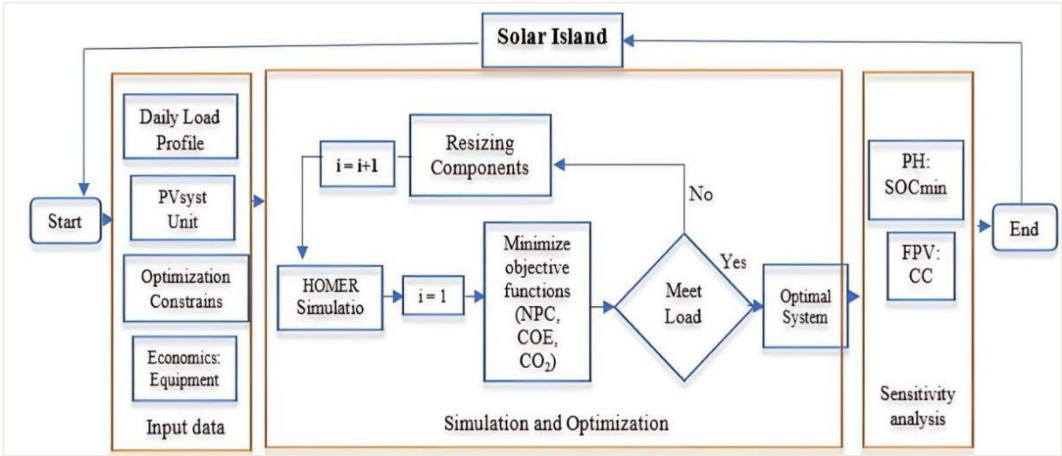


Figure 23. Simulation and Optimization flowchart.

The optimization and simulation process in this dissertation was guided by Figure 13 and Figure 22. The objective functions, as outlined in the flowchart, were used in conjunction with detailed economic modeling in Homer Pro (as described in [101] and section 3.7.2). Furthermore, sensitivity analyses were conducted to optimize the proposed system, aligning it with the (E-W-F-N) approach, as illustrated in Figure 24 and Figure 19.

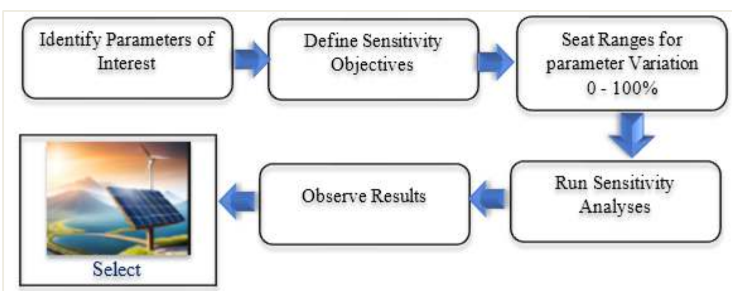


Figure 24. Sensitivity analysis procedure followed

We presented the sensitivity analysis by considering the main parameters, specifically the pumped hydro storage (PHS) minimum state of charge (SOCmin) or the water level in the upper reservoir (Figure 12), (FPV: CCM),Solar irradiance and diesel fuel price (Table 7). By varying these parameters, we assessed their impact on the system's performance and economic indicators.

Furthermore, we provided a justification for selecting sensitivity values for the floating PV capital cost multiplier (FPV: CCM) (1 and 0.5), based on the Solar Futures Study conducted by the Department of Energy. This study indicates that the cost of solar PV systems is expected to decrease in the future due to technological advancements and increased production scale (Solar Futures Study | Department of Energy).

In addition to the priority given by the Homer software to selecting the optimal system type stated in the economic modeling section, the authors go beyond this and include the SOCmin situation of the storage system as a selection metric, i.e., an optimal system type which can support the novel HDGEs design and management strategy proposed in this study and discussed in the previous section. CCs (charge following strategy) and LLs (Load following strategy) are modeled by Homer and considered in this study. The search space, constraints, and sensitivity variables given as input for homer while running the simulations is indicated in the Table 7.

Table 7. Simulation and optimization inputs

| | Search space | Sensitivity values | Constraints | Value |
|---|---|---|---|---|
| Wind speed, WTa | 0,…20 (Qty) | 4,4.5,5,5.86,5.9,6 (m/s) | Cs | 0, 5% |
| Solar (KWh/m$^2$ ), PV | 0,5,15,35,50 (KW) | 3-7 (KWh/m$^2$) | Or | 5% |
| PH: SOCmin, PHS | 0.1,2,3,4,5,8 (Qty) | 0 - 80 % | PLa | 10% |
| FPV: CCM | | 0.5,1 | | |
| CCM of PHS | | 0.5,1,1.5,2 | | |
| DGe | 0, 45KW | | WTa-out | 60% |
| Diesel cost $/L | | 0.5, 0.6, 0.7, 0.85,1,1.05 | | |
| Deferrable Load | Storage capacity:19.24 to 40 (KWh) Peak Load : 9.26,15,20 KW | | | |
| Key: Cs (capacity shortage), Or (operating reserve), PLa (Peak Load yearly) | | | PV-out | 35% |

# CHAPTER 4: RESULTS AND DISCUSSION

## 4.1. Assessment of Sustainable Energy Resources in the E.C.R.V.

This section presents the findings of the resource assessment conducted to evaluate the potential of wind, solar, and pumped hydro storage (PHS) as sustainable energy sources for electrifying the E.C.R.V. The analysis aims to quantify the available resources, identify promising locations for energy generation, and provide a foundation for the design of hybrid microgrid systems tailored to the specific conditions of the region.

### 4.1.1. Wind Energy Potential

To assess the wind energy potential of the E.C.R.V., both primary and secondary wind data were collected and analyzed. Primary data, consisting of wind speed and direction measurements, were gathered using a wind mast erected at the location indicated in Figure 6 and Figure 7. These measurements were taken at heights of 10m, 50m, and 70m above ground level for the years 2017 and 2018. For comparison, secondary wind data from the NASA database, covering the period 1978-2018, were also utilized (Figure 25).

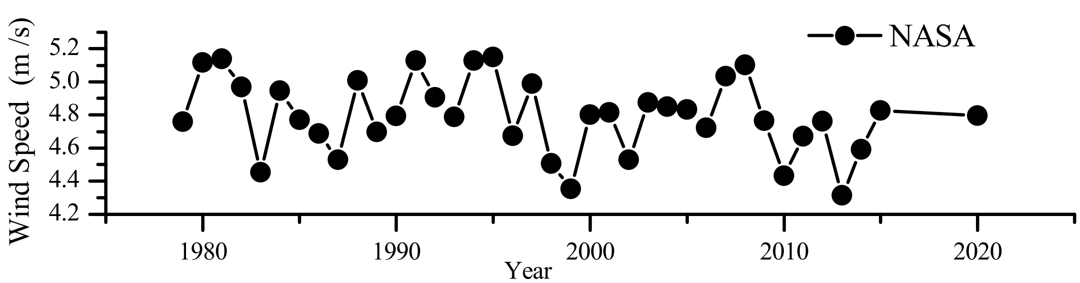


Figure 25. Time series of monthly wind speeds for the study area at 50m

The measured data were compared with the NASA data at a height of 50 meters, revealing a positive correlation with an $R^2$ value of 0.73 (Figure 26 ). This strong correlation, combined with the fact that the collected field data spans at least one year, aligns with the requirements for accurate resource assessment outlined in the literature [102-104].

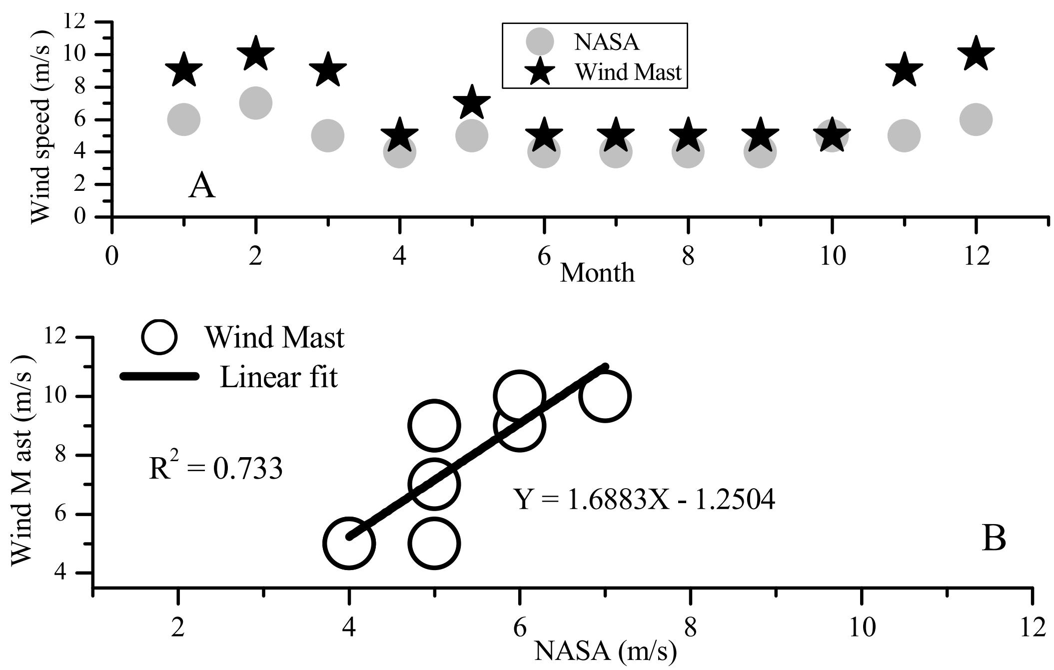


Figure 26 (A, B). Comparison of measured and data from NASA at 50m, measured VS NASA data

The results obtained here, in the opinion of the authors, should be sufficient to move the research on designing hybrid energy supply systems to the next stage, and eventually to the realization of the results as a project.

Figure 27 illustrates the fluctuation in wind speed at 70 meters over the measurement period, with the highest speeds occurring in December and January and the lowest in June, July, and August. The average wind speed at 50 meters was found to be 7 m/s, and the average power density suggests that the wind regime in the E.C.R.V falls within Class 4 of the international wind power classification. This classification, coupled with the fact that wind speeds exceed the start-up speed of typical wind turbines for over 89% of the time, indicates that wind power in the region is economically feasible and suitable for wind farm development [105].

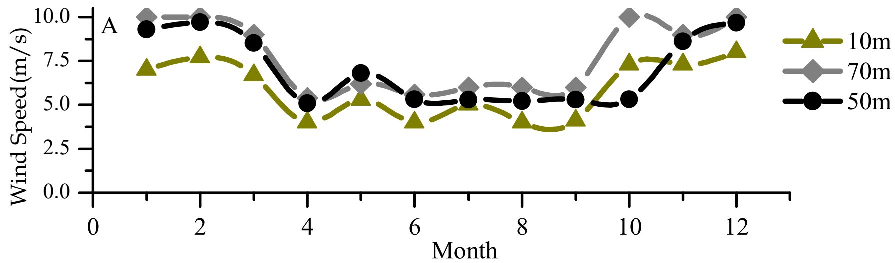

Figure 27. Monthly variation of averaged wind speed at research area (Field data, 2018)

The monthly variations in the most probable wind speed (Vmp) and the maximum energy-carrying wind speed (VmaxE) are depicted in Figure 28. These speeds range from 2.85 m/s to 9.14 m/s for Vmp and from 7.49 m/s to 13.06 m/s for VmaxE. Figure 29 further illustrates the scale factor (c) and shape factor (k) of the Weibull distribution, which were calculated using MATLAB and the least-square curve fitting method (Equation 3.3).

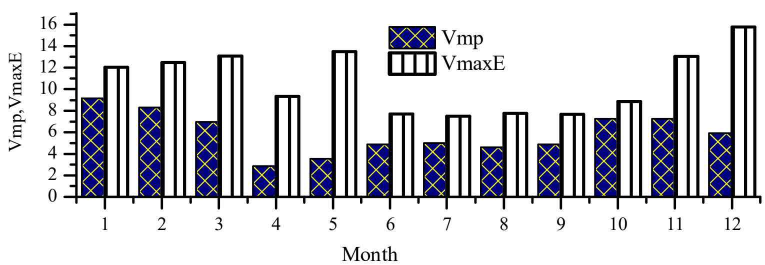

Figure 28. Monthly variation of Vmp & VmaxE

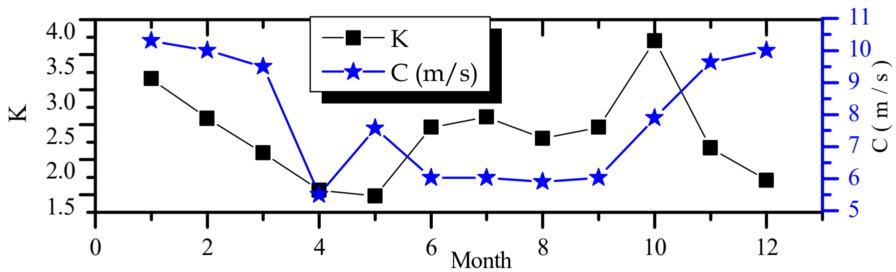

Figure 29. Scale factor and the shape factor of the study area.

The wind power density (WPD) and wind energy density (WED) were estimated using Equations 3.4-3.8. The WPD varies between 144 W/m² and 997 W/m² from July to December, with the lowest wind energy density (WED) of 107 kWh/m² recorded in July and the highest of 741.8 kWh/m² in December (Figure 30).

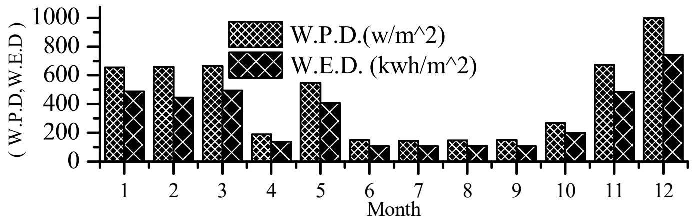


Figure 30. The power density & energy density of the study area.

The Weibull distribution of wind speeds was calculated using Equation 3.2, with F (0) = 0 and F (∞) = 1. This distribution, along with the cumulative and probability density functions, is presented in Figure 31 (A,B and C). The analysis confirms that the wind speed in the E.C.R.V. falls within the operational range (2.7 m/s to 5.86 m/s) of typical 5.1 kW and 3.3 kW wind turbines for a significant percentage of the time, further supporting the viability of wind energy in the region.

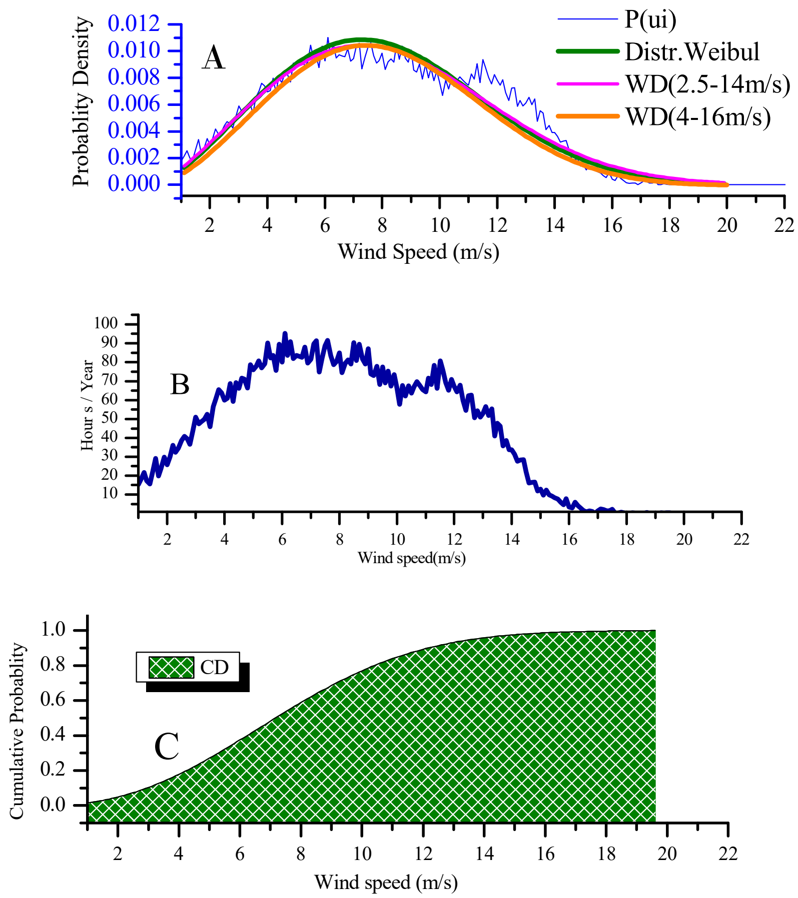


Figure 31.  A, B, & C Wind resource, cumulative distribution, and Probability Density function

#### 4.1.1.1.Implications for Wind Turbine Design and Development

The lack of reliable wind data has been a significant barrier to the advancement of small-scale wind energy technologies in many developing countries, including Ethiopia [106]. This study's rigorous collection of wind speed data at multiple heights and time intervals addresses this gap and offers several key benefits for wind turbine design and development [4]:

- **Accurate Resource Assessment:** The detailed dataset enables a more precise evaluation of the wind energy potential in the E.C.R.V., informing decisions about turbine placement and sizing.
- **Tailored Design:** The data can be used to design wind turbines that are specifically optimized for the local wind conditions, leading to improved efficiency and performance.
- **Local Manufacturing Potential:** The availability of reliable wind data could incentivize the development of local wind turbine manufacturing capabilities, reducing reliance on imported technologies and fostering economic growth.
- **Research and Development:** The dataset can serve as a valuable resource for future research on wind energy in the E.C.R.V., contributing to the advancement of knowledge and innovation in this field.

### 4.1.2. Solar Energy Potential

The solar resource potential of the E.C.R.V. was assessed using data from various sources, including PV-GIS, NASA Power, and the metronome 8 database. Additionally, locally measured sunshine hour data from five geographical coordinate points (Figure 6) were converted to their irradiance equivalent using Equations 3.11-3.16.

#### 4.1.2.1.Solar Irradiance Analysis

The solar resource assessment revealed that the E.C.R.V. is endowed with abundant solar energy (Figure 33). The monthly and hourly radiation profiles (Figure 32 A, B, C& D) demonstrate a high level of solar irradiance throughout most of the year, with a slight dip during the rainy months of July and August (Figure 31). The PVGIS 5.2, NASA Power, metronome 8, and SolarGi data showed good correlation, with an average irradiance of 6.10 kWh/m²/day, further supported by the calculated value of 6.3 kWh/m²/day.

In order to account for the lowest solar energy production periods in the E.C.R.V., the simulation employed a scaled annual average solar irradiance of 5.04 kWh/m²/day. The average temperature in the region was determined to be 21°C, with a cleanliness index of 0.6 (Figure 36).

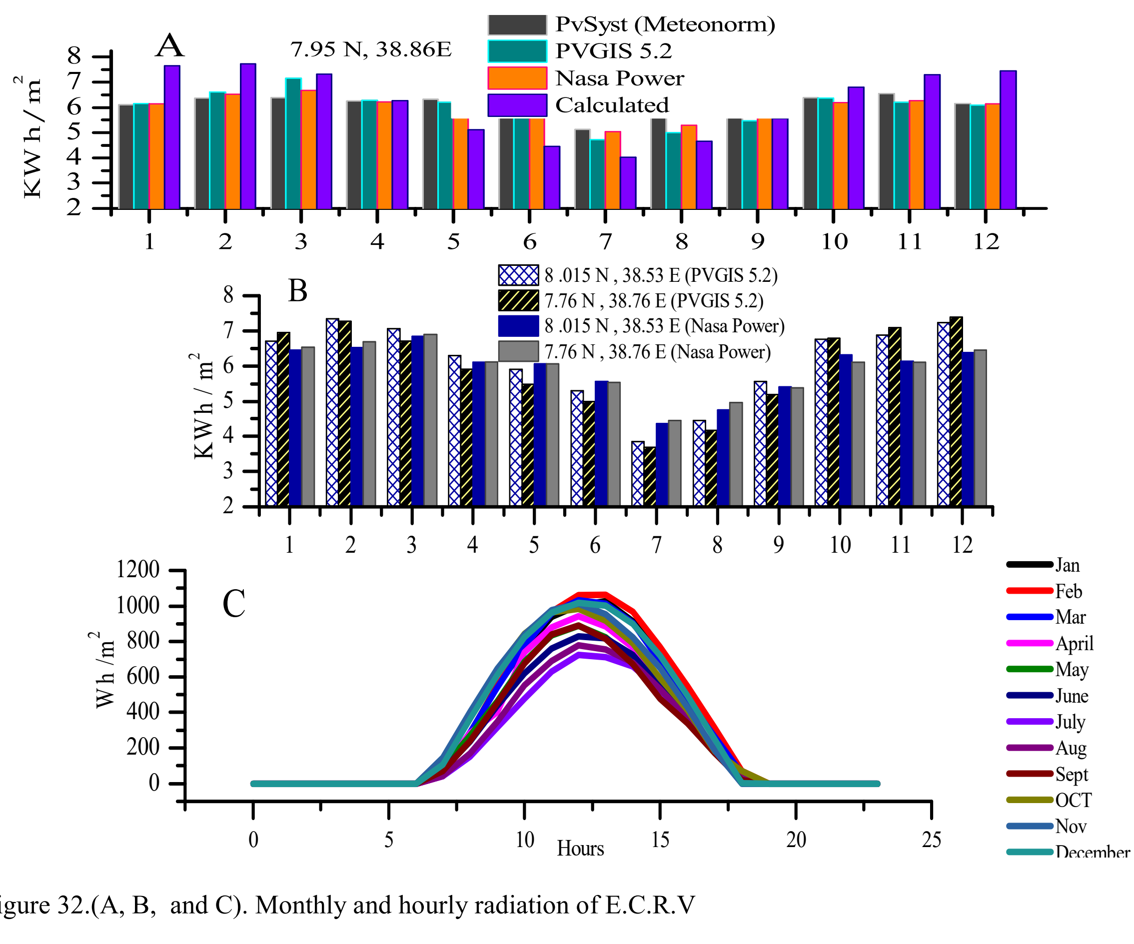


Figure 32.(A, B, and C). Monthly and hourly radiation of E.C.R.V

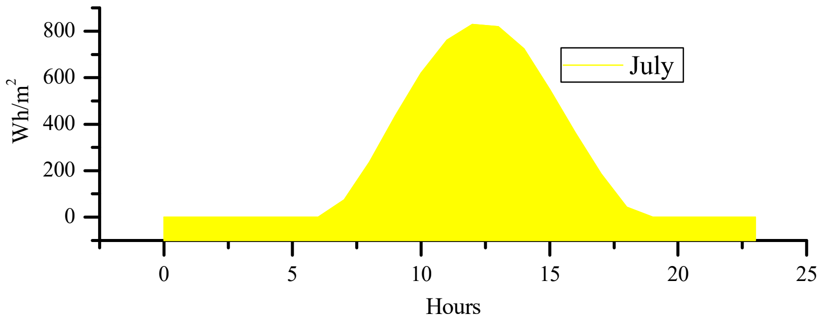

Figure 33. Daily irradiance for the worst reference day (July)

In order to account for the lowest solar energy production periods in the E.C.R.V., the simulation employed a scaled annual average solar irradiance of 5.04 kWh/m²/day. The average temperature in the region was determined to be 21°C, with a cleanliness index of 0.6 (see Figure 36).

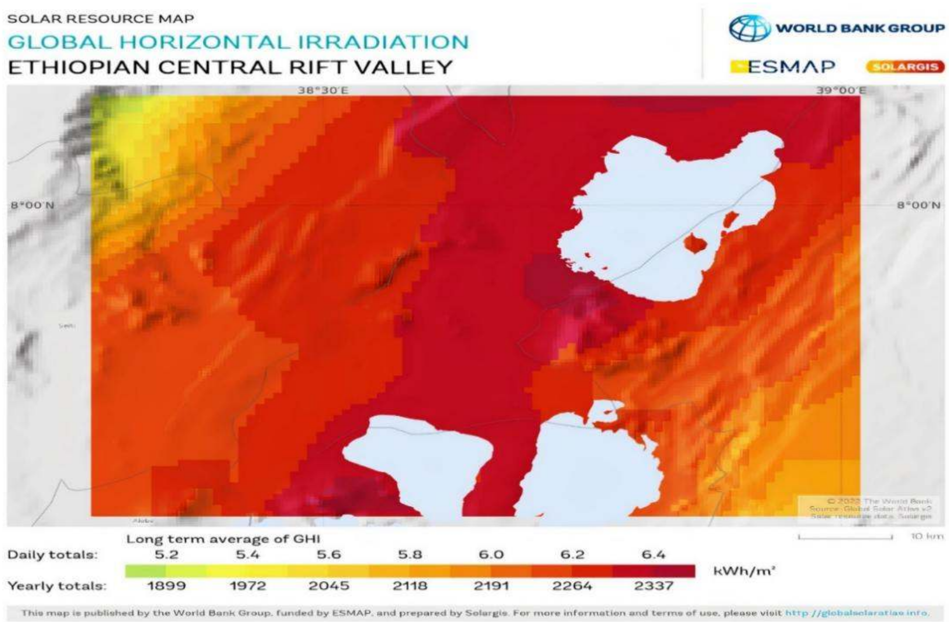


Figure 34. E.C.R.Vs Solar resource potential (July,2022): http://globalsolaratlas.info

#### 4.1.2.2.Determination of the Optimal PV panel Inclination

To optimize solar energy harvesting, the ideal tilt angle for photovoltaic (PV) modules was determined. Figure 35 illustrates the monthly average irradiation at varying tilt angles facing south. The analysis reveals that steeper angles (e.g., 25°) maximize irradiation during dry seasons when the sun is positioned to the south, while shallower angles (e.g., 5°) are more advantageous during the rainy season when the sun is positioned to the north.

A 12° tilt angle (Hopt) was found to maximize the annual average daily global radiation, ranging from 5.61 kWh/m²/day to 6 kWh/m²/day, with a peak of 6.1 kWh/m²/day. Notably, the impact of shading on energy capture is minimal at this optimal angle.

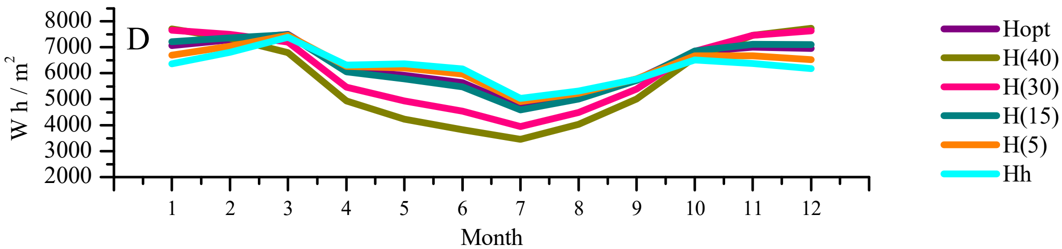


Figure 35. Monthly average irradiation at different tilt angle

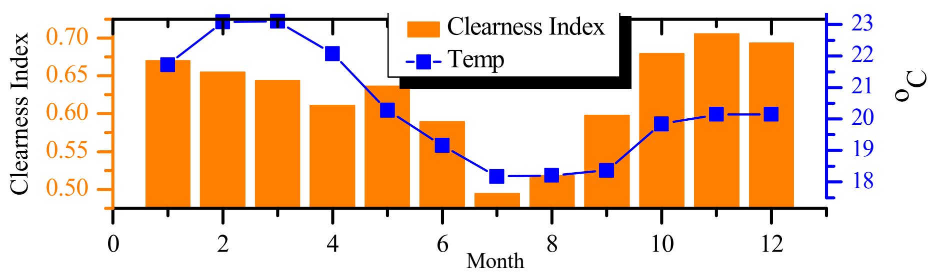


Figure 36. Temprature and Cleanness index of the E.C.R.Vs

Figure 35. demonstrates that adjusting the tilt angle of photovoltaic (PV) modules influences the amount of solar irradiation received throughout the year. Steeper angles yield higher irradiation during dry seasons (southern sun position), while shallower angles are more beneficial during rainy months (northern sun position). The average daily global radiation across a year ranges from 5.6 kWh/m²/day to 6 kWh/m²/day, peaking at 6,100 Wh/m²/day with a 12° tilt angle (Hopt). Notably, shadowing losses are negligible, indicating an efficient panel arrangement.

### 4.1.3. Pumped Hydro Storage Potential (PHSP)

The potential for pumped hydro storage (PHS), often referred to as a "water battery," was assessed for the three islands in Lake Ziway: Tulugudo, Funduro, and Tsedecha (Figure 36). A 12.5m digital elevation model (DEM) derived from Light Detection and Ranging (LiDAR) data was used to evaluate the topography and identify suitable locations for UR and LR. Selection criteria included topography, available space for an upper reservoir, elevation difference (head), proximity to the community, and relatively low slope. Figure 37 provides an aerial view of the focus area, highlighting the three islands.

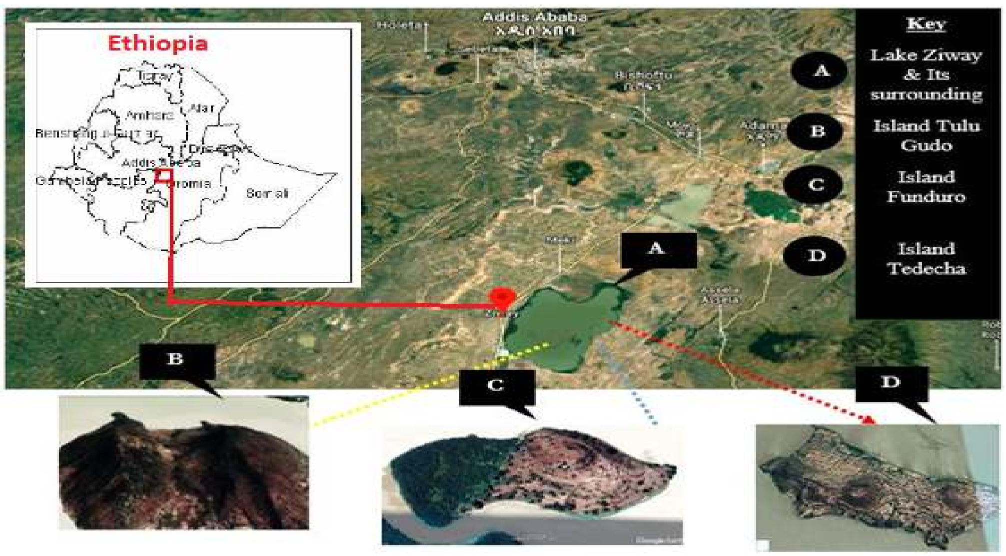


Figure 37. Potential locations for (PHS) on Lake Ziway Islands (source: Google Earth 2021)

#### 4.1.3.1. Determination of Head

Figure 38 presents a 3D visualization of the available head for each island, calculated using the LiDAR DEM. The head, or elevation difference between the upper and lower reservoirs, is a critical factor influencing the energy storage capacity and power output of a PHS system. The analysis revealed that Tulugudo Island has the highest available head (50-300 m), followed by Tedecha (50-200 m) and Funduro (50-100 m).

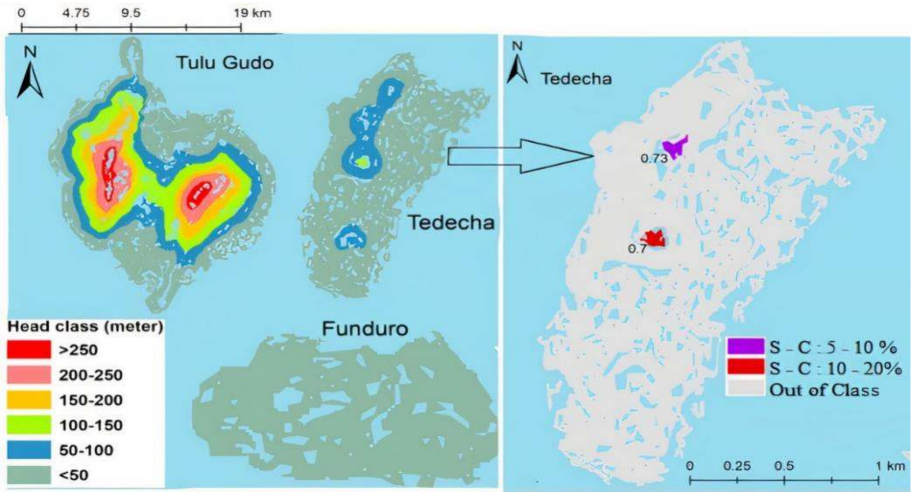


Figure 38. Head, slop class, and area (hec) of the Islands.

Given the importance of head in determining the potential energy storage capacity of PHS, Tulugudo Island initially appeared to be the most promising candidate. However, further analysis of the slope revealed that Tedecha Island offered a more suitable topography for PHS development. Tedecha's lower slope (0-10 degrees) aligns with the optimal range for PHS sites, as it provides sufficient flatness for reservoir construction while still allowing for adequate head [107]. Tulugudo Island, despite its higher head, exhibited a steeper slope, making it less ideal for PHS implementation. Funduro Island, with the lowest head and slope, was considered the third potential candidate.

To identify specific locations for upper reservoirs, areas with slopes between 0 and 30 degrees were reclassified and converted into polygon areas (Figure 39). These polygonal regions represent potential sites for upper reservoirs. For instance, one identified reservoir site on Tedecha Island has a capacity of 51,100 $m^3$ of water and a head ranging from 50 to 100 meters. Based on these parameters, a small-scale PHS system with a minimum storage capacity of 5,976 kWh could be developed, assuming a 60-meter head, a discharge time of 0.0833 hours, and a generating efficiency of 70%.

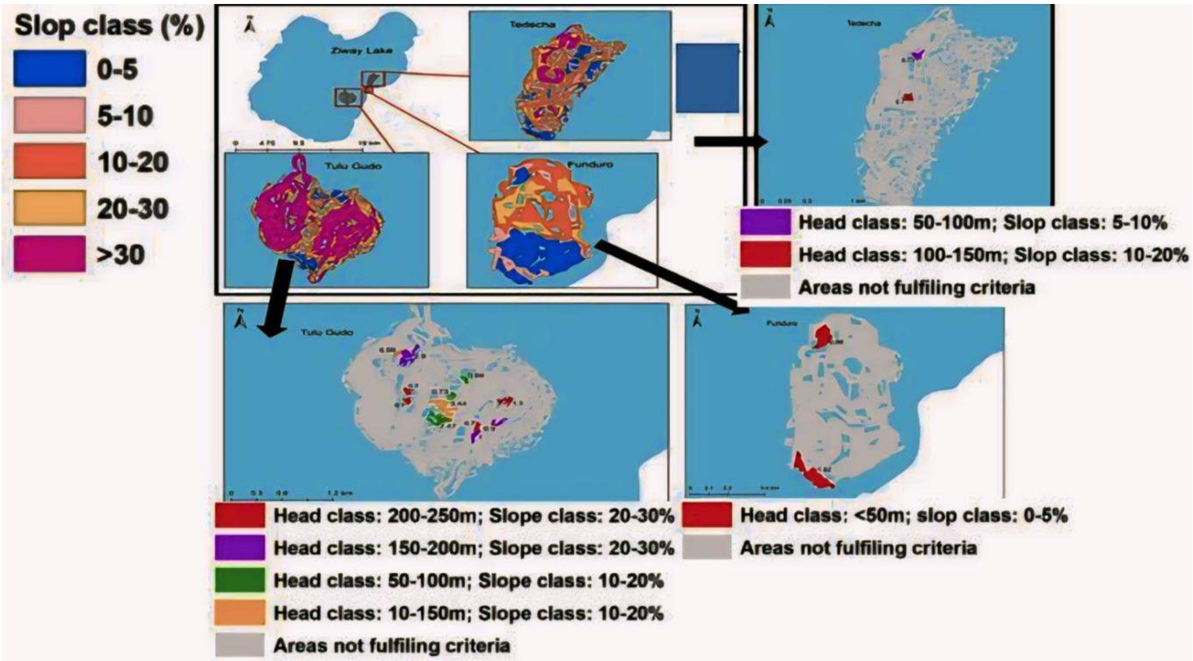


Figure 39. Slop class, area, and corresponding head according to (LiDAR, DEM,2021)

Figure 40 summarizes the PHS potential of the three islands, highlighting Tedecha as the most suitable candidate due to its combination of adequate head and favorable topography.

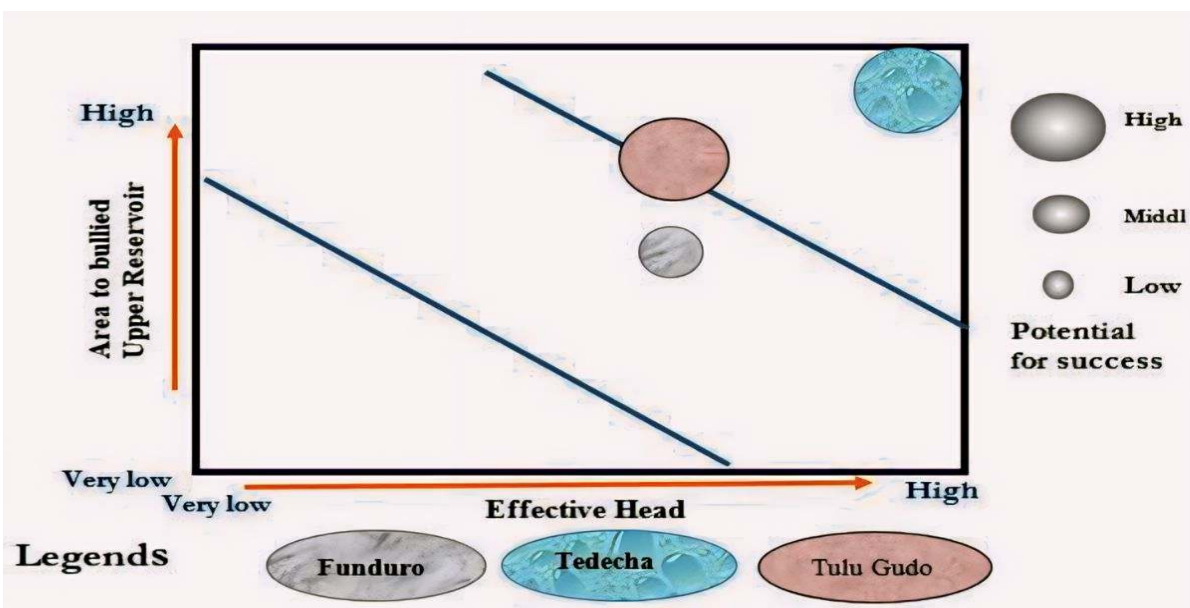


Figure 40. Pumped hydro-storage potential of the islands


Figure 41. Natural volcanic crater pond on Tedecha Island with solar PV and wind turbine .

### 4.1.4. Conclusions

The assessment of sustainable energy resources in the E.C.R.V. reveals a region endowed with significant potential for both wind and solar energy generation. The average wind speed of 7 and 7.63 m/s at 50 and 70m height, coupled with a favorable Weibull distribution, indicates a Class 4 wind regime suitable for wind farm development. The average annual solar irradiance of 6.1 kWh/m²/day further confirms the viability of solar energy utilization in the region.

Utilizing LiDAR-derived digital elevation models (DEMs) and GIS-based analysis, the PHS potential of the E.C.R.V. islands was investigated. Twelve potential upper reservoir sites were identified, with Tedecha Island emerging as the most promising candidate due to its favorable topography and head. The analysis demonstrates the feasibility of developing a small-scale PHS system with a minimum storage capacity of 5,976 kWh, leveraging the natural volcanic crater pond (see Figure 41) on Tedecha Island as an upper reservoir. This innovative approach presents a sustainable and cost-effective solution for energy storage in the region. This comprehensive resource assessment not only confirms the feasibility of harnessing renewable energy in the E.C.R.V. but also provides crucial data for informing the design and optimization of hybrid microgrid systems tailored to the specific conditions of the region. The availability of detailed wind and solar data, along with the identified PHS potential, lays a strong foundation for the subsequent development of sustainable energy solutions that can address the energy challenges faced by both mainland and island communities.

### 4.2. Load Demand Estimation and Profiling

The electricity demand for the E.C.R.V community was assessed using the end-use model from UNEP [108]. A comprehensive inventory of electrical equipment and their power ratings for 250 households and community-serving sectors was conducted (Appendix 1). This information was used to develop hourly, daily, and monthly load profiles (Figure 41 and 42), providing a nuanced understanding of the community's energy consumption patterns.

To capture the diverse nature of energy usage and account for future load growth, the load profile was categorized into two distinct types: primary and deferrable loads. This distinction allows for more accurate modeling and optimization of the microgrid system.

1. **Primary Load:** This encompasses essential and non-negotiable electricity demands, primarily driven by household appliances, lighting, and critical community services. The annual average primary load was estimated to be 136.76 kWh/day, totaling 49,917.4 kWh/year.
2. **Deferrable Load:** This category includes flexible loads that can be shifted or delayed to periods of excess energy generation, primarily associated with vegetable irrigation in this study. Each household equipped with a 0.37 kW electric pump (Figure 41) is estimated to consume 19.24 kWh/day for irrigation. With 10.4% of the 250 households (26 households) (see in the Appendix 1) utilizing irrigation pumps, the total annual deferrable load for irrigation is estimated to be 7,022.2 kWh/year. To enhance energy efficiency and reduce

reliance on diesel fuel, the study proposes replacing traditional diesel irrigation pumps with more efficient electric pumps (Figure 41).

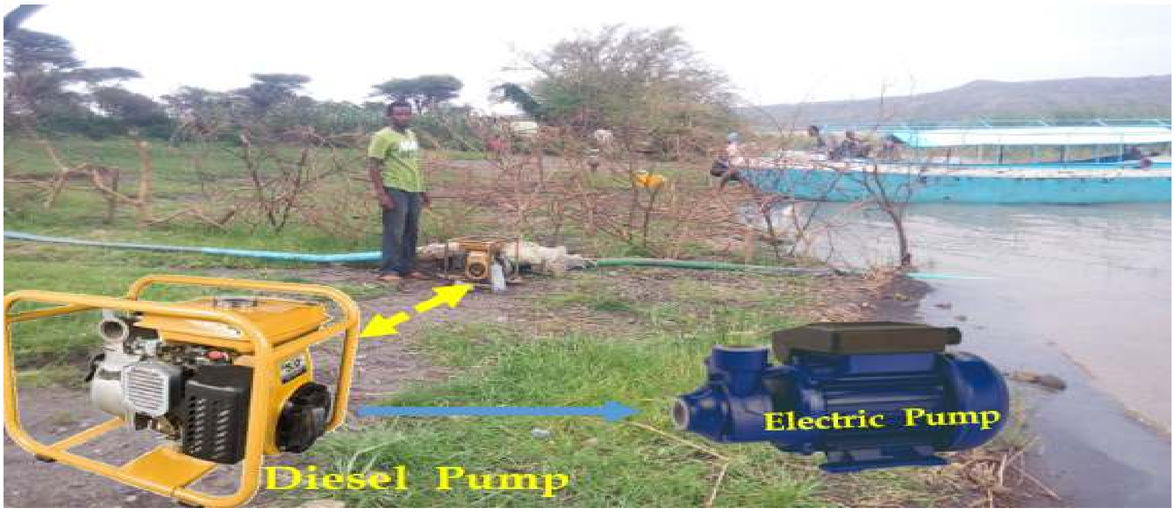


Figure 42. Farmer with diesel irrigation Pump and electric pump equivalent.

#### 4.2.1. Hourly, and Seasonal Load Profiles

Figure 43 illustrates the hourly electricity demand profile for the island, combining both primary and deferrable loads. This aggregated profile reveals a peak demand of 26.58 kW, typically occurring when both load types coincide. The average daily consumption, considering both primary and deferrable loads, is 156 kWh. To account for real-world fluctuations, a daily inconsistency of 20% and a 15% variability in time steps were incorporated into the model, resulting in an annual energy consumption of 56,940 kWh.

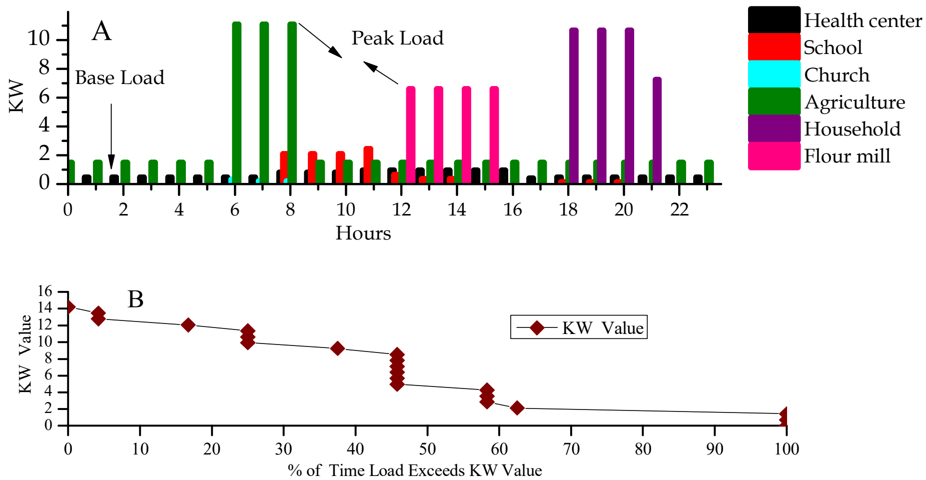


Figure 43. Hourly electricity requirement of the community and Load-duration curve

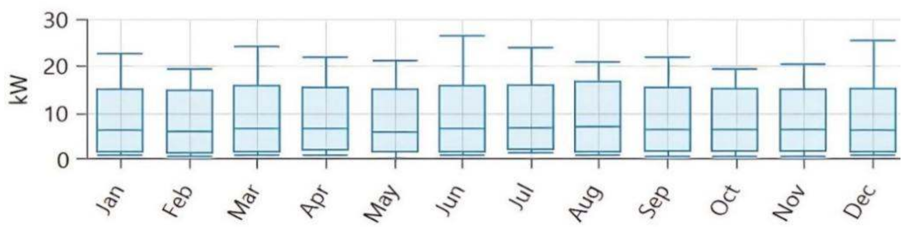


Figure 44. Monthly Load profile

The monthly load profile Figure 44 demonstrates the combined primary and deferrable load throughout the year. The slight increase in certain months reflects the seasonal variation in irrigation demand. To accommodate both current and future energy needs, the deferrable load was analyzed separately, resulting in a total annual deferrable load from irrigation of 7,022.2 kWh. This figure aligns with the difference between the total annual load (56,940 kWh) and the annual primary load (49,917.4 kWh), validating the accuracy of the load estimation.

### 4.3. Design and Evaluation of HDGEs for the E.C.R.V.

#### 4.3.1. Simulation and Optimization Results

This section assesses the performance of hybrid decentralized green energy systems (HDGEs) utilizing various energy storage technologies within proposed microgrid (MiG) configurations. The MiGs integrate power sources like photovoltaic (PVs) panels, wind turbines (WTa), and diesel generators (DGe) with energy storage options such as PHS, (Lib), and (Lab) batteries. Multiple simulation batches were conducted in HOMER Pro software based on the MiG configurations detailed in Figure 21 and as detailed in the (Appendix 2) . Initial simulations focused on three configurations: WTa-PVs-DGe with PHS, WTa-PVs-DGe with Lib, and WTa-PVs-DGe with Lab.

**Initial Simulations and Comparative Analysis**

Initial simulations were conducted using HOMER Pro software, focusing on three configurations:

- WTa-PVs-DGe with PHS
- WTa-PVs-DGe with Lib
- WTa-PVs-DGe with Lab

Using HOMER Pro software, the investigation involved multiple simulation batches based on the microgrid configurations shown in and further detailed in Figure 21 and Appendix 2. The objective was to identify the optimal system for each storage scenario, considering factors such as net present cost (NPC), levelized cost of electricity (LCOE), (RF), and the capacity to support the Energy-Water-Food Nexus (E-W-F-N).

Figure 45(a) and
Table **8** illustrate the results of the first scenario (WTa-PVs-DGe with PHS), where the most optimal system comprises 41 kW of PVs, one PHS unit (245 kWh), and a 19.1 kW converter, operating with cycle charging (CC). This system's LCOE ranges from $0.0677 to $0.151 / kWh, and the NPC is between $63,381 and $159,657, well within both the proposed (MiGs) tariff for Ethiopia and the new on-grid tariff reform (Figure 46 and Figure 47). Notably, this configuration achieves a 100% renewable energy fraction and effectively manages a 13.2% deferrable load.

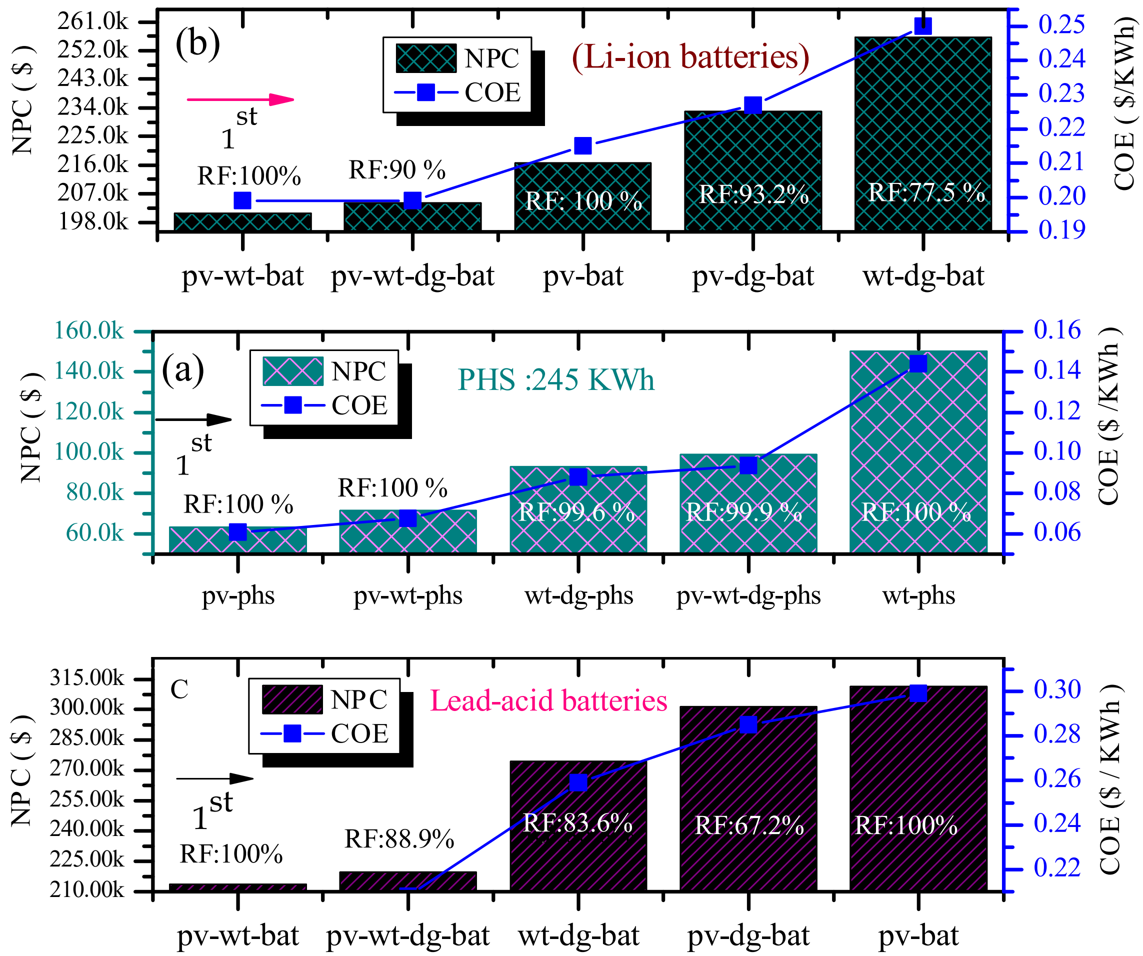


Figure 45. Optimal hybrid (MGi) Configurations for different Storage Scenarios: (a) PVs-WTa-DGe-PHS (b) PV-WT-DGe-Lib (c) PV-WTa-DGe-Lab

Figure 45(b),(c) and Table 9 show the results for the scenarios incorporating electrochemical storage (Lib and Lab). For Lib, the most optimal system (1st) combines 20.4 kW WTa, 35.8 kW PV, and 72 Lib batteries, resulting in an NPC ranging from \$198,738 to \$245,915 and an LCOE ranging from \$0.190/kWh to \$0.232/kWh. This configuration also achieves 93.2-100% RF and serves 13.2% deferrable load. However, for the Lab scenario, the optimal system is less cost-effective compared to the proposed tariff (Figure 46 and Figure 47), with NPC and LCOE ranging from \$213,533 to \$311,359 and \$0.208/kWh to \$0.3/kWh, respectively. The most optimal system (1st) comprises 27.9 kW PV, 30.6 kW WTa, and 118 Lab batteries and serves a similar 13.2% deferrable load.

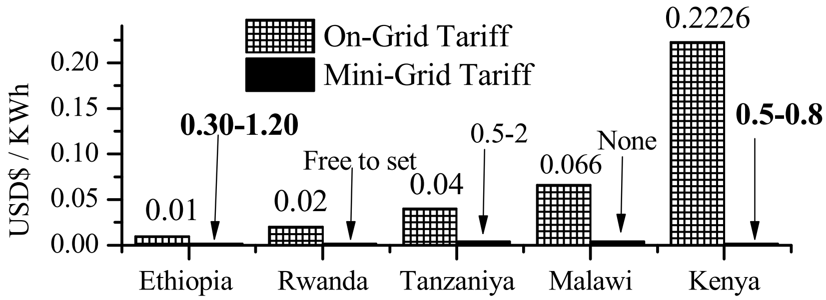


Figure 46. Comparison of On-Grid and proposed mini-Grid Electricity tariffs in selected East African Countries (USD$/kWh) [109].

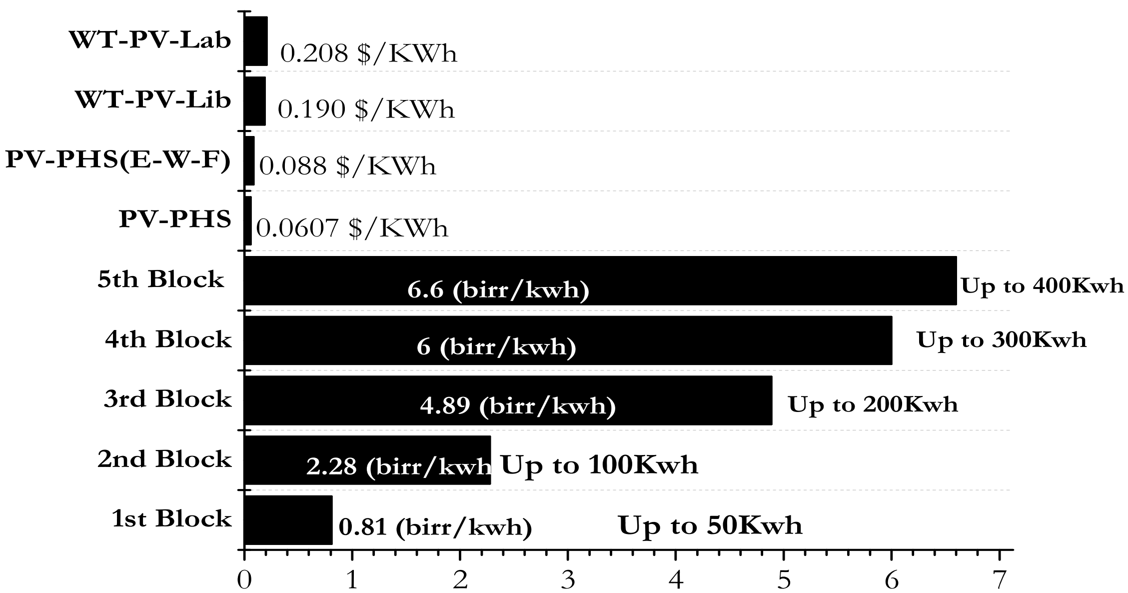


Figure 47. Comparison of On-Grid and proposed mini-Grid in light of the new tariff reform[15]and [110].

Table 8. Economic, technical and performance indicators of optimal hybrid (MiGs) for the Island Community

| Main category | Technology specification | unit | Smart hybrid system configuration /group(G) | | | | | |
|---|---|---|---|---|---|---|---|---|
| | | | G- 1 | G-2 | G- 3 | G-4 | G-5 | G-6 |
| HESS architecture | Wind turbine (AWS5.1KW) | KW | 0 | 5.1 | - | 56.1 | 11 | 40.8 |
| | PH 245(Pumped hydro) | KWh | 254 | 254 | 508 | 508 | 254 | 254 |
| | CS6K_259(Solar energy gen) | KW | 41 | 37.3 | 41.2 | 36.8 | - | - |
| | CAT-45(Diesel gen) | KW | - | - | 45 | 45 | - | 45 |
| | Power Converter | KW | 19.1 | 18.9 | 26.8 | 27.1 | 15.5 | 19.4 |
| | Dispatch strategy | (CC, LF) | CC | CC | LF | LF | CC | LF |
| Cost | LCOE (Cost of energy) | $/KW-h | 0.0607 | 0.0677 | 0.0880 | 0.0937 | 0.144 | 0.151 |
| | NPC | $ | 63,381 | 71,381 | 93,195 | 99,264 | 150,354 | 159,657 |
| MiGs components and performance indicators | AWS5.1KW | KW-h/Year | - | 11,564 | - | 11,567 | 127,253 | 92,534 |
| | CS6K_259 | KW-h/Year | 64,704 | 58,880 | 65,124 | 58,040 | - | - |
| | Diesel gen | KW-h/Year | - | - | 214 | 56.3 | - | 4,085 |
| | Net power production | KW-h/Year | 64,704 | 70,447 | 65,338 | 69,663 | 127,253 | 96,620 |
| | AC (Primary Load Consumption) | KW-h/Year | 45,775 | 46,251 | 46,497 | 46,497 | 45,732 | 46,497 |
| | Capacity shortage | % | 5.02 | 2.45 | 0 | 0 | 5.04 | 0 |
| | Unmet electrical load | % | 1.41 | 0.460 | 0 | 0 | 1.50 | 0 |
| | Excess energy generation | % | 8 | 16.4 | 7.53 | 15 | 55.9 | 41.0 |
| Capacity factor | Wind turbine (AWS5.1KW) | % | - | 25.9 | - | 25.9 | 25.9 | 25.9 |
| | CS6K_259 (PV array) | % | 18.0 | 18.0 | 18.0 | 18.0 | - | - |
| | Diesel gen | % | - | - | 0.0542 | 0.0143 | - | 1.04 |

Table 9. Economic, technical and performance indicators of optimal hybrid (MiGs) for the Mainland community

| Main category | Technology specification | unit | Smart hybrid system configuration /group(G) — Mainland Community Electricity options (G1 to G4) | | | |
|---|---|---|---|---|---|---|
| | | | G- 1 | G-2 | G- 3 | G-4 |
| HESS architecture | WTa (AWS5.1KW) | KW | 20.4 | 20.4 | - | - |
| | Lib (battery) | KWh | 72 | 36 | 98 | 94 |
| | CS6K_259(Solar energy gen) | KW | 35.8 | 23.1 | 63.4 | 52.0 |
| | CAT-45(Diesel gen) | KW | - | 45 | - | 45 |
| | Power Converter | KW | 23.9 | 19.2 | 27.5 | 22.2 |
| | Dispatch strategy | (CC, LF) | CC | LF | CC | LF |
| Cost | LCOE (Cost of energy) | $/KW-h | 0.190 | 0.188 | 0.211 | 0.223 |
| | NPC | $ | 198,738 | 199,410 | 219,785 | 236,448 |
| MiGs components and performance indicators | AWS5.1KW | KW-h/Year | 46,267 | 46,267 | - | - |
| | CS6K_259 | KW-h/Year | 56,526 | 36,435 | 100,116 | 82,071 |
| | Diesel gen | KW-h/Year | - | 7,207 | - | 3;329 |
| | Net power production | KW-h/Year | 102,793 | 89,909 | 100,116 | 85,400 |
| | AC (Primary Load Consumption) | KW-h/Year | 45,814 | 46,467 | 45,690 | 46,497 |
| | Capacity shortage | % | 5.09 | 0 | 5.08 | 0 |
| | Unmet electrical load | % | 1.31 | 0 | 1.50 | 0 |
| | Excess energy generation | % | 46.8 | 38.9 | 43.7 | 33.2 |
| Capacity factor | Wind turbine (AWS5.1KW) | % | 25.9 | 25.9 | - | - |
| | CS6K_259 (PV array) | % | 18.0 | 18.0 | 18.0 | 18.0 |
| | Diesel gen | % | - | 1.83 | - | 0.844 |

#### 4.3.1.1. Component Cost Analysis

Figure 48 illustrates the percentage share of component costs within the total NPC for the optimal system types in each scenario. The battery component emerges as the most significant contributor to the project cost, accounting for 56.18% in the (Lib) - scenario and 52.7% in the (Lab)-scenario. Notably, the lead-acid scenario exhibits higher operation and maintenance (O&M) costs. Solar PV also plays a substantial role, contributing between 11.93% and 58.17%, while WTa contribute 22.9% to 32.4% across scenarios.

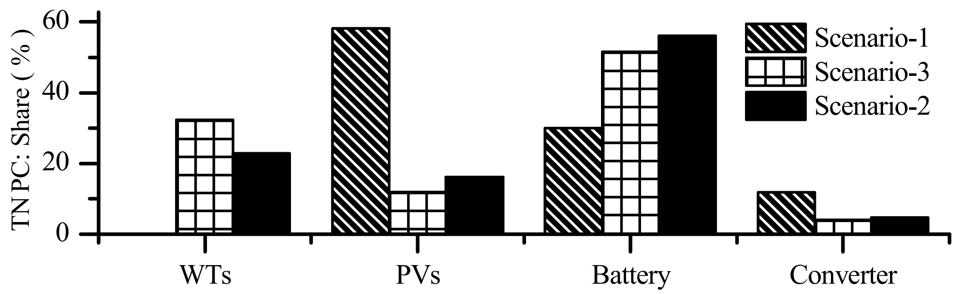


Figure 48. Cost breakdown of components in optimal hybrid MiGs

It's important to note that the specific cost difference between the two technologies can vary depending on the project's scale, location, and specific operating conditions. Therefore, a detailed techno-economic analysis is always recommended to assess the most suitable battery technology for a given microgrid project. The simulation results obtained for the lithium-ion (Li-ion) and lead-acid (Lab) battery-based microgrid configurations (Figure 45(b & c) andTable 9) are consistent with the findings reported in the literature [88] . As observed in Figure 45 (c), the Lab scenario resulted in a higher range of net present cost (NPC) and levelized cost of electricity (LCOE) compared to the Lib scenario, ranging from $213,533 to $311,359 and $0.208/kWh to $0.3/kWh, respectively. This aligns with previous research demonstrating that lead-acid batteries, while potentially cheaper upfront, tend to be less cost-effective in the long run due to their shorter lifespan, lower efficiency, and higher maintenance requirements compared to Li-ion batteries [88].

The simulation results underscore that, with the exception of the initial two optimal systems, microgrids utilizing lead-acid batteries are not economically viable within the proposed Ethiopian microgrid tariff structure. This finding aligns with existing research, emphasizing the need for careful consideration of the long-term costs and benefits of different battery technologies when designing rural electrification projects.

#### 4.3.1.2. Detailed Analysis of Optimal System (G-1) for the Island Community

The PV-WT-DGe-PHS system, designated as G-1 in Table 7, was chosen for in-depth analysis due to its superior performance in cost-effectiveness (COE), renewable energy utilization (RF), and potential to support the (E-W-F-N) approach (Figure 21). This system, which generates 64,704 kWh/year entirely from (CS6K-295MS, Figure 49), exhibits a capacity factor of 18.1 percent.

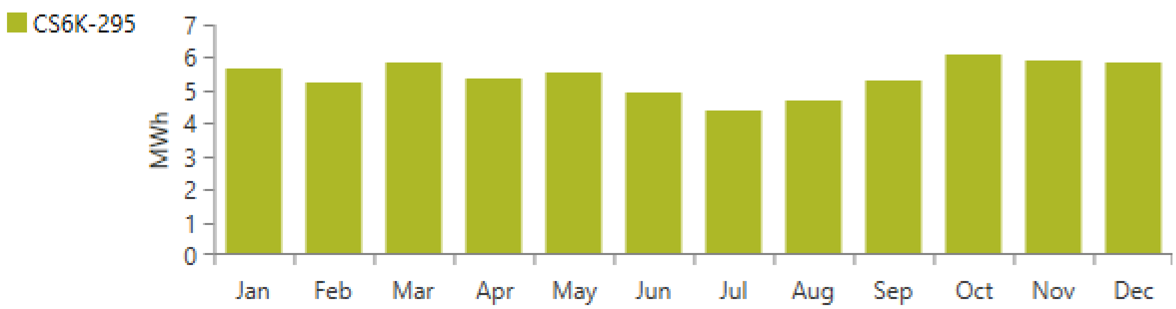


Figure 49. Electricity generation of the optimal system type

This efficiency is attributed to low levels of excess energy production (8%) and unmet system load (5, 1.4 % for the unmet load and capacity shortage). Figure 49 provides further insight into G-1's technical performance by depicting electricity generation, PHS input power, upper reservoir (UR) level, and load demand over a simulated year and for a specific day in August with challenging conditions.

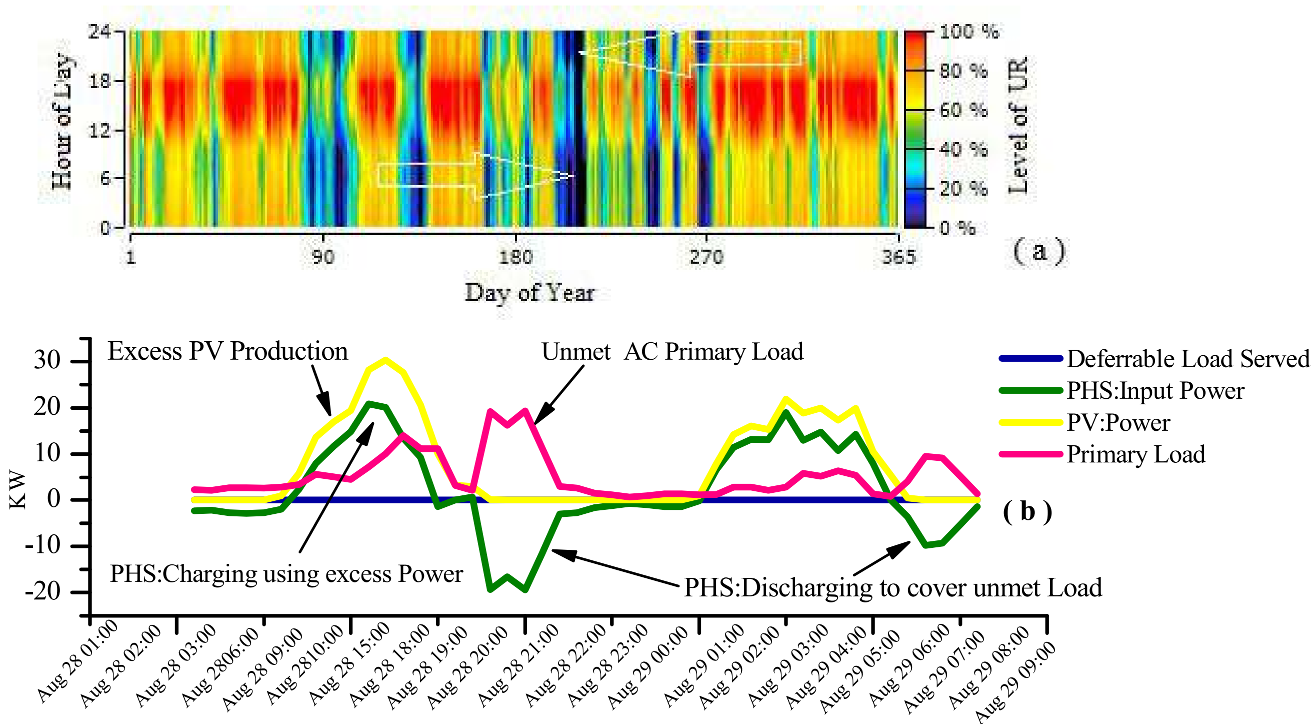


Figure 50 (a**&**b)**.** Proposed microgrid Performance under cloudy conditions (PHS-SOCmin), hourly analysis for a representative day in August.

As shown in Figure 49(b), when solar PV production is insufficient, the PHS system steps in to meet the energy demand, as evidenced by the mirroring patterns of the unmet primary load (olive) and PHS input power. The positive and negative values of energy output signify the PHS charging and discharging processes, respectively. To thoroughly analyze the microgrid's (MiGs) performance, various aspects were examined, including Photovoltaics generation, pumped hydro storage input power, total load served, and PHS minimum state of charge (SOCmin) over a week in March (Figure 50), as well as during the design reference month (Figure 51).

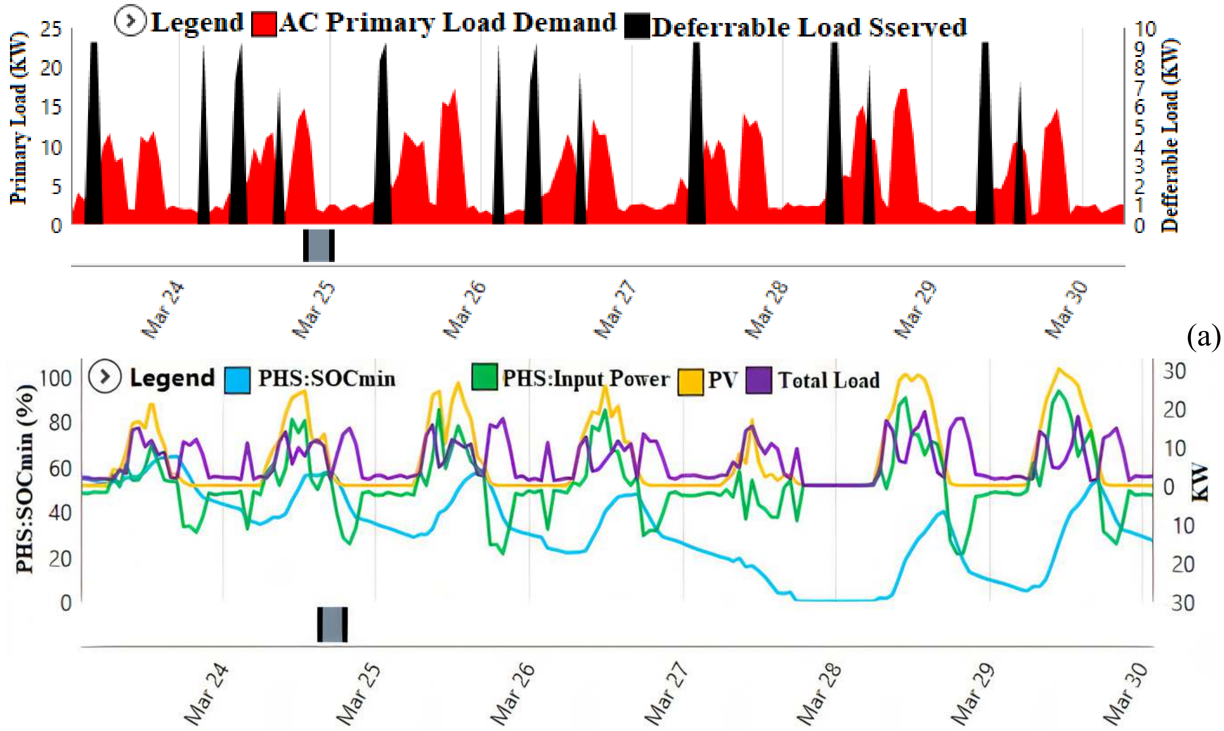


(b)

Figure 51(a and b). MiGs operation during one week in March: interactions between loads served (Primary and deferrable), PV generation, PHS input power, and SOCmin.

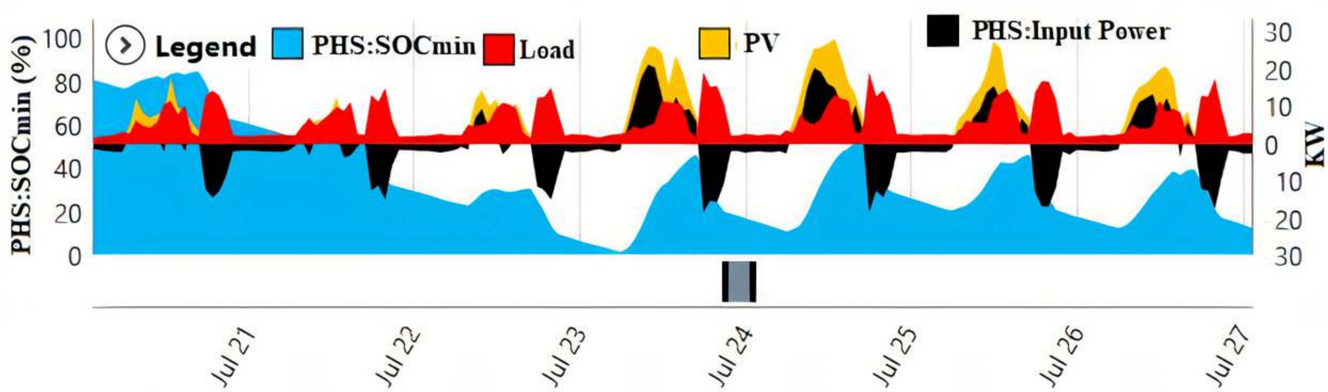


Figure 52. Proposed (MiGs) performance for the worst scenario month July

The analysis revealed that the system effectively supplemented the PV system during cloudy and rainy periods in March, specifically from the 28th to the 30th. However, in July, as depicted in

Figure 49(a), the upper reservoir level reached 0% from the 23rd to the 26th , leading to a shortfall in solar PV production and necessitating PHS to take over the load supply (Figure 52).

#### 4.3.1.3. Sensitivity Analysis and E-W-F-N Integration Potential

Given the inherent uncertainties in meteorological variables, climatic conditions, and human requirements, sensitivity analysis is crucial for robust microgrid design [111]. This study emphasizes the importance of sensitivity analysis, incorporating on-site measured wind data, multi-source solar radiation data, and actual load and economic indicators to ensure accurate and reliable results.

The sensitivity analysis investigates the impact of independent variables, such as solar irradiance, wind speed, PHS minimum state of charge (SOCmin), and load, on the designed system's performance (Table 10). This analysis not only assesses the system's robustness to variations in these parameters but also evaluates the potential for integrating an innovative energy-water-food nexus (E-W-F-N) microgrid management strategy, as illustrated in Figure 53.

Table 10 reveals that varying the PHS SOCmin, representing the minimum water level in the upper reservoir, does not significantly affect the unmet load or capacity shortage of the system. However, increasing the SOCmin does lead to higher levelized cost of electricity (LCOE) and net present cost (NPC) due to increased pumping energy requirements.

Importantly, the analysis demonstrates that even at higher SOCmin levels (up to 75%), the resulting LCOE remains within acceptable limits ($0.0882/kWh).

Table 10. Sensitivity analysis for different range of radiation and SOCmin level

| Solar ($KWh/m^2$) | Variables | | | | | |
|---|---|---|---|---|---|---|
| | PHS:SOCmin (%) | LCOE($) | NPC($) | Unmet load (%) | Capacity shortage (%) | Mass of ($H_2O$) at UR |
| | 0 | 0.0753 | 78,586 | 1.44 | 4.97 | |
| | 15 | 0.0771 | 80,495 | 1.37 | 5.10 | |
| (3.5) | 25 | 0.0803 | 82,225 | 1.43 | 5.02 | |
| | 35 | 0.0813 | 84,810 | 1.50 | 5.06 | |
| | 50 | 0.0885 | 92,351 | 1.40 | 5.08 | |
| | 55 | 0.0943 | 98,502 | 1.41 | 5.08 | 0 Kg |
| | 75 | 0.106 | 110,779 | 1.65 | 5.09 | 150,000 Kg |
| | 0 | 0.0692 | 72,254 | 1.47 | 5.04 | 350,000 Kg |
| | 15 | 0.0711 | 74,275 | 1.37 | 5.03 | 250,000 Kg |
| | 25 | 0.0725 | 75,659 | 1.45 | 5.09 | 500,000 Kg |
| (4) | 35 | 0.0745 | 77,743 | 1.50 | 5.05 | 550,000 Kg |
| | 50 | 0.0822 | 85,786 | 1.40 | 5.08 | 750,000 Kg |
| | 55 | 0.0850 | 88,723 | 1.42 | 5.09 | |
| | 75 | 0.0990 | 103,016 | 1.75 | 5.07 | |
| | 0 | 0.0607 | 63,381 | 1.41 | 5.02 | |
| | 15 | 0.0624 | 65,178 | 1.39 | 5.04 | |
| | 25 | 0.0634 | 66,107 | 1.46 | 5.09 | |
| (5.04) | 35 | 0.0650 | 67,771 | 1.50 | 5.07 | |
| | 50 | 0.0719 | 75,091 | 1.38 | 5.10 | |
| | 55 | 0.0754 | 78,731 | 1.40 | 5.08 | |
| | 75 | 0.0882 | 91,916 | 1.63 | 5.06 | |

while yielding a substantial surplus of 750,000 kg of water. This surplus water can be effectively utilized for various household activities, livestock watering, micro-irrigation, and sanitation, aligning with the E-W-F-N concept of resource optimization.

Figure 53 provides further insight into the optimal microgrid configuration under varying solar irradiance and PHS SOCmin. It reveals that for lower solar irradiance (3-4.2 kWh/m²/day), the PV-WTa-PHS system is preferred across all SOCmin values. However, for higher solar irradiance (4.8-6 kWh/m²/day), the PV-PHS system becomes more favorable, especially at higher SOCmin levels. This shift is influenced by the decrease in PHS autonomy hours as solar irradiance increases.

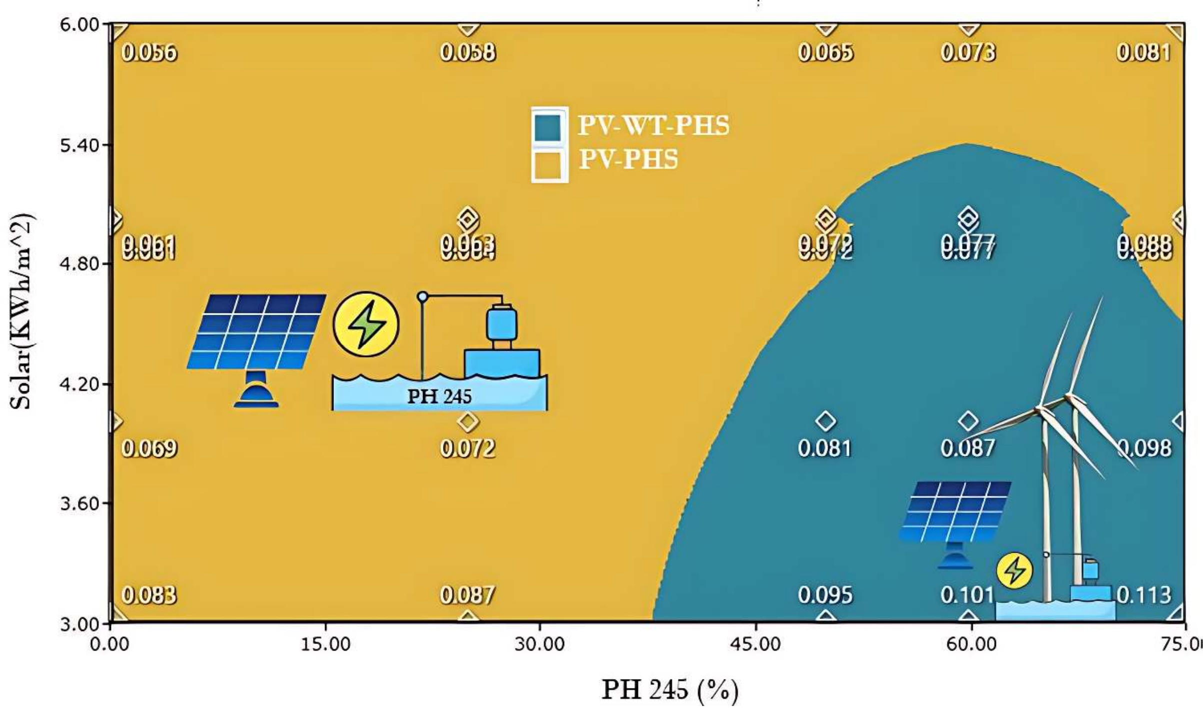


Figure 53. Optimal MiGs type for a fixed wind speed of 5.86m/s, radiations, and % of PHS: SOCmin

#### 4.3.1.4. Analysis of Optimal System (G-1 and G-2) for the Mainland Community

The simulation and optimization results for the mainland community revealed six optimal systems (G1-G6: see, Table 9), two of the configurations: G1 (PV-WTa-Lib, CC) and G2 (PV-WTa-Lib-DGe, LF) found to be promising. G1, operating under cycle charging, boasts the lowest levelized cost of electricity (LCOE) of \$0.190/kWh and the lowest net present cost (NPC) of \$198,738, highlighting its economic advantage. It achieves a 100% renewable energy fraction (RF), relying solely on solar PV and wind energy, but experiences a 5.09% capacity shortage and 1.31% unmet load, indicating potential for occasional outages. In contrast, G2, operating under load following with the inclusion of a diesel generator (DGe), offers superior reliability with no capacity shortage or unmet load, albeit at a relative LCOE of $0.188/kWh and NPC of $199,410. While G2 also achieves a 100% RF when the DGe is not running, its operation incurs a minimal environmental impact due to diesel emissions. Furthermore, the absence of a diesel generator in G1 simplifies the system, reducing maintenance requirements and contributing to long-term cost savings. Therefore, G1 presents a more sustainable and environmentally friendly option for the mainland community, aligning with the region's need for clean and affordable energy solutions.

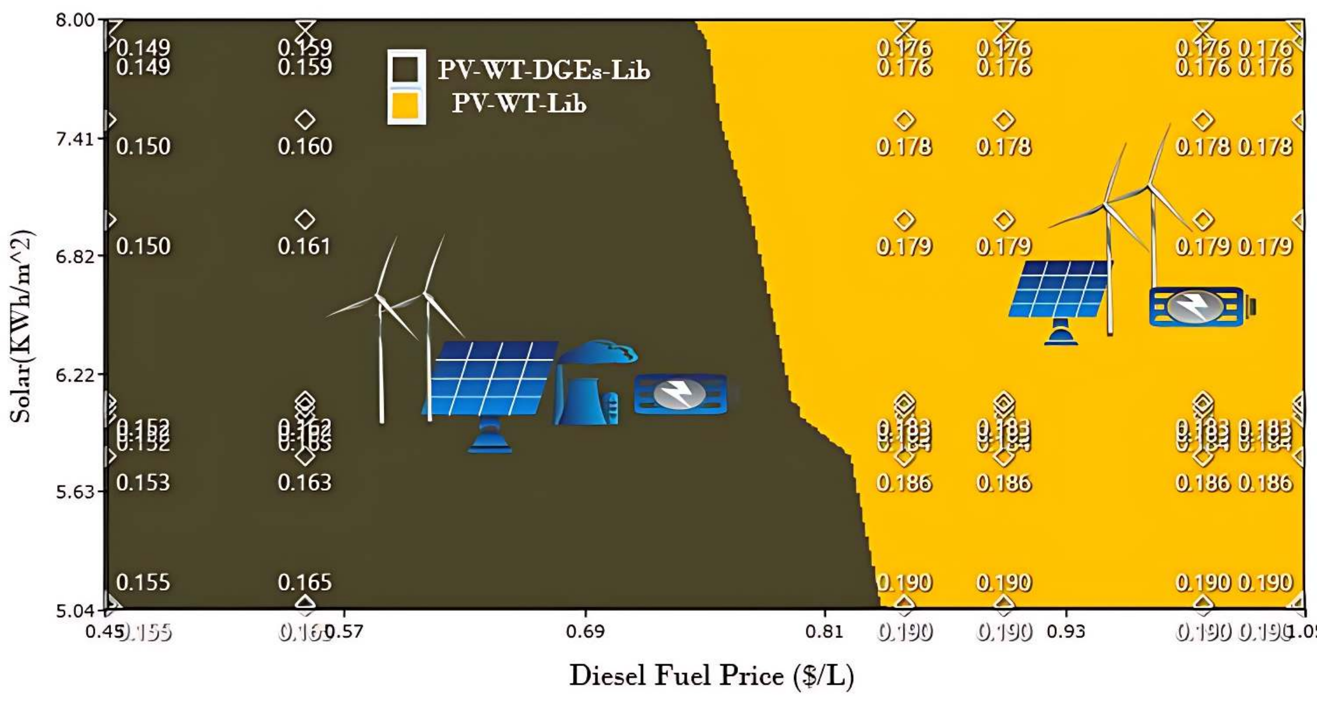


Figure 54. (G-2) Main Land/Island optimal system fuel price Vs solar radiation sensitivity

Sensitivity analysis (Figure 53) revealed that the LCOE of G2 remains constant at its optimal COE regardless of diesel price variations, suggesting minimal DGe utilization. However, as diesel prices rise, the economic advantage of G2 over the 100% renewable G1 diminishes. This highlights the importance of considering long-term fuel price trends and the potential for increased reliance on the DGe, which could offset the initial cost savings.

### 4.3.2. Conclusions

This dissertation demonstrates the potential of microgrids to provide sustainable and affordable electricity to underserved communities in Ethiopia, focusing on the unique energy landscape of Central Rift Valley. Through rigorous field measurements and advanced modeling techniques, the study identifies optimal hybrid energy solutions that integrate renewable sources like wind, solar, and pumped hydro storage (PHS) with various battery technologies (Table 7 and 8). For the island community, the most cost-effective solution was a hybrid system comprising solar PV, PHS, and a converter, achieving an LCOE of $0.061/kWh and complete reliance on renewable energy (Table 7). This design leverages the island's volcanic crater pond (as described in Figure 40) as a natural reservoir for PHS, showcasing innovative and contextually appropriate approach to energy storage. This integrated system not only addresses energy poverty but also contributes to water resource management and agricultural productivity, demonstrating the potential of MiGs to support broader sustainable development goals through the Energy-Water-Food Nexus (E-W-F-N).

For the mainland community, the optimal system (G-1) (Table 8) combined solar PV, wind, and lithium-ion batteries, offering an LCOE of $0.190/kWh.

The island community could also consider adopting the mainland's optimal configurations, G1 or G2, as alternative solutions.

- G1 (PVs-WTa-Lib, CC): This system, composed of solar PV, wind turbines, and lithium-ion batteries, offers the lowest LCOE ($0.190/kWh) among the evaluated options. However, due to the lower efficiency of solar PV compared to wind energy, it requires a larger surface area for the PV array, which could potentially impact land availability on the island.

- G2 (PVs-WTa-Lib-DGe, LF): This configuration is cost-effective, LCOE $0.188/kWh while not environmentally friend, includes a diesel generator for backup power, ensuring higher reliability. By reducing the reliance on solar PV, this system can potentially have a smaller footprint compared to G1, minimizing the impact on land use for agriculture.

The choice between these two options would involve a trade-off between cost-effectiveness (favoring G1) and land utilization for agriculture (favoring G2 with potentially smaller PV array). The island community would need to weigh these factors against their specific priorities and resource constraints to determine the most suitable solution.

The study's detailed sensitivity and performance analysis underscore the robustness of the island's optimal system (G-1) (Table 8) to varying conditions and future load increases. However, the lack of a similar analysis for the mainland systems and the exclusion of biomass data in the simulations highlight avenues for future research. The findings of this dissertation have significant implications for policymakers, energy planners, and communities in the E.C.R.V. and other regions facing similar challenges. By demonstrating the technical and financial feasibility of hybrid microgrids, this research contributes to the knowledge base for expanding energy access and promoting sustainable development in underserved areas.

**4.4.FPV-Based Microgrid Design and Evaluation**

This section delves into the design and evaluation of a floating photovoltaic (FPV)-based microgrid system for the E.C.R.V (Tulu Gudo island community). It begins with a comprehensive FPV system modeling, examining the thermal behavior of PV panels in the aquatic environment and optimizing their configuration for maximum energy yield. A PVsyst unit is then developed and integrated into HOMER Pro for simulating the entire FPV-DGe-PHS microgrid system (as represented in (Appendix 2). The simulation results are analyzed, assessing the system's performance under various conditions and conducting sensitivity analysis to evaluate its robustness. Finally, the accuracy of the simulation results is validated by comparing them with simulations from other software System Advisor model (SAM), MATLAB/Simulink) and relevant literature on FPV systems. This rigorous approach ensures the reliability and validity of the proposed microgrid design, providing a comprehensive understanding of its potential for implementation in the E.C.R.V.

#### 4.4.1. Thermal Modelling and Homer Pro-PVsyst unit Configuration

This section discusses the result related to PV panel field behaviour, optimization of the solar geometry for high energy yield and finally, availing the PVsyst unit of the Homer Pro component through 3D construction. The choice of the tilt angle is based on the self-sufficiency of the village, in particular for the worst productive month of the year, July (see Figure 33 ). The optimum slope angle is 15° ($\gamma$ = 0° to the south); for self-cleaning with rainfall, the floating structure literature recommends an angle of 15° [51]. Based on equations (3.18-3.21), the field behaviour of the selected (SPR-E20-327) PV panel for the terrestrial PV system was analyzed in Figure 55. As seen from the curve, the solar generator efficiency comes down to 16.61% at STC due to the PV cell's exposure to high temperatures.

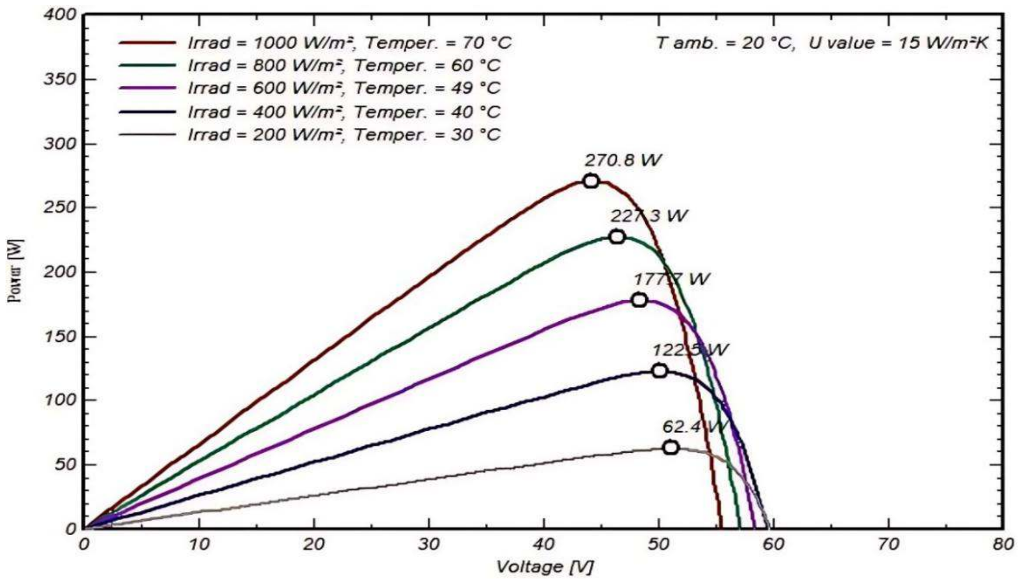


Figure 55. PV cell temperature and power characteristics of SPR-E20-327 at Tulugudo.

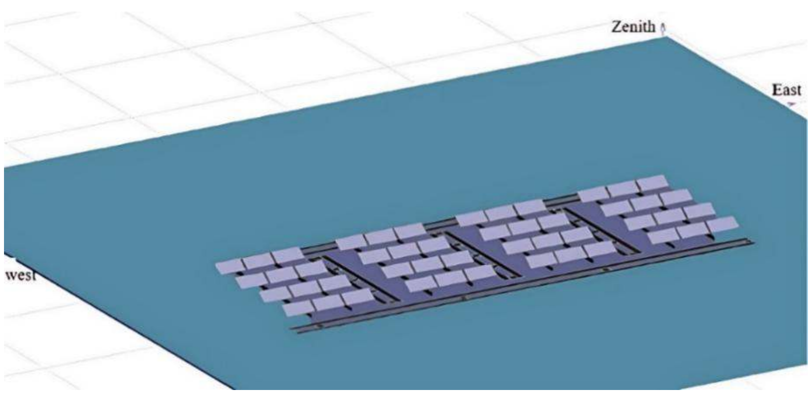


Figure 56. 15.7 KWp PVsyst Unit configuration and 3D construction for shading simulation in PVsyst.

Figure 55 shows the ground-mounted PV system field behaviour of selected (SPR-E20-327) PV panel 327Wp each at the site (7.95° N and 38.86° E) with an ambient temperature of 20°C and thermal factor Ut of 15W/m$^2$.K. The thermal loss factor (Ut), which is used in module temperature modelling, is a significant parameter for FPV. Due to the higher cooling effect of water on the module, the (Ut) value for floating photovoltaics is higher in magnitude than that of ground-mounted photovoltaics [51]. This analysis aims to understand the floatvoltaic cooling effect recovery from temperature loss in contrast to the onshore PV system. Shading can have a significant impact on photovoltaic performance (energy yield). The shading simulation for the 3D structure was computed in

Figure 56 in the PVsyst software. To avoid this, tilt angles or pitches are arranged to reduce shade losses to acceptable levels. Figure 57 shows the associated optimized *iso* shading curve for the entire year in the islands of Ziway. The broken line curved paths in this figure represent the losses due to shadings, and the pitches distance considered across the path was 5m. The loss due to shading is zero for all paths.

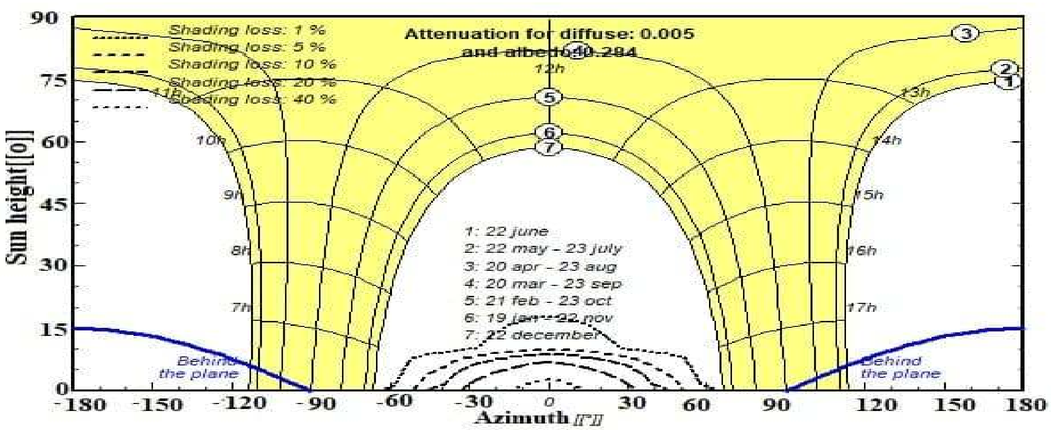


Figure 57. sun-path diagram (Linear calculation: beam-shading factor)

From Path 7 (December 22) to Path 5 (February 21- October 23), Figure 57, the sun travels to the north, bringing it closer to the FPV modules. The sun is getting away from the floatvoltaic after path 5, so the solar radiation is moving to the south. As a result, the PV modules need to be installed facing south. To allow the system to extract maximum energy throughout the year. The highest transposition factor is found at the optimum tilt angle. The greatest transposition factor in this study is 1.02 at a 15-tilt angle Figure 58.

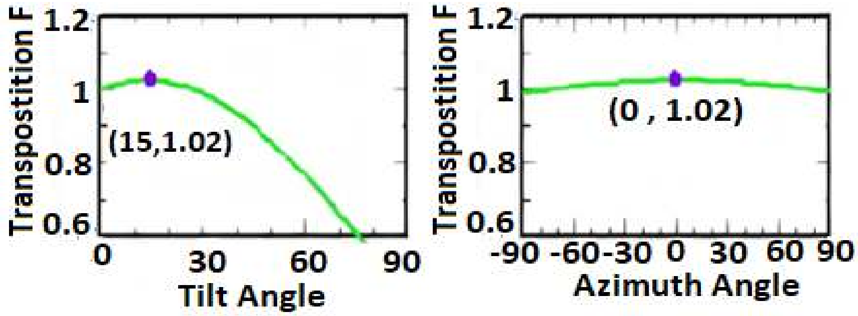


Figure 58: Transposition factor

FPV has the ability to recover energy from different factors, as mentioned before, i.e., temperature (thermal factor), albedo effect and soiling. This study neglected gains from albedo while exporting the 15.7KWp PVsyst Homer Pro component. The PV power capacity in PVsyst has been set to a symbolic size due to the sizing process in Homer Pro Software's feasibility simulation. In Homer Pro Software, this symbolic size is represented as a PVsyst unit with a PV capacity of 15.7 KWp Figure 56.

The PV system's output is determined by the amount of solar energy received and the temperature. According to site data, the PV array in this position receives 2226 kWh/m$^2$ of electricity per year. Due to various variables, photovoltaics cannot convert 100% of radiation into electricity. (SPR-E20-327) PV 327Wp each has 20.12% of efficiency at STC. After detailed loss inventory and recovery in contrast to land mounted PV, a Homer Pro PVsyst unit,78m$^2$ area produced 33.810 MWh of electricity per year. Loss due to temperature was found to be -11.8 and -2.4% for the onshore and offshore and equivalent to 3258 and 845 KWh/PVsyst unit, for the entire system is 6,679 and 1,732.3 KWh electrical energy loss for the whole year with corresponding floating cooling and soiling effect recovery of 4.95MWh.

### 4.4.2. Optimization Results

HOMER Pro optimization identified the most cost-effective system configuration for the island community, as shown in Table 11. This configuration comprises 98 PV modules (32.2 kWp) utilizing a PVsyst Homer Pro unit, two PHS units with 245 kWh storage capacity each (totaling 508 kWh), and a 33.9 kW power converter, all operating under the cycle charging (CC) strategy. The FPV system, modeled in PVsyst and integrated into HOMER Pro, generated 69.3 MWh of electricity annually, with an average daily output of 197 kWh/day and a capacity factor of 20.5% (Figure 59).

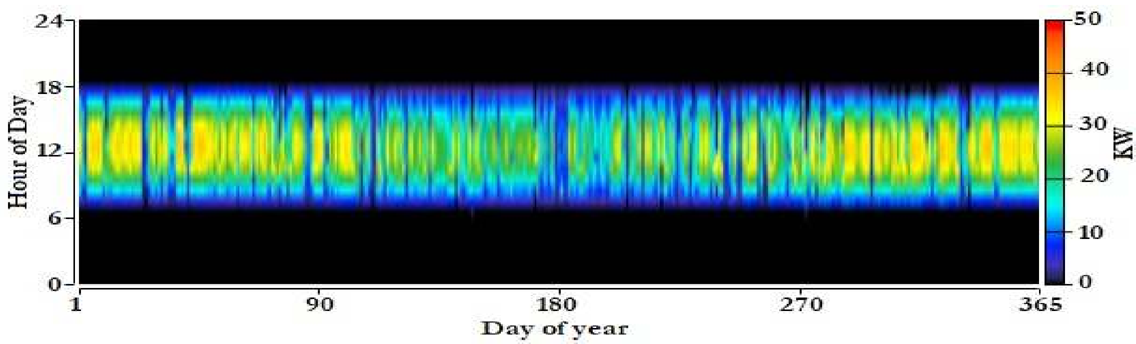


Figure 59. PVsyst generation output (KW)

Figure 59 illustrates the hourly FPV performance throughout the year, revealing consistent generation except during the rainy season (around day 180), as previously noted in the resource assessment Figure 32 and Figure 33.

Figure 60 illustrates the dynamic operation of the pumped hydro storage (PHS) system throughout the year. The state of charge (SOC) consistently exhibits daily cycling, increasing during sunlight hours when excess solar energy is used for pumping and decreasing at night during energy consumption. Seasonal variations are also evident, with higher SOC levels during sunnier months and lower levels during periods of reduced solar irradiance, likely coinciding with the rainy season.

The system maintains a minimum SOCmin of approximately 15%, ensuring consistent power supply even during low renewable generation. Overall, the PHS effectively manages energy storage and dispatch, enhancing the microgrid's reliability and maximizing the utilization of solar energy.

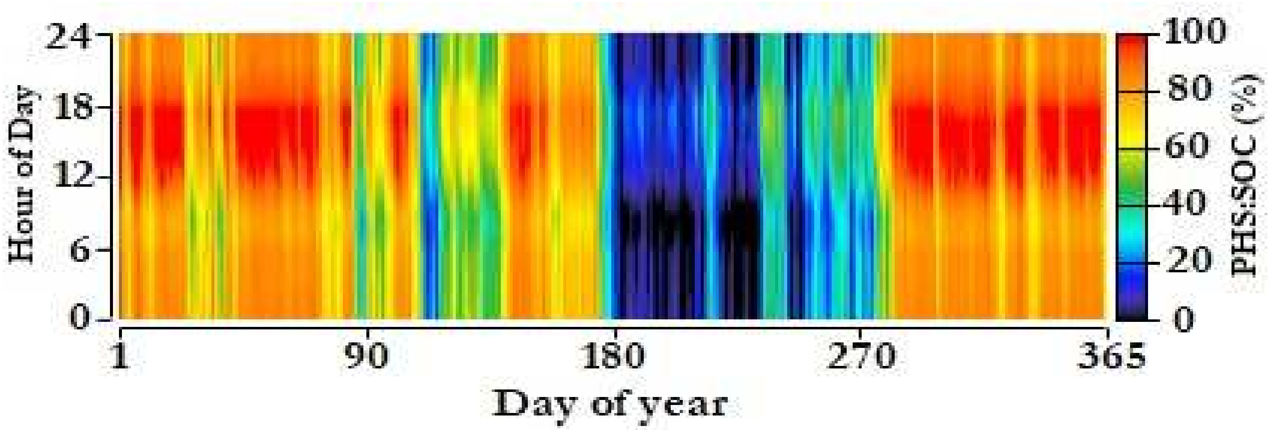


Figure 60. PHS: Level of the upper reservoir (SOCmin)

Table 11. Comparative analysis of the top two optimal power supply system type

| Rank | Sub-system | Capacity | Unit | NPC($) | COE($/KWh) | Fuel(L) | DiSp |
|---|---|---|---|---|---|---|---|
| | PHS:245 | 2,(508) | qty,KWh | | | | |
| 1st | PVsyst | 2.05,(32.2) | unit, KWp | 154,265 | 0.140 | 0L | CCs |
| | Converter | 33.9 | KW | | | | |
| | PHS:245 | 2,(508) | qty,KWh | | | | |
| 2nd | PVsyst | 2.01,(31.6) | unit, KWp | 172,680 | 0.153 | 928L | CCs |
| | Converter | 31.2 | KW | | | | |
| | DGEs | 45 | KW | | | | |

The optimal configuration's levelized cost of electricity (LCOE) is \$0.140/kWh, with a total net present cost (NPC) of \$154,265, positioning it as a cost-effective solution compared to the proposed off-grid electricity tariff in Ethiopia (Table 11 ) and (Figure 45).

### 4.4.3. Sensitivity Analysis and E-W-F-N Integration Potential

To explore the robustness of the design and the potential for Energy-Water-Food Nexus (E-W-F-N) integration, a sensitivity analysis was conducted for the first optimal system (Table 11 ). Figure 61 illustrates the impact of varying PHS SOCmin on the unmet electric load (UEL), COE, and PHS capacity. As the SOCmin increases, the COE also rises, indicating the trade-off between energy storage capacity and economic viability. Notably, even at a high SOCmin, the COE and unmet electric load (UEL) showed slight increment, with a significant amount of water available for E-W-F-N applications.

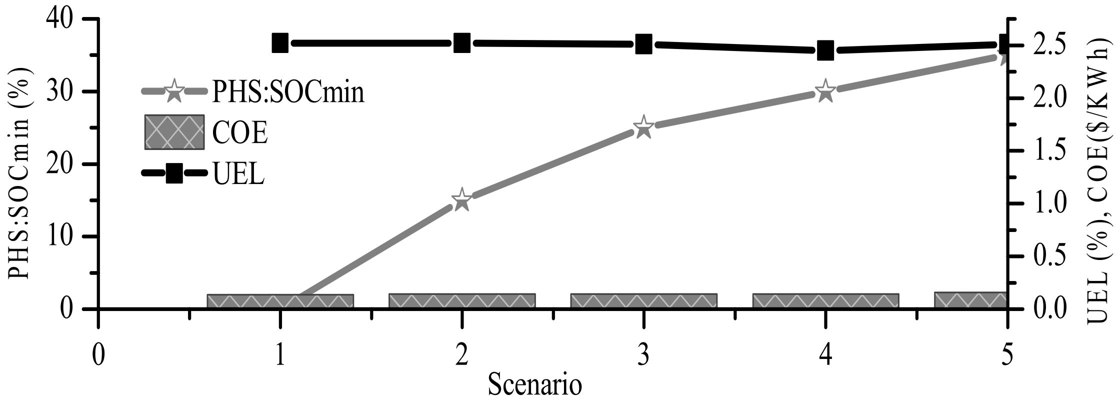


Figure 61. Unmet electrical load (UEL), COE and PHS: SOCmin sensitivity

Figure 62 further examines the effect of PHS SOCmin and FPV capital cost multiplier (CCM) on the NPC of the optimal system, both under current conditions and considering potential future reductions in solar PV costs.

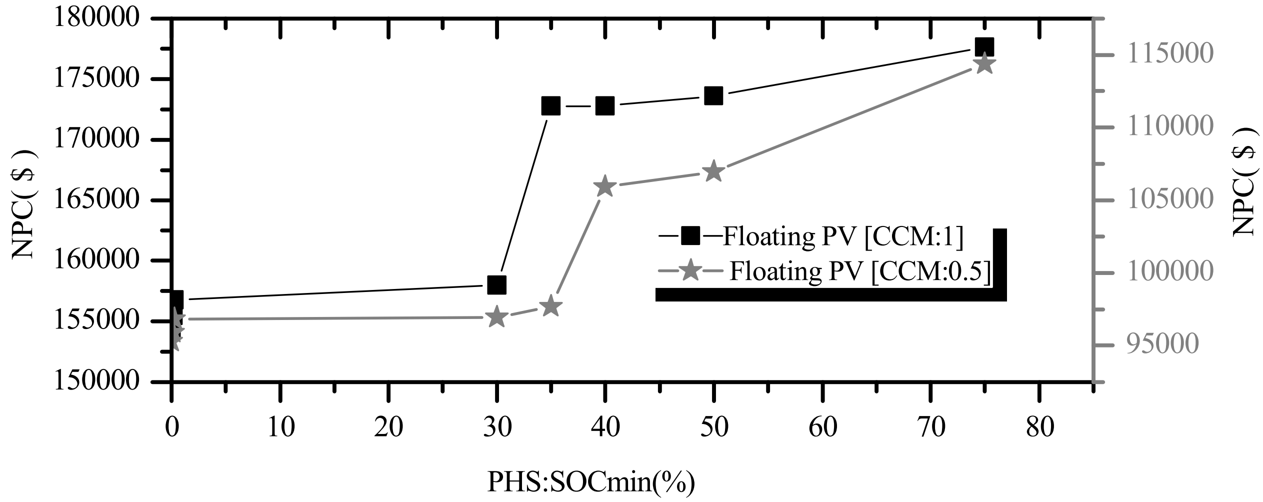


Figure 62. Effect of the PHS:$SOC_{min}$ (%) and PVSyst (CCM) on NPC of the optimal system.

This sensitivity analysis highlights the system's flexibility in accommodating variations in PHS SOCmin and the potential for E-W-F-N integration without compromising energy services or economic viability. Additionally, the robustness of the system to future load increments and the potential for cost reduction through FPV advancements further solidifies its suitability for the Tulu Gudo island community.

#### 4.4.4. Operational Performance Analysis for the Most Optimal system

The operational performance of the designed FPV-PHS microgrid system is illustrated in Figure 63 (a–c ). Figure 63 ( a & b) depict the system's behavior during typical good production seasons, where the photovoltaic (FPV) system generates sufficient power to meet the demand, and excess energy is stored in the pumped hydro storage (PHS) system. The positive (+) and negative (-) kW values in Figure 62(a) indicate the PHS charging (positive) and discharging (negative) cycles, respectively.

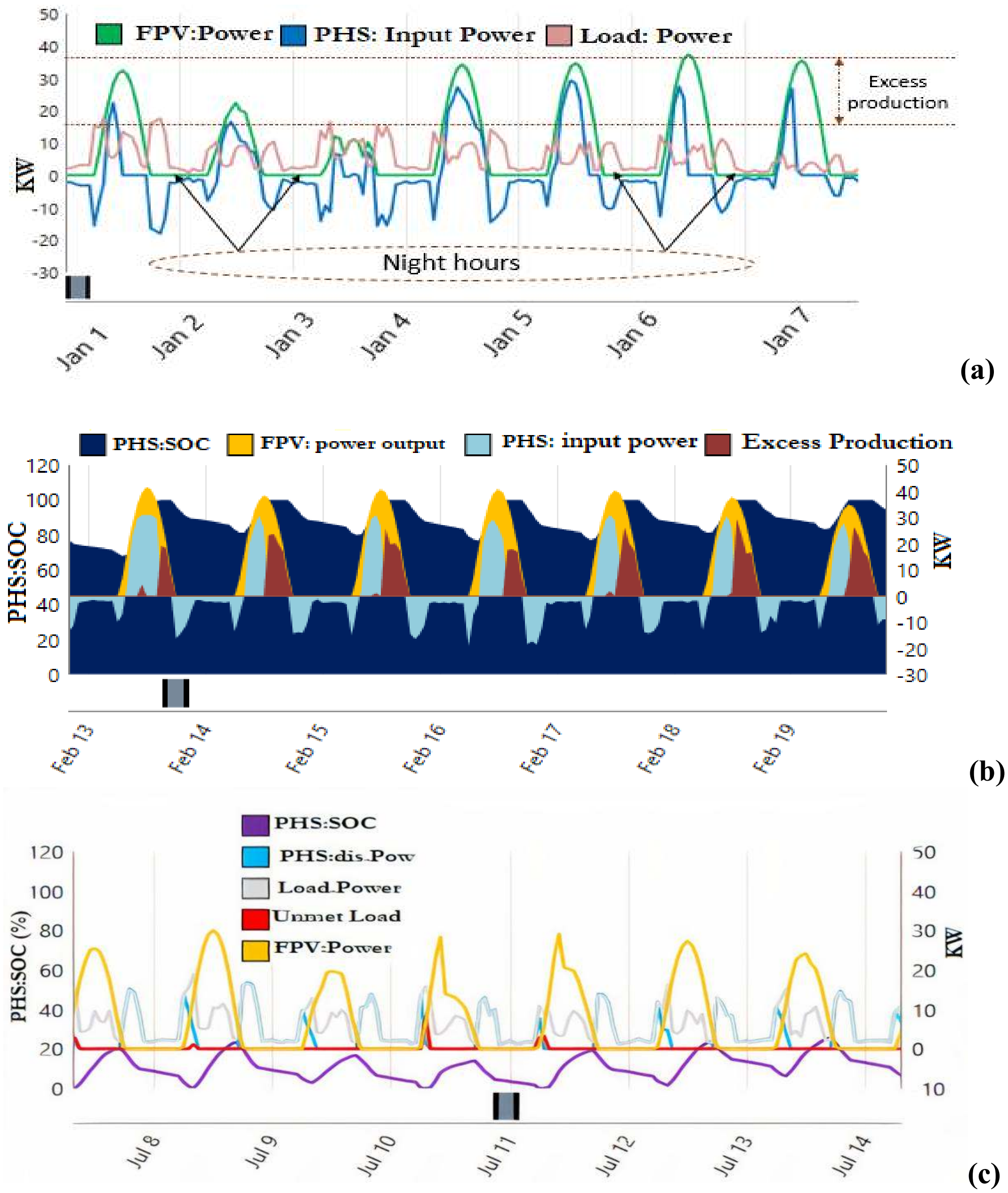


Figure 63. (a ,b, &c) Performance of the system for typical good and worst season of production

In contrast, Figure 63 (c) demonstrates the system's performance during the worst production season (July), characterized by the region's rainy season and reduced solar irradiance (Figure 31(a) and Figure 32). During this period, the PV system struggles to meet the load, resulting in the PHS discharging stored energy to compensate. This is evident in the fluctuation of the PHS minimum state of charge (SOCmin) between 0% and 20%.

#### 4.4.4.1.Performance Comparison and Water Saving Potential

A comparison between the aquatic (FPV) and terrestrial PV systems revealed a significant 7% increment in electricity generation efficiency for the FPV system, along with a higher capacity factor of 2.4%. The levelized cost of electricity (LCOE) for the floating PV system is $0.140/kWh, notably lower than the $0.240/kWh for the ground-mounted system. This aligns with the literature[92, 112], which reports energy yield gains of 2-7% and reduced LCOE for FPV systems due to the cooling effect of water.

Furthermore, the water-saving potential of the FPV system was estimated using equations (3.28-3.30) and the evaporation modeling framework presented in Section. With a total FPV array area of 160m², the system is projected to save 8,760 m³ of water annually, as indicated by the monthly evapotranspiration (ETo) data for the study area (Figure 64).

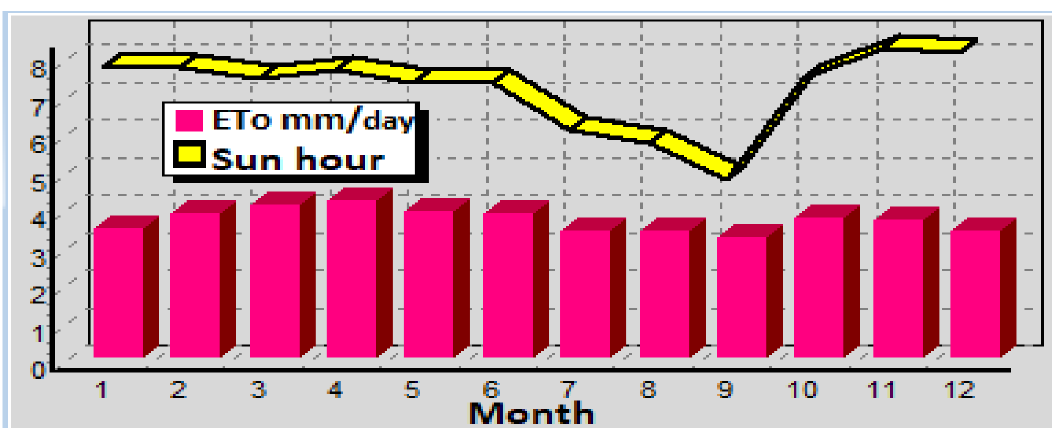


Figure 64. ETo for the study area

### 4.4.5. Validation of PVsyst Simulation Results

To validate the accuracy of the PVsyst simulation for the FPV system, a two-pronged approach was employed: comparison with other software and validation against existing literature.

#### 4.4.5.1.Validation with other Software

The FPV system's monthly energy generation predicted by PVsyst was compared with simulations from System Advisor Model (SAM), scaled by 110% to account for a hypothesized 9% underestimation in actual system performance. Table 12,

Table 13 and Figure 65 detail this comparison. While PVsyst slightly overestimated energy production by 1.81% compared to the scaled SAM results, this error falls within the expected range, suggesting that PVsyst can accurately estimate energy production with an error margin of approximately 7.2%.

Additionally, MATLAB Simulink simulations based on a temperature model (Figure 16,Table 4) [69] were conducted to further validate the PVsyst results (Appendix 4(b). These simulations showed strong agreement with PVsyst generation, reinforcing the reliability of the FPV system model.

Table 12. Monthly PVsyst (FPV) and SAM energy generation simulation

| Month | PVsyst (kWh) | SAM (kWh) | Difference | RMSE | MBE | MAPE (%) |
|---|---|---|---|---|---|---|
| January | 6,861.47 | 6090.91 | 770.56 | 591.12 kWh/month | 573.33 kWh/month | 9.64% |
| February | 6116.50 | 5500 | 616.50 | | | |
| March | 6,426.01 | 6272.73 | 153.28 | | | |
| April | 5,739.95 | 5136.36 | 603.59 | | | |
| May | 5,685.75 | 5090.91 | 594.84 | | | |
| June | 5,227.17 | 4681.82 | 545.35 | | | |
| July | 4,601.74 | 4090.91 | 510.83 | | | |
| August | 5,340.58 | 4727.27 | 613.31 | | | |
| September | 5,329.11 | 4818.16 | 510.95 | | | |
| October | 6,679.04 | 6045.45 | 633.59 | | | |
| November | 7027.36 | 6363.64 | 663.72 | | | |
| December | 7,004.30 | 6340.91 | 663.39 | | | |
| Yearly | 72,038.98 | 65159.07 | 770.56 | | | |

Table 13. Monthly PVsyst SAM*110% energy generation simulation

| Month | (SAM)X 1.1 KWh | PVsyst KWh | Difference KWh/month | RMSE KWh/month | MBE KWh/month | MAPE % |
|---|---|---|---|---|---|---|
| 1 | 6,700.00 | 6,861.47 | 0.00 | | | |
| 2 | 6,050.00 | 6116.50 | 20.00 | | | |
| 3 | 6,900.00 | 6,426.01 | 565.60 | | | |
| 4 | 5,650.00 | 5,739.95 | -0.01 | | | |
| 5 | 5,600.00 | 5,685.75 | -2.01 | | | |
| 6 | 5,150.00 | 5,227.17 | 0.00 | 160.72 | 109.33 | |
| 7 | 4,500.00 | 4,601.74 | 0.00 | kWh/month | kWh/month | 1.81 |
| 8 | 5,200.00 | 5,340.58 | -390.30 | | | |
| 9 | 5,300.00 | 5,329.11 | -221.81 | | | |
| 10 | 6,650.00 | 6,679.04 | 0.00 | | | |
| 11 | 7,000.00 | 7027.36 | 11.98 | | | |
| 12 | 6,975.00 | 7,004.30 | -2.21 | | | |
| Yearly | 71,674.98 | 72,038.98 | -18.76 | | | |

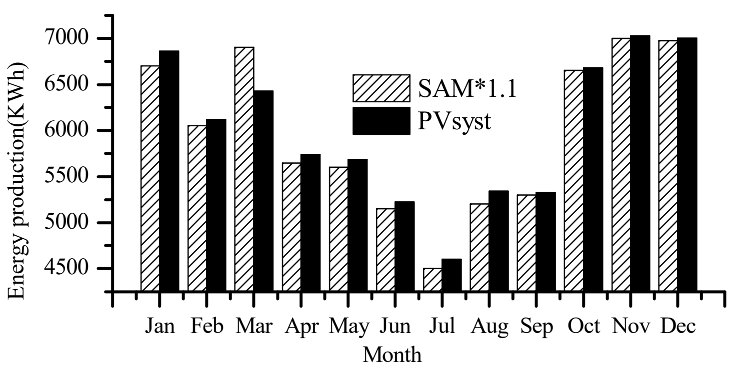


Figure 65. Comparison of the PVsyst simulation of FPV and SAM with scale factor 110%

#### 4.4.5.2.Validation Based on Related Literature

The findings of this study were further validated by comparing them to similar studies on FPV systems in Ethiopia and globally (Table 14). The observed 7% energy gain compared to land-mounted PV is consistent with previous research in Ethiopia, reporting gains of 3% and 6.9% [49, 113]. This increase also aligns with the 5-10% range documented globally by the World Bank [114].

Furthermore, the estimated water savings of 8,760 m³ annually, although from a smaller system, corroborates the water conservation benefits highlighted in other studies [113, 115]. The LCOE of $0.140/kWh for the FPV-PHS system demonstrates its cost-effectiveness, especially when compared to smaller systems with higher LCOEs [44]. While larger FPV projects can achieve even lower LCOEs [91], our findings demonstrate the competitiveness of small-scale FPV-PHS systems in off-grid settings.

Table 14. Review of Literature in Comparable Weather Conditions

| Authors | Objective | Location | HESS | EgoLMPV | COEs/kWh |
|---|---|---|---|---|---|
| [115] | Modelling and designing to supply electricity for small community | Turkey | FPV-hydrogen fuel cell | - | 0.612 |
| [44] | Techno-economic sizing to power aquaculture aeration | Thailand | FPV-Battery | - | 0.61 |
| [49] | Design FPVs to increases efficiency of solar cell and save land | Ethiopia | FPV-Battery | 3% | - |
| [113] | A techno-economic comparative analysis | Ethiopia | FPV/LMPV-Grid | 6.9% | 0.043 |
| [116] | A techno-economic & environmental feasibility | Bangladesh | FPV-Gird | - | 0.051 |

### 4.4.6. Applicability to other Contexts

The solar island microgrid system developed for E.C.R.V (Lake Ziway Tulu Gudo island), while tailored to its specific context, offers a versatile framework for broader application. The adaptable design methodology (Figure 14) allows for customization to various geographical, energy demand, and meteorological conditions. This scalability enables the system to be tailored to different community sizes and to incorporate technological advancements in renewable energy and storage solutions.

Beyond customization, the system's effectiveness and sustainability can be further enhanced through various adaptations. Integrating complementary renewable sources, such as wind or biogas, can bolster reliability and potentially reduce costs. Additionally, where feasible, interconnecting the microgrid with the existing power grid allows for energy export and grid support during periods of low renewable generation. Critically, robust community engagement throughout the project's lifecycle is essential for ensuring long-term sustainability, fostering local ownership, and maximizing the system's benefits.

While the system emphasizes sustainability, a comprehensive ecological assessment is necessary for responsible implementation. This evaluation should examine potential impacts on aquatic life and ecosystems, particularly in relation to floating photovoltaic panels and the construction of the pumped hydro storage system's upper reservoir. Key considerations include habitat loss, soil erosion, and effects on local flora and fauna, both during and after construction. Adherence to environmental regulations and the implementation of mitigation measures, such as habitat restoration and erosion control, are crucial for achieving a balance between renewable energy generation and environmental preservation.

#### 4.4.7. Conclusions

This research successfully designed and simulated a hybrid floating photovoltaic (FPV)-pumped hydro storage (PHS) microgrid system with diesel generator (DGe) backup for the remote Lake Ziway Tulu Gudo island community in Ethiopia. The integrated assessment methodology (Figure 13), utilizing HOMER Pro and PVsyst, enabled comprehensive modeling and optimization to meet the community's load profile while achieving economic and environmental objectives.

The optimal FPV-PHS hybrid configuration (32.2 kWp FPV, 508 kWh PHS) demonstrated technical and economic viability, achieving a levelized cost of electricity (LCOE) of $0.140/kWh. This represents a significant reduction compared to the island's existing diesel-based generation, the national off-grid rate, and other potential system configurations (Figure 45, Table 10). This finding translates to immediate cost savings and a pathway towards greater energy independence for the community.

Furthermore, the FPV system demonstrated a 7% increase in annual electricity generation and an 8,760 $m^3$ reduction in water consumption compared to a land-mounted PV system of equivalent capacity. This dual benefit addresses both energy and water scarcity challenges, highlighting the potential for FPV to contribute to sustainable development in water-stressed regions.

The study also explored the integration of the microgrid with the Energy-Food-Water (EFW) Nexus. Results indicate that up to 700,000 kg of water could be allocated annually for agricultural use without compromising energy services or economic viability. This innovative approach demonstrates the potential for FPV-based microgrids to contribute to sustainable development beyond energy provision.

This research offers a comprehensive methodological framework for designing and optimizing FPV-based microgrids in similar island and lakeside communities globally. Future work should expand the scope to include additional renewable resources, such as biogas and electrolyzers, and conduct detailed geological assessments to further validate the feasibility and optimize the design of the PHS reservoir.

By demonstrating the technical, economic, and environmental advantages of integrated FPV-PHS systems, this study represents a significant step towards accelerating the adoption of sustainable energy solutions for remote and underserved populations.

# CHAPTER 5: SUMMARY AND OUTLOOK

Driven by the urgent need to address energy poverty and promote sustainable development in underserved regions, this dissertation has investigated advanced hybrid microgrid systems as a promising solution. With a focus on harnessing renewable energy sources and utilizing innovative technologies like floating photovoltaics (FPV) and pumped hydro storage (PHS), this research aims to pave the way for a cleaner and more equitable energy future.

The dissertation is structured into four chapters. Chapter 1 (Introduction) and Chapter 2 (Literature Review) provide a comprehensive overview of the global and regional energy landscape, emphasizing the challenges faced by the Ethiopian Central Rift Valley (E.C.R.V.) in terms of electricity access and the potential of hybrid microgrids to address these challenges. The literature review also identifies key research gaps, highlighting the need for innovative approaches that integrate the proposed MiGs with multiple benefits.

Chapter 3 (Methodology) outlines the rigorous methodological framework employed in this study, encompassing resource assessment, hybrid microgrid design, simulation, optimization, and validation. The chapter details the tools and techniques used, including HOMER Pro and PVsyst software, and explains the rationale behind the selection of specific system configurations and parameters.

In this concluding chapter, we will synthesize the key findings presented in Chapter 4, providing a concise overview of the research outcomes. Additionally, I will offer a brief outlook on the potential implications of this work and suggest directions for future research.

## 5.1. Summary of the main results

### Sustainable Energy resource potential of the E.C.R.V

The E.C.R.V. boasts ample wind and solar resources, with an average wind speed of 7 m/s at 50m height and an average annual solar irradiance of 6.1 kWh/m²/day. Additionally, the unique topography of Tedecha Island presents a promising location for a small-scale pumped hydro storage (PHS) system, leveraging a natural volcanic crater pond as an upper reservoir.

### Hybrid Microgrid Optimization:

### Mainland Community

For the mainland community, the optimal configuration was found to be a 35.8 kW solar PV system coupled with four 5.1 kW wind turbines and 72 lithium-ion batteries, achieving a levelized cost of electricity (LCOE) of $0.190/kWh (G-1in Table 9). An alternative configuration with a diesel generator backup was also explored (G-2 in Table 9), providing higher reliability but operating under load following with the inclusion of a diesel generator (DGe), albeit at a relative LCOE of $0.188/kWh and NPC of $199,410. While it also achieves a 100% RF when the DGe is not running, its operation incurs a minimal environmental impact due to diesel emissions.

### Island Community

For the island community, the optimal solution was a hybrid system combining a 41 kW of PV(CS6K_259) array with one PHS unit of 245 kWh storage capacity, and a 19.1 kW power converter, operating under the cycle charging (CC) dispatch strategy, resulting in an LCOE of $0.0677/kWh, falling within the acceptable range of the proposed microgrid tariff for Ethiopia (Figure 45)

The sensitivity analysis conducted on the optimal PV(CS6K_259)-PHS microgrid system (G1), Table 8) demonstrates its robust performance and potential for E-W-F N integration. By varying the (SOCmin) of the PHS system from 0% to 75%, we assessed the impact on both energy services and water availability. Key findings:

- **Resilient Energy Services:** The microgrid maintains reliable energy services, even at varying PHS: SOCmin levels. The unmet load and capacity shortage remain relatively low (around 1.4-1.65% and 5.02-5.09%, respectively (see Table 8) across all scenarios. This indicates that the system can consistently meet the community's electricity demand, even when the PHS reservoir has lower water levels.
- **Economic Viability:** While the levelized cost of electricity (LCOE) increases with higher SOCmin, the values remain within the affordable range of $0.0607/kWh to $0.0882/kWh. This demonstrates the economic viability of the system even when a significant portion of the PHS capacity is reserved for E-W-F-N purposes.
- **Water Availability for E-W-F-N:** At a SOCmin of 75%, the system still generates a substantial surplus of 750,000 kg of water. This surplus can be effectively utilized for various E-W-F-N applications, such as household use, livestock watering, micro-irrigation, and sanitation, without compromising the microgrid's primary function of providing electricity.

**Implications:**

These results underscore the potential of the PV-PHS microgrid system to simultaneously address energy and water challenges in the island community. By operating the PHS at a higher SOCmin, the system can provide a reliable electricity supply while also contributing to water security and agricultural productivity. This integrated approach demonstrates the feasibility and effectiveness of the E-W-F-N concept in real-world applications, offering a sustainable solution for off-grid communities. And this dissertation provides empirical evidence for the effectiveness of small-scale PHS in supporting the E-W-F-N, offering a valuable model for other regions facing similar challenges.

**The simulation results for lead-acid battery-based MiGs in the E.C.R.V** indicate limited economic feasibility compared to the proposed Ethiopian off-grid electricity tariff (Table 11). The higher levelized cost of electricity (LCOE) and net present cost (NPC) associated with these systems align with existing literature, which demonstrates that lead-acid batteries tend to be more expensive in the long run due to their shorter lifespan, lower efficiency, higher maintenance requirements, and lower energy density compared to lithium-ion alternatives [88]. These findings underscore the importance of carefully considering the long-term costs and benefits of different battery technologies when designing microgrid systems for rural electrification projects in Ethiopia.

**Solar-Island (FPV-Based-Hybrid Microgrid Optimization):**

This system is specific to the island community, the optimal solution was a hybrid system combining a 32.2 kWp floating PV (FPV) array with 508 kWh PHS, resulting in an LCOE of $0.140/kWh and a 7% increase in energy yield compared to land-mounted PV. This is a substantial reduction compared to the island's current diesel-based generation, the national off-grid rate, and other potential system configurations, as demonstrated in (Table 11 and Figure 45).

The accuracy of the simulation results was confirmed through validation with other software (SAM and MATLAB/Simulink) and related literatures. Notably, this research fills a crucial gap in the literature by providing empirical evidence for the effectiveness and cost-competitiveness of small-scale FPV-PHS systems within the 20-50 kWp range, thus validating their potential as a sustainable solution for electrifying remote communities.

The FPV-based microgrid system, designed for Tulu Gudo Island, offers a customizable framework (see Figure 14 ) adaptable to diverse geographical and energy contexts. Its integration with other renewable sources and potential grid connection can further enhance its effectiveness.

However, responsible implementation necessitates a comprehensive ecological assessment to mitigate potential environmental impacts.

Limited Exploration of Local Materials for FPV Platforms: This study focused on conventional FPV designs using imported materials. The potential cost reduction and sustainability benefits of utilizing locally available floating structures, such as bamboo, were not explored due to the scope of this research.

**Impacts of Ethiopia's on-grid New Tariff Reform and Floating Exchange Rate on the Cost Competitiveness of Proposed Microgrid**

As shown in Figure 65, the optimal microgrid configurations proposed for the island community are already cost-competitive under the new tariff structure. This is largely due to the inherent challenges and high costs associated with extending the grid to geographically isolated islands.

On the mainland, while the best-performing microgrid (lithium-ion based) has a slightly higher LCOE than the new grid tariff, the government's incentives for electric vehicle (EV) adoption present a significant opportunity. The anticipated increase in EV demand creates a potential revenue stream for microgrids through charging services, enhancing their financial viability and competitiveness.

Furthermore, the government's focus on green energy and the possibility of future tariff adjustments further strengthen the case for microgrid adoption. Microgrids can play a key role in enabling the transition to electric mobility, especially in areas with limited grid access, while also providing grid support services and contributing to a cleaner energy future.

Overall, while the new tariff reform and floating exchange rate introduce some complexities, the supportive policy environment and the potential for EV integration create a favorable outlook for microgrid development in Ethiopia. Careful planning and collaboration among stakeholders will be essential to navigate the challenges and maximize the benefits of microgrids in this evolving landscape.

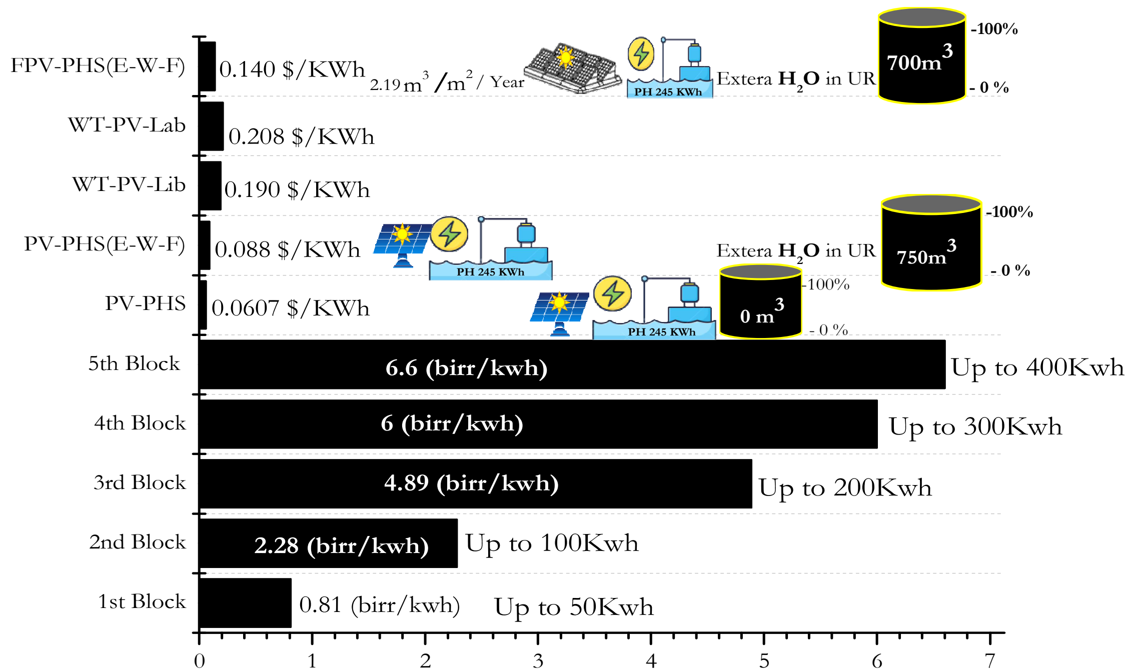


Figure 66. Overall performance of the proposed MiGs with proposed on-grid tariff reform [15,106].

## 5.2.Outlook

Building on the findings of this dissertation, several promising avenues for further research emerge, both from a technical and implementation perspective.

1. A key area for future investigation is the development of an automated control system to optimize the E-W-F-N integration within the proposed microgrids. Although the theoretical feasibility of this integration has been confirmed through sensitivity analysis in

HOMER Pro, the practical implementation requires a robust control mechanism that can balance energy production, storage, and consumption while dynamically allocating excess energy to E-W-F-N applications (e.g., irrigation, water pumping).

2. Incorporation of Biomass Energy: Due to data limitations, this study did not consider biomass as a potential energy source. Future research should investigate the feasibility of integrating biomass into hybrid microgrid systems in the E.C.R.V., assessing its impact on system performance, cost-effectiveness, and environmental sustainability.
3. Detailed Social and Economic Impact Assessment**:** A comprehensive assessment of the social and economic impacts of the proposed microgrid systems on local communities is warranted. This would involve investigating changes in livelihoods, employment opportunities, health outcomes, and overall quality of life.
4. Mainland Microgrid Performance Analysis: A detailed analysis of the performance of the optimal microgrid configurations for the mainland communities is needed, assessing their long-term reliability, efficiency, and adaptability to varying conditions.
5. Geological Assessment of the Natural Crater Pond: A comprehensive geological assessment of the natural crater pond on Tedecha Island is crucial to ensure the safe and sustainable implementation of the proposed pumped hydro storage (PHS) system. This assessment should evaluate the pond's geological stability, potential for leakage or erosion, and any associated environmental risks
6. Grid Integration and Energy Trading: Investigating the potential for integrating the proposed microgrids with the national grid could open up opportunities for energy trading and revenue generation for the communities. This would involve studying the technical and regulatory requirements for grid integration, as well as the economic feasibility of energy trading models.

7. Investigating Locally Sourced FPV Platforms: Future research should explore the feasibility, durability, and environmental impact of utilizing locally available materials like bamboo for FPV platforms. This could lead to significant cost reductions and increased accessibility of FPV systems for off-grid communities in Ethiopia.

By addressing these future research directions, we can build upon the insights gained from this dissertation and pave the way for a more sustainable and equitable energy future for remote communities in Ethiopia and other regions facing similar challenges.

# REFERENCES


[1] Outlook, A.E., A focus on energy prospects in Sub-Saharan Africa. International Energy Agency IEA, 2014.

[2] perkovic, M. How Business Leaders Can Prepare For The Sustainable Energy World Of 2050. 2021 19 May 2022]; Available from: https://www.forbes.com/sites/forbesbusinesscouncil/2021/02/26/how-business-leaders-can-prepare-for-the-sustainable-energy-world-of-2050/#:~:text=Canadian%20film%20director%20James%20Cameron,consumption%20will%20double%20by%202050.

[3] IRENA, J., Offshore Renewables: An Action Agenda for Deployment. 2021, International Renewable Energy Agency Abu Dhabi, United Arab Emirates.

[4] Tiruye, G.A., et al., Opportunities and challenges of renewable energy production in Ethiopia. Sustainability, 2021. **13**(18): p. 10381.

[5] IEA, I., UNSD, World Bank, WHO, Access to electricity (% of population). 2023: Washington DC. ©World Bank.

[6] IEA, sdg7-data-and-projections. 2023, iea: paris.

[7] INERNSUS, CLEAN ENERGY MINI-GRID POLICY DEVELOPMENT GUIDE, UNIDO, Editor. 2020, UNIDO, Department of Energy: Germany.

[8] Power, E.E. Installed capacity (MW) of ICS as of 2015 EFY (2022/23 G.C.). 2024 30 Augest 2024]; Available from: https://www.eep.com.et/?page_id=1033.

[9] Van-Hein Sackey, C. and D. Nock, The need for agricultural productive uses in the national electrification plan of sub-Saharan African countries—a call to action for Ethiopia. Environmental Research: Infrastructure and Sustainability, 2022. **2**(2): p. 023001.

[10] Ministry of Water, I., and Energy, Federal Democratic Republic of Ethiopia. National Electrification Program 2.0., I. Ministry of Water, and Energy, and Ethiopian Electric Utility., Editor. 2019: Addis Ababa.

[11] Gizaw, M. and G. Bekele, Study of the potential of Sea-water pumped storage for Power Generation: Zway Islands in Ethiopia. 2021, EasyChair.

[12] Gizaw, M. and G. Bekele, Investigation of Sustainable Technology Options: Wind, Pumped-hydro-storage and Solar potential to Electrify Isolated Ziway Islanders in Ethiopia. EAI Endorsed Transactions on Energy Web, 2023. **10**.

[13] Gizaw, M. and G. Bekele, Design of a solar island with a water-battery storage system for Lake Ziway islanders in Ethiopia. Cogent Engineering, 2024. **11**(1): p. 2363001.

[14] Tibebe, D., et al., Assessment of spatio-temporal variations of selected water quality parameters of Lake Ziway, Ethiopia using multivariate techniques. BMC chemistry, 2022. **16**(1): p. 1-18.

[15] Africa, P., Off-grid solar market assessment. US Agency of International Development (USAID): Washington, DC, USA, 2019: p. 1-47.

[16] Aga, W.S., et al., Rural electrification with hybrid renewable energy-based off-grid technology: a case study of Adem Tuleman, Ethiopia. Energy, Ecology and Environment, 2023. **8**(5): p. 420-438.

[17] Bedo, D., A. Mekuriaw, and A. Bantider, Vulnerability of household livelihoods to climate variability and change in the central rift valley sub-basin of Ethiopia. Heliyon, 2024. **10**(3).

[18] Kjeldstad, T., et al., Cooling of floating photovoltaics and the importance of water temperature. Solar Energy, 2021. **218**: p. 544-551.

[19] Elminshawy, N.A., et al., A technical and economic evaluation of floating photovoltaic systems in the context of the water-energy nexus. Energy, 2024: p. 131904.

[20] Rogner, M. and N. Troja, The world's water battery: Pumped hydropower storage and the clean energy transition. The International Hydropower Association (IHA), Chancery House, St Nicholas Way, Sutton, London SM1 IJB, United Kingdom, 2018.

[21] Goshime, D.W., et al., Implications of water abstraction on the interconnected Central Rift Valley Lakes sub-basin of Ethiopia using WEAP. Journal of Hydrology: Regional Studies, 2021. **38**: p. 100969.

[22] Zhongming, Z., et al., IRENA Outlines Action Agenda on Offshore Renewables for G20. 2021.

[23] Franz, M., et al., Mini-grid policy toolkit. EUEI-PDF, ARE and REN21, Tech. Rep, 2014.

[24] Chaudhary, G., et al., Review of energy storage and energy management system control strategies in microgrids. Energies, 2021. **14**(16): p. 4929.

[25] Georgious Zaher Georgious, R., et al., Review on energy storage systems in microgrids. Electronics (Switzerland), 2021.

[26] Kwon, K., et al., Integrated Battery and Hydrogen Energy Storage for Enhanced Grid Power Savings and Green Hydrogen Utilization. Applied Sciences, 2024. **14**(17): p. 7631.

[27] Oulis Rousis, A., et al., Design of a hybrid AC/DC microgrid using Homer Pro: Case study on an islanded residential application. Inventions, 2018. **3**(3): p. 55.

[28] Benti, N.E., Y.S. Mekonnen, and A.A. Asfaw, Combining green energy technologies to electrify rural community of Wollega, Western Ethiopia. Scientific African, 2023. **19**: p. e01467.

[29] Benti, N.E., et al., Techno-economic analysis of solar energy system for electrification of rural school in Southern Ethiopia. Cogent Engineering, 2022. **9**(1): p. 2021838.

[30] Gebrehiwot, K., et al., Optimization and cost-benefit assessment of hybrid power systems for off-grid rural electrification in Ethiopia. Energy, 2019. **177**: p. 234-246.

[31] Bekele, G., Study into the potential and feasibility of a standalone solar-wind hybrid electric energy supply system. 2009, KTH.

[32] Berihun, G., modeling and simulating of a micro hydro wind hybrid power generation system for rural area of Ethiopia. Mater thesis in Addis Ababa University, 2013.

[33] Bekele, G. and G. Tadesse, Feasibility study of small Hydro/PV/Wind hybrid system for off-grid rural electrification in Ethiopia. Applied Energy, 2012. **97**: p. 5-15.

[34] Jahangir, M.H. and R. Cheraghi, Economic and environmental assessment of solar-wind-biomass hybrid renewable energy system supplying rural settlement load. Sustainable Energy Technologies and Assessments, 2020. **42**: p. 100895.

[35] Zhang, W., L. Zhang, and J. Liu, Satellite-based re-examination of changes in terrestrial near-surface wind speed in the last 30 years. Frontiers in Earth Science, 2024. **12**: p. 1398638.

[36] Kolhe, M.L., K.I.U. Ranaweera, and A.S. Gunawardana, Techno-economic sizing of off-grid hybrid renewable energy system for rural electrification in Sri Lanka. Sustainable Energy Technologies and Assessments, 2015. **11**: p. 53-64.

[37] Olatomiwa, L., S. Mekhilef, and O.S. Ohunakin, Hybrid renewable power supply for rural health clinics (RHC) in six geo-political zones of Nigeria. Sustainable Energy Technologies and Assessments, 2016. **13**: p. 1-12.

[38] Alonso, J.B., P. Sandwell, and J. Nelson, The potential for solar-diesel hybrid mini-grids in refugee camps: A case study of Nyabiheke camp, Rwanda. Sustainable Energy Technologies and Assessments, 2021. **44**: p. 101095.

[39] Boussetta, M., et al., Assessing the potential of hybrid PV–Wind systems to cover public facilities loads under different Moroccan climate conditions. Sustainable Energy Technologies and Assessments, 2017. **22**: p. 74-82.

[40] Agyekum, E.B. and C. Nutakor, Feasibility study and economic analysis of stand-alone hybrid energy system for southern Ghana. Sustainable Energy Technologies and Assessments, 2020. **39**: p. 100695.

[41] Gebreyes, M., et al., Local perceptions of water-energy-food security: livelihood consequences of dam construction in Ethiopia. Sustainability, 2020. **12**(6): p. 2161.

[42] Ferroukhi, R., et al., Renewable energy in the water, energy & food nexus. IRENA, Abu Dhabi, 2015: p. 1-125.

[43] Ladu, N.S.D., et al., Feasibility Study of a Standalone Hybrid Energy System to Supply Electricity to a Rural Community in South Sudan. Scientific African, 2022: p. e01157.

[44] Jamroen, C., Optimal techno-economic sizing of a standalone floating photovoltaic/battery energy storage system to power an aquaculture aeration and monitoring system. Sustainable Energy Technologies and Assessments, 2022. **50**: p. 101862.

[45] Agrawal, K.K., et al., Assessment of floating solar PV (FSPV) potential and water conservation: Case study on Rajghat Dam in Uttar Pradesh, India. Energy for Sustainable Development, 2022. **66**: p. 287-295.

[46] Nagananthini, R. and R. Nagavinothini, Investigation on floating photovoltaic covering system in rural Indian reservoir to minimize evaporation loss. International Journal of Sustainable Energy, 2021: p. 1-25.

[47] Liu, L., et al., Evaluating the benefits of integrating floating photovoltaic and pumped storage power system. Energy Conversion and Management, 2019. **194**: p. 173-185.

[48] Nyeche, E. and E. Diemuodeke, Modelling and optimisation of a hybrid PV-wind turbine-pumped hydro storage energy system for mini-grid application in coastline communities. Journal of cleaner production, 2020. **250**: p. 119578.

[49] Taye, B.Z., A.H. Nebey, and T.G. Workineh, Design of floating solar PV system for typical household on Debre Mariam Island. Cogent Engineering, 2020. **7**(1): p. 1829275.

[50] Bekele, G. and B. Palm, Feasibility study for a standalone solar–wind-based hybrid energy system for application in Ethiopia. Applied energy, 2010. **87**(2): p. 487-495.

[51] Program, E.S.M.A. and S.E.R.I.o. Singapore, Where Sun Meets Water: Floating Solar Handbook for Practitioners. 2019, World Bank.

[52] Rachoutis, E. and D. Koubogiannis. Energy Payback Time of a Rooftop Photovoltaic System in Greece. in IOP Conference Series: Materials Science and Engineering. 2016. IOP Publishing.

[53] Rogers, T., et al., Onshore wind energy potential for Small Island Developing States: Findings and recommendations from Barbados. Energy for Sustainable Development, 2019. **52**: p. 116-127.

[54] Ohunakin, O.S. and O.O. Akinnawonu, Assessment of wind energy potential and the economics of wind power generation in Jos, Plateau State, Nigeria. Energy for Sustainable Development, 2012. **16**(1): p. 78-83.

[55] Cooney, C., et al., Performance characterisation of a commercial-scale wind turbine operating in an urban environment, using real data. Energy for Sustainable Development, 2017. **36**: p. 44-54.

[56] Soulouknga, M., et al., Analysis of wind speed data and wind energy potential in Faya-Largeau, Chad, using Weibull distribution. Renewable energy, 2018. **121**: p. 1-8.

[57] Said, M., et al., Improved framework for techno-economical optimization of wind energy production. Sustain Energy Technol Assess, 2017. **23**: p. 57-72.

[58] Pishgar-Komleh, S., A.J.S.E.T. Akram, and Assessments, Evaluation of wind energy potential for different turbine models based on the wind speed data of Zabol region, Iran. Sustain Energy Technol Assess, 2017. **22**: p. 34-40.

[59] Nayak, A., et al., An integrated optimal operating strategy for a grid-connected AC microgrid under load and renewable generation uncertainty considering demand response. Sustain Energy Technol Assess, 2021. **45**: p. 101169.

[60] Mathew, S., Wind energy: fundamentals, resource analysis and economics. 2006: Springer.

[61] Amente, G. and M. Gizaw, Analysis of Wind Power Potential for Jijiga Area. 2012, Haramaya University.

[62] Fadare, D., The application of artificial neural networks to mapping of wind speed profile for energy application in Nigeria. Applied Energy, 2010. **87**(3): p. 934-942.

[63] Promsen, W., S. Janjai, and T. Tantalechon, An Analysis of Wind Energy Potential of Kampot Province, Southern Cambodia. Energy Procedia, 2014. **52**: p. 633-641.

[64] Amri, F., et al., Toward an evolutionary multi-criteria model for the analysis and estimation of wind potential. Journal of Power and Energy Engineering, 2015. **3**(11): p. 14.

[65] Khosravi, A., et al., Prediction of wind speed and wind direction using artificial neural network, support vector regression and adaptive neuro-fuzzy inference system. Sustain Energy Technol Assess, 2018. **25**: p. 146-160.

[66] Quan, P., T.J.S.E.T. Leephakpreeda, and Assessments, Assessment of wind energy potential for selecting wind turbines: An application to Thailand. Sustain Energy Technol Assess, 2015. **11**: p. 17-26.

[67] Hatata, A., et al., An optimization method for sizing a solar/wind/battery hybrid power system based on the artificial immune system. Sustain Energy Technol Assess, 2018. **27**: p. 83-93.

[68] Jahangir, M.H., R.J.S.E.T. Cheraghi, and Assessments, Economic and environmental assessment of solar-wind-biomass hybrid renewable energy system supplying rural settlement load. Sustain Energy Technol Assess, 2020. **42**: p. 100895.

[69] De Kooning, J.D., et al., Techno-economic optimisation of small wind turbines using co-design on a parametrised model. 2021. **45**: p. 101165.

[70] Kharrich, M., O.H. Mohammed, and M. Akherraz, Design of hybrid microgrid PV/Wind/Diesel/Battery system: case study for rabat and baghdad. EAI Endorsed Transactions on Energy Web, 2020. **7**(27).

[71] Chouaib, A., H. Messaoud, and M. Salim, Sizing, modelling and simulation for Hybrid Central PV/wind turbine/diesel generator for feeding rural village in South Algeria. EAI Endorsed Transactions on Energy Web, 2017. **4**(15).

[72] Beza, T.M., C.-H. Wu, and C.-C. Kuo, Optimal Sizing and Techno-Economic Analysis of Minigrid Hybrid Renewable Energy System for Tourist Destination Islands of Lake Tana, Ethiopia. Applied Sciences, 2021. **11**(15): p. 7085.

[73] Javed, M.S., et al., Hybrid pumped hydro and battery storage for renewable energy based power supply system. Applied Energy, 2020. **257**: p. 114026.

[74] Sahu, A., N. Yadav, and K. Sudhakar, Floating photovoltaic power plant: A review. Renewable and sustainable energy reviews, 2016. **66**: p. 815-824.

[75] World Bank Group, E. and SERIS, Where sun meets water: floating solar market report. 2018, World Bank Washington, DC.

[76] Abuzaid, H., L.A. Moeilak, and A. Alzaatreh, Customers' perception of residential photovoltaic solar projects in the UAE: A structural equation modeling approach. Energy Strategy Reviews, 2022. **39**: p. 100778.

[77] Ghabuzyan, L., et al., Thermal Effects on Photovoltaic Array Performance: Experimentation, Modeling, and Simulation. Applied Sciences, 2021. **11**(4): p. 1460.

[78] Micheli, L., Energy and economic assessment of floating photovoltaics in Spanish reservoirs: cost competitiveness and the role of temperature. Solar Energy, 2021. **227**: p. 625-634.

[79] Song, J. and Y. Choi, Analysis of the potential for use of floating photovoltaic systems on mine pit lakes: Case study at the Ssangyong open-pit limestone mine in Korea. Energies, 2016. **9**(2): p. 102.

[80] Suh, J., Y. Jang, and Y. Choi, Comparison of electric power output observed and estimated from floating photovoltaic systems: A case study on the hapcheon dam, Korea. Sustainability, 2019. **12**(1): p. 276.

[81] Kumar, N.M., et al., Advancing simulation tools specific to floating solar photovoltaic systems–Comparative analysis of field-measured and simulated energy performance. Sustainable Energy Technologies and Assessments, 2022. **52**: p. 102168.

[82] Charles Lawrence Kamuyu, W., et al., Prediction model of photovoltaic module temperature for power performance of floating PVs. Energies, 2018. **11**(2): p. 447.

[83] Kichou, S., N. Skandalos, and P. Wolf, Floating photovoltaics performance simulation approach. Heliyon, 2022. **8**(12).

[84] Fereshtehpour, M., et al., Evaluation of factors governing the use of floating solar system: A study on Iran's important water infrastructures. Renewable Energy, 2021. **171**: p. 1171-1187.

[85] Gabr, M.E., Modelling net irrigation water requirements using FAO-CROPWAT 8.0 and CLIMWAT 2.0: a case study of Tina Plain and East South ElKantara regions, North Sinai, Egypt. Archives of Agronomy and Soil Science, 2021: p. 1-16.

[86] Nzotcha, U., Promoting Pumped Hydroelectric Energy Storage for Sustainable Power Generation in Cameroon: An Assessment of Local Opportunities. 2020, Université de Yaoundé I, Ecole Nationale Supérieure Polytechnique de Yaoundé.

[87] Dhundhara, S., Y.P. Verma, and A. Williams, Techno-economic analysis of the lithium-ion and lead-acid battery in microgrid systems. Energy Conversion and Management, 2018. **177**: p. 122-142.

[88] Makola, C.S., P.F. Le Roux, and J.A. Jordaan, Comparative analysis of lithium-ion and lead–acid as electrical energy storage systems in a grid-tied microgrid application. Applied Sciences, 2023. **13**(5): p. 3137.

[89] Pandyaswargo, A.H., et al., Estimating the energy demand and growth in off-grid villages: Case studies from Myanmar, Indonesia, and Laos. Energies, 2020. **13**(20): p. 5313.

[90] Swisher, J.N., G.d. Martino Jannuzzi, and R.Y. Redlinger, Tools and methods for integrated resource planning. Improving energy efficiency and protecting the environment. 1997, United Nations Environmental Programme.

[91] Ramasamy, V. and R. Margolis, Floating Photovoltaic System Cost Benchmark: Q1 2021 Installations on Artificial Water Bodies. 2021, National Renewable Energy Lab.(NREL), Golden, CO (United States).

[92] Hafeez, H., et al., Techno-economic perspective of a floating solar PV deployment over urban lakes: A case study of NUST lake Islamabad. Solar Energy, 2022. **231**: p. 355-364.

[93] sunpower Corporation. SunPower SPR-E20-327 solar panel. 2020,August 20; Available from: https://www.solarreviews.com/manufacturers/sunpower/solar-panels/sunpo19768eseriesspre20327.

[94] SOLARIS. FRONIUS SYMO LITE 24.0 24KW 3-PH INVERTER. 2022,April 7; Available from: https://www.solaris-shop.com/fronius-symo-lite-24-0-24kw-3-ph-inverter/.

[95] Hicham, M., Assessment of the feasibility of hybrid renewable power for supply pumping system for irrigation. Turkish Journal of Computer and Mathematics Education (TURCOMAT), 2021. **12**(4): p. 1434-1454.

[96] Xiamen Sto Energy Tech. Co., L. HDPE Solar Floating Mounting System. 2022, February 14; Available from: https://www.enfsolar.com/pv/mounting-system-datasheet/6229?utm_source=ENF&utm_medium=mounting_system_list&utm_campaign=enquiry_product_directory&utm_content=51973.

[97] Deane, J.P., B.Ó. Gallachóir, and E. McKeogh, Techno-economic review of existing and new pumped hydro energy storage plant. Renewable and Sustainable Energy Reviews, 2010. **14**(4): p. 1293-1302.

[98] Behabtu, H.A., et al., A review of energy storage technologies' application potentials in renewable energy sources grid integration. Sustainability, 2020. **12**(24): p. 10511.

[99] Sabihuddin, S., A.E. Kiprakis, and M. Mueller, A numerical and graphical review of energy storage technologies. Energies, 2015. **8**(1): p. 172-216.

[100] Keiner, D., et al., Powering an island energy system by offshore floating technologies towards 100% renewables: A case for the Maldives. Applied Energy, 2022. **308**: p. 118360.

[101] Hossen, M.D., et al., Design and implementation of a hybrid solar-wind-biomass renewable energy system considering meteorological conditions with the power system performances. International journal of photoenergy, 2022. **2022**.

[102] Ganesan, S. and S. Ahmed, Assessment of wind energy potential using topographical and meteorological data of a site in Central India (Bhopal). International Journal of Sustainable Energy, 2008. **27**(3): p. 131-142.

[103] Bailey, B.H., et al., Wind resource assessment handbook: Fundamentals for conducting a successful monitoring program. 1997, National Renewable Energy Lab., Golden, CO (US); AWS Scientific, Inc ….

[104] Al-Yahyai, S., Y. Charabi, and A. Gastli, Review of the use of numerical weather prediction (NWP) models for wind energy assessment. Renewable and Sustainable Energy Reviews, 2010. **14**(9): p. 3192-3198.

[105] Ahmad, J., et al., Techno economic analysis of a wind-photovoltaic-biomass hybrid renewable energy system for rural electrification: A case study of Kallar Kahar. Energy, 2018. **148**: p. 208-234.

[106] Gebreslassie, M.G., Development and manufacturing of solar and wind energy technologies in Ethiopia: Challenges and policy implications. Renewable Energy, 2021. **168**: p. 107-118.

[107] AHMADI, H. and A. SHAMSAI, Preliminary Site Selection of Pumped Storage Hydropower Plants-A GIS-based approach. 2009.

[108] Chimtavee, A. and N. Ketjoy, PV generator performance evaluation and load analysis of the PV microgrid system in Thailand. Procedia Engineering, 2012. **32**: p. 384-391.

[109] IPE Global Limited, N.C., Financing Gaps and Business Models Off-grid Energy Sector in Ethiopia, I.a.E. Ethiopian Ministry of Water, Editor. 2019, IPE GLOBAL. p. 15.

[110] Fortune. Revised electricity tariffs 2024 31 Augest 2024]; Available from: https://addisfortune.news/fed-bets-on-revised-electric-tariffs-to-lure-investors/#:~:text=The%20new%20tariffs%20will%20be,for%20commercial%20and%20industrial%20users.

[111] Investopedia. Sensitivity Analysis. 2020,May 28; Available from: https://www.investopedia.com/terms/s/sensitivityanalysis.asp.

[112] Kougias, I., et al., The potential of water infrastructure to accommodate solar PV systems in Mediterranean islands. Solar Energy, 2016. **136**: p. 174-182.

[113] Mekonnen, T., et al., Techno-economic comparative analysis of floating/on-ground solar PV system for electrification of Gilgel Gibe i Auxiliary load in Ethiopia. International Journal of Energy Economics and Policy, 2024. **14**(2): p. 218-225.

[114] Group, W.B., Where Sun Meets Water: Floating Solar Market Report. 2019: World Bank.

[115] Temiz, M. and N. Javani, Design and analysis of a combined floating photovoltaic system for electricity and hydrogen production. International Journal of Hydrogen Energy, 2020. **45**(5): p. 3457-3469.

[116] Kowsar, A., et al., Optimization and techno-economic assessment of 50 MW floating solar power plant on Hakaluki marsh land in Bangladesh. Renewable Energy, 2023. **216**: p. 119077.

# APPENDICES

| Load Category | Electrical equipment's | Power rating(w) | Total number |
|---|---|---|---|
| Agriculture (fishing activities + irrigation) | Irrigation water pump (PM45) | 370 | 26 |
| | Refrigerator (Micro-fishing association) BDF-60H1184 | 370 | 4 |
| Flour-mill | Flour-mill | 2200 | 3 |
| Household | Light bulb (LED) | 8.5 | 500 |
| | TV | 65 | 40 |
| | Radio | 12 | 250 |
| | Cellphone charger | 3.3 | 250 |
| Health center | Refrigerator (Vaccine) | 200 | 2 |
| | Room Light (CFL) | 13 | 5 |
| | Sterilization equipment | 60 | 1 |
| | TV | 150 | 2 |
| | Desktop computer | 150 | 2 |
| | Office printer | 100 | 1 |
| School | Light bulb (CLF) | 13 | 10 |
| | Desktop computer | 150 | 12 |
| | Plasma TV | 100 | 3 |
| | Ceiling fan | 50 | 7 |
| | Office printer | 100 | 2 |
| Church | Light bulb (CLF) | 13 | 8 |
| | Ceiling fan | 50 | 4 |

Appendix 1. Electricity Load of the case study

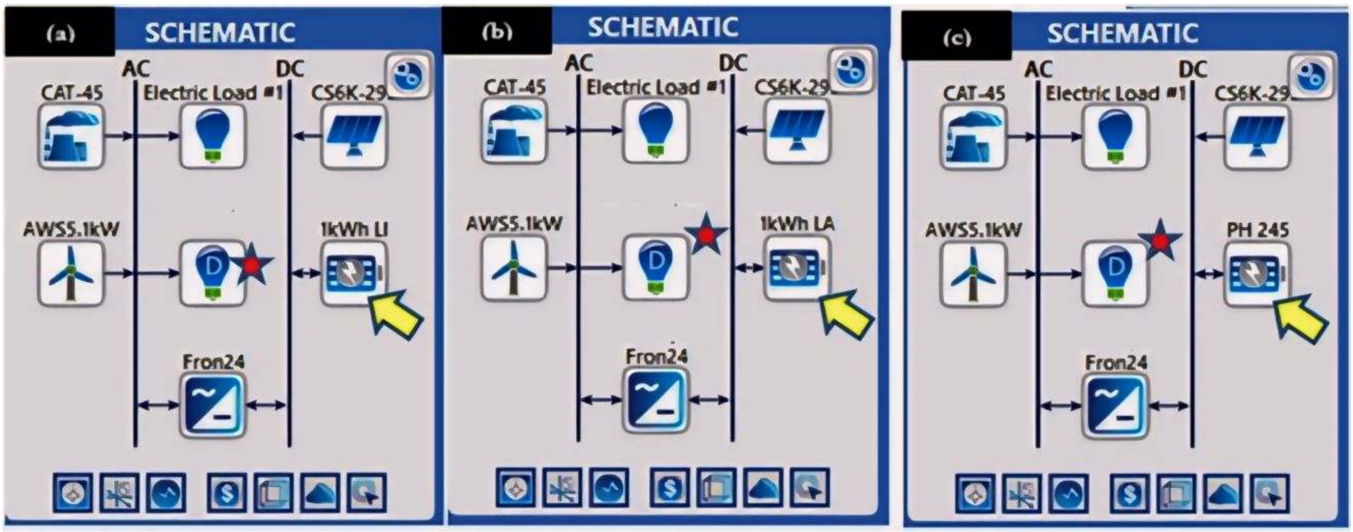


Appendix 2. (a&b), (c). PV-WT-DGe-electro-chemical battery, and PV-WT-DGe-PH 245 Homer pro configuration.

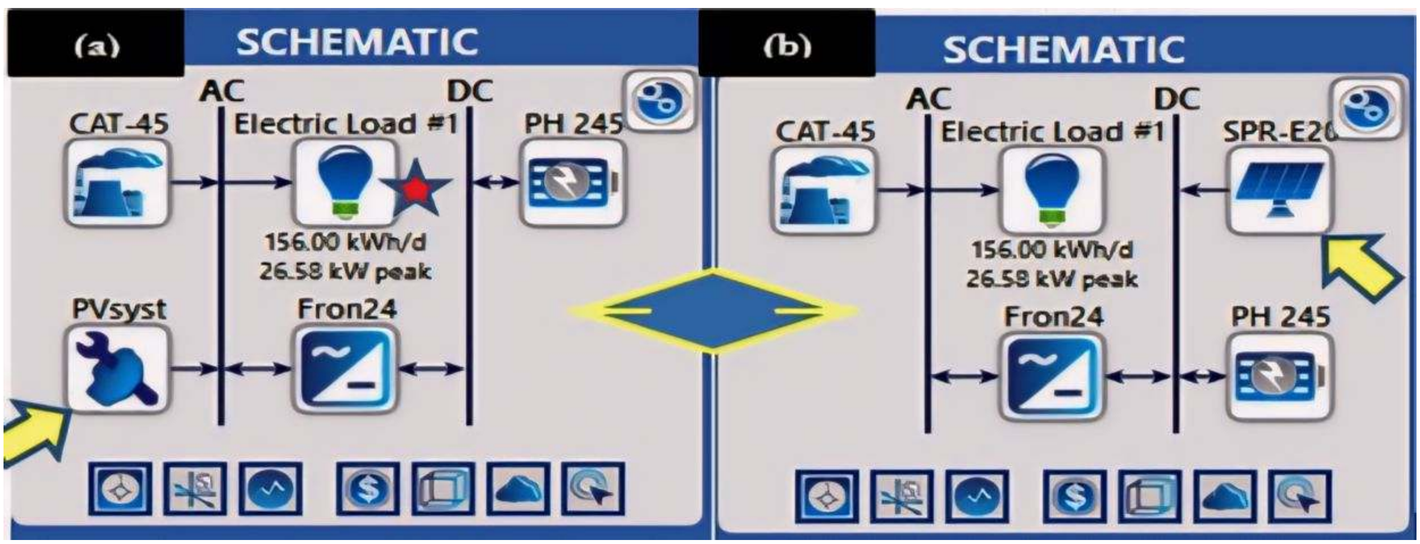


Appendix 3. Homer pro and pvSyst unit configuration schematic

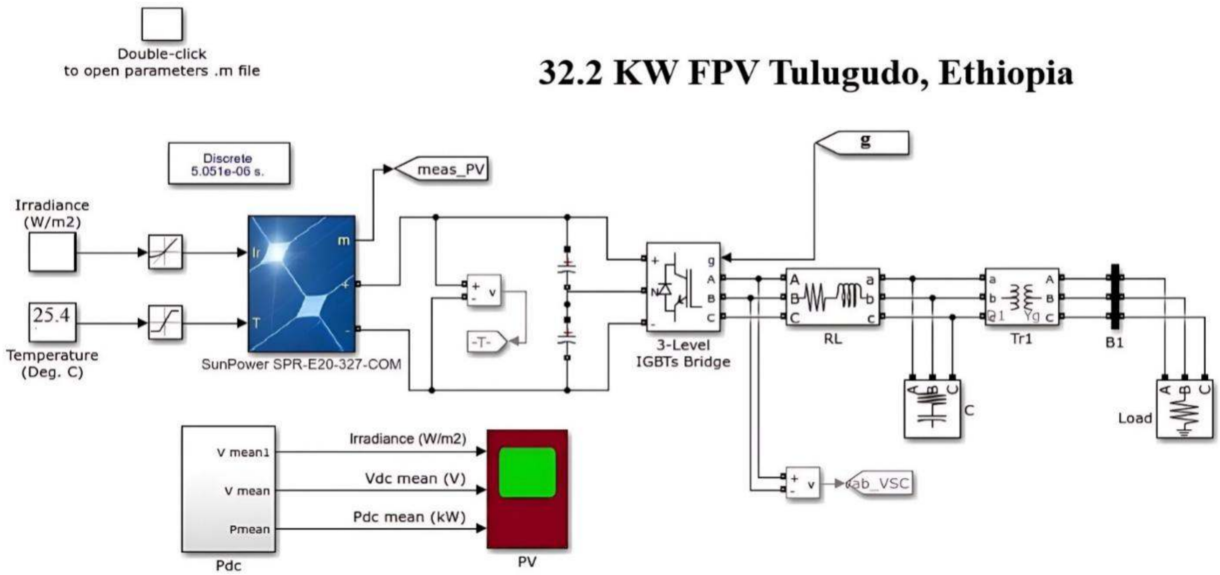


(a)

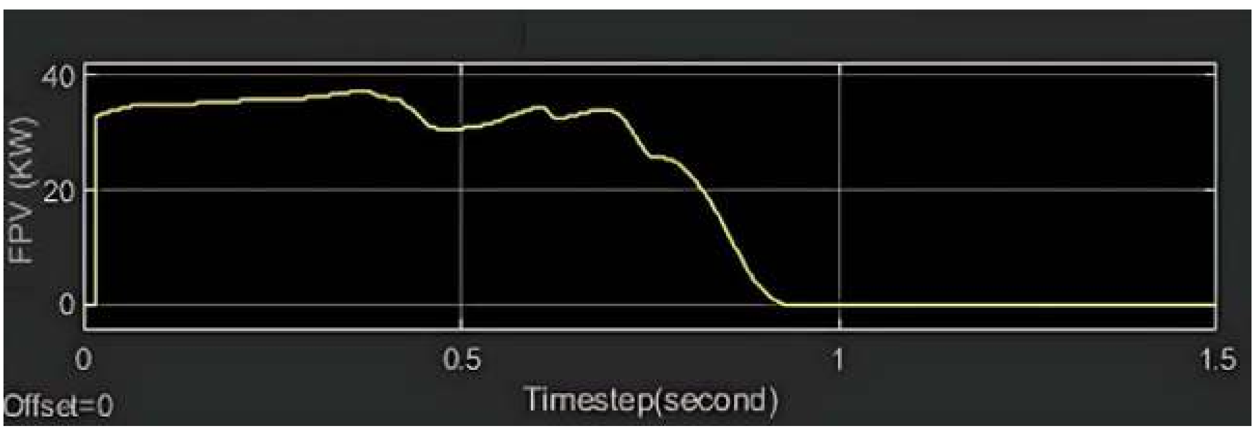


(b)

Appendix 4.(a&b) FPV Mat lab Simulink Model with the corresponding power output

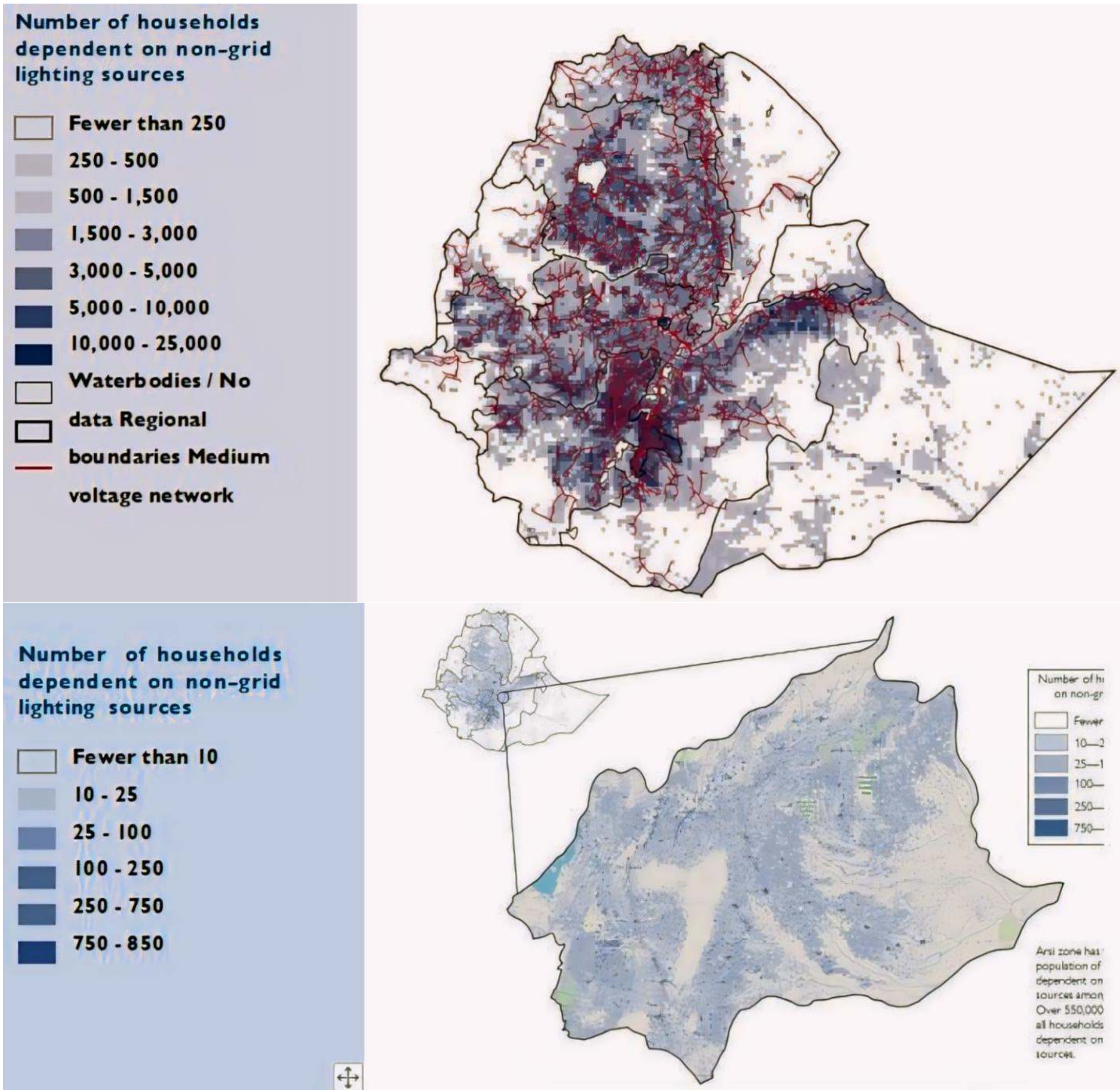


| E.C.R.V (Arsi Zone Characteristics) | |
|---|---|
| Total households | 800,000 |
| Modest consumption power households | 330,000 |
| Medium comsumption power households | 125,000 |
| High consumption power households | 75,000 |
| Non-grid lighting households within 10 km of power lines | 525,000 |

Source: Power Africa Geospatial Analysis 2019

Appendix 5. Households(HH) dependent on non-grid lighting sources


(a)


(b)

Appendix 6(a & b). E.C.R.V Livelihood activates, (Captured during field observation, 2021)..